Dynamic Spectrum Sharing in Cognitive Radio and Device-to-Device Systems

by

Ruochen Zeng

A Dissertation Presented in Partial Fulfillment
of the Requirements for the Degree
Doctor of Philosophy

Approved October 2017 by the
Graduate Supervisory Committee:

Cihan Tepedelenlioğlu, Chair
Antonia Papandreou-Suppappola
Daniel W. Bliss
Oliver Kosut

ARIZONA STATE UNIVERSITY

December 2017

ABSTRACT

Cognitive radio (CR) and device-to-device (D2D) systems are two promising dynamic spectrum access schemes in wireless communication systems to provide improved quality-of-service, and efficient spectrum utilization. This dissertation shows that both CR and D2D systems benefit from properly designed cooperation scheme.

In underlay CR systems, where secondary users (SUs) transmit simultaneously with primary users (PUs), reliable communication is by all means guaranteed for PUs, which likely deteriorates SUs performance. To overcome this issue, cooperation exclusively among SUs is achieved through multi-user diversity (MUD), where each SU is subject to an instantaneous interference constraint at the primary receiver. Therefore, the active number of SUs satisfying this constraint is random. Under different user distributions with the same mean number of SUs, the stochastic ordering of SU performance metrics including bit error rate (BER), outage probability, and ergodic capacity are made possible even without observing closed form expressions. Furthermore, a cooperation is assumed between primary and secondary networks, where those SUs exceeding the interference constraint facilitate PUs transmission by relaying its signal. A fundamental performance trade-off between primary and secondary networks is observed, and it is illustrated that the proposed scheme outperforms non-cooperative underlay CR systems in the sense of system overall BER and sum achievable rate.

Similar to conventional cellular networks, CR systems suffer from an overloaded receiver having to manage signals from a large number of users. To address this issue, D2D communications has been proposed, where direct transmission links are established between users in close proximity to offload the system traffic. Several new cooperative spectrum access policies are proposed allowing coexistence of multiple D2D pairs in order to improve the spectral efficiency. Despite the additional inter-

ference, it is shown that both the cellular users (CU) and the individual D2D user's achievable rates can be improved simultaneously when the number of D2D pairs is below a certain threshold, resulting in a significant multiplexing gain in the sense of D2D sum rate. This threshold is quantified for different policies using second order approximations for the average achievable rates for both the CU and the individual D2D user.

To My Family.

ACKNOWLEDGMENTS

First and foremost I wish to express utmost gratitude to my Ph.D advisor and mentor, Dr. Cihan Tepedelenlioğlu, for his constant support and encouragement. His strong dedication, immense knowledge, and serious attitude towards research are one of the main reasons that help me achievable my best in development of my research. Dr. Tepedelenlioglu has never turned down my request of meeting, and I could not have imagined a better advisor and mentor for my Ph.D study. Once again, my heartfelt thanks to Dr. Tepedelenlioglu.

Besides my advisor, I would like to thank Dr. Daniel W. Bliss, Dr. Antonia Papandreou-Suppappola, and D. Oliver Kosut for their precious time in serving on my thesis committee member, and for their insightful comments and valuable feedback. In addition, I would like to thank Dr. Tolga Duman for asking me a good number of questions as well as providing helpful suggestions at the early stage of my research, which surely help me form my work in a better shape. I also wish to extend my appreciation to the School of Electrical, Computer and Energy Engineering at Arizona State University for providing me this opportunity to pursue my Ph.D degree.

I would like to thank all my present and previous colleagues Adithya Rajan, Sivaraman Dasarathan, Jonghoon Lee, Yuan Zhang, Ahmed Ewaisha, Xiaofeng Li, Sai Zhang, and Xue Zhang, who help me cope with all kinds of difficulties in my research.

Last but not least, I am totally indebted to my family for their unconditional love and endless support. My parents not only support me financially, but also guide me through all those toughness in my life abroad. Without my dear wife's immense faith in my abilities, I could not have come this far.

TABLE OF CONTENTS

CHAPTER Page

CHAPTER Page

APPENDIX Page

LIST OF ABBREVIATIONS

5G	Fifth Generation
AF	Amplify-and-forward
AWGN	Additive White Gaussian Noise
BC	Broadcast Channel
BER	Bit Error Rate
BS	Base Station
CR	Cognitive Radio
CDF	Cumulative Distribution Function
c.m.	completely monotonic
c.m.d.	completely monotonic derivative
CSI	Channel State Information
CU	Cellular User
D2D	Device-to-device
DF	Decode-and-forward
DT	Device-to-device Transmitter
DR	Device-to-device Receiver
DU	Device-to-device User
DPSK	Differential Phase Shift Keying
FDMA	Frequency Division Multiple Access
i.i.d.	independently identically distributed
MAC	Multiple Access Channel
M-DPSK	M-level Differential Phase Shift Keying

MGF	Moment Generating Function
MIMO	Multi-input Multi-output
MRC	Maximal Ratio Combining
MUD	Multi-user Diversity
NB	Negative Binomial
non-i.i.d.	non-independently identically distributed
OFDM	Orthogonal Frequency Division Multiplexing
PAC	Parallel-access Channel
PB	Poisson Binomial
PDF	Probability Density Function
PGF	Probability Generating Function
PR	Primary Receiver
PU	Primary User
SC	Selection Combining
SINR	Signal-to-Interference plus Noise power Ratio
SMUD	Selective Multi-user Diversity
SNR	Signal to Noise Ratio
SR	Secondary Receiver
SU	Secondary User
LoS	Light of Sight
LT	Laplace Transform
LTE	Long Term Evolution
QoS	Quality of Service

LIST OF FIGURES

Figure Page

Chapter 1

INTRODUCTION

1.1 Cognitive Radio Systems

As a result of multimedia applications becoming common in wireless networks, the need for high data rate service has increased dramatically in the past decade. Due to the nature of the limitation of the spectrum and high price to gain new spectrum resource, and the fact that spectrum utilization depends strongly on time and place [1, 2], static spectrum access scheme can not accommodate the rise in the number of high data rate devices [3]. The concept of cognitive radio (CR) was first proposed by Joseph Mitola in 1998 [4], and has become very popular since it is considered as an promising and opportunistic spectrum usage solution to dynamically utilize the spectrum resources [5]. In CR systems, frequency bands are not used exclusively by their licensed users (primary users), who own the right to get access to the channel in an arbitrary time as needed.

Most CR paradigms can be categorized into two kinds: overlay and underlay. In the overlay paradigm, unlicensed users (secondary users) continuously monitor the available spectrum holes and the activities of the primary users. Once the primary user (PU) is silent, the secondary users (SUs) are allowed to transmit [6, 7]. With perfect sensing from SUs, the spectrum resources can be shared by large number of clients and PUs do not suffer from cross interference caused by SUs [4]. In the underlay system, SUs transmit simultaneously with PUs, where interference temperature at the primary receiver (PR) is kept below a certain threshold to satisfy a strict interference constraint [8].

In the overlay CR systems, one of the most important components is the SU's sensing ability to be aware of the idleness of the PU so that SUs only transmit during these idle periods [9,10]. This awareness can be obtained by the local sensing results at SUs via a number of different methods. Energy detector based approach is the most common way due to its low computational and implementation complexities, where the received signal at the SU is detected by comparing the output of the energy detector with a threshold [11]. The probability of detection averaged over Rayleigh fading channel is derived in [12]. The performance of energy detector with low signal-to-noise-ratio (SNR) values and noise estimation errors scenarios are studied in [13, 14]. By exploiting the cyclostationary features of the received signal at the SU such as the mean and autocorrelation, cyclostationarity-based sensing method has been introduced to spectrum sensing in CR systems [2, 15]. Cyclostationarity-based sensing of orthogonal-frequency-division-multiplexing (OFDM) specific [16,17] as well as general types of signals [18] are developed. Assuming that the transmitted signal from the PU is known at the SU, match-filtering is the optimal approach to detect the PU's presence. The complexity and power consumption issues have been discussed in [2] and compared with other spectrum sensing approaches. Based on the local sensing results at peer SUs, cooperative sensing scheme is proposed to decrease the miss-detection, false alarm probabilities, and solve the hidden PU problem issue [19, 20]. A pairwise cooperation scheme is proposed in [21], where a SU far from the PR will collaborate with a user nearby to utilize the spatial diversity. Recently, consensus is applied to share messages among all SUs in the decentralized as well as distributed spectrum sensing [22–29]. Optimal power control and scheduling on the sensing and throughput trade-off has been studied from the MAC layer perspective [30–34].

In the underlay scheme, since SUs are transmitting over the licensed spectrum band simultaneously with the PU, managing the interference at the PR is the main

goal. Most of the literature impose the interference model into the transmission power of the SU, so that the interference temperature can be strictly controlled [35]. An power control strategy is proposed in [36], which enables the SU to maximize its transmission rate while guaranteeing the outage probability of the PU not degraded. SU's rate is maximized with respect to a peak transmitting power and peak interference power constraint in [37]. Multiple-input-multiple-output (MIMO) antenna arrays can be exploited to create degrees of freedom to align interference into the PU's orthogonal signal spaces [38]. Capacity for Gaussian MIMO channels under received-power constraints in underlay cognitive radio systems is studied in [39]. Transmitting beamforming coefficients are optimized in order to maximize the transmit SNR of the secondary users with respect to the interference to the PUs. In addition, a zero-forcing beamforming scheme incorporated with a user selection algorithm is proposed in [40] to maximize the sum rate. In [41], an algorithm which computes the power control values and the beamforming weights in turn, is proposed to minimize the total transmission power of the CR system and to satisfy the minimum performance requirements for both the primary and secondary networks.

A hybrid CR system is proposed in [42], where the SU initially senses the available spectrum and adjusts its access strategies between overlay and underlay according to the sensing decision. A power allocation algorithm to maximize the throughput of the secondary link is studied in [43], where the achievable rates of the secondary system in underlay, overlay, and hybrid options are compared. The access strategy of the SU entering the overlay, underlay, and hybrid modes in terms of maximizing the secondary achievable rates has been studied in [44]. The mode switching rate, which is the rate that SUs switch between overlay and underlay modes is optimized in [45, 46]. It is shown that the hybrid CR system with the optimal switching rate significantly improves the average throughput and also is robust to detection errors

[45]. Outage performance of the hybrid CR systems are studied and compared with the conventional CR system in [45–47].

1.1.1 Underlay Cognitive Radio System with Multi-user Diversity

In the underlay CR systems, the primary network's performance is guaranteed by all means, which potentially deteriorates SUs' performance. To exploit the spatial and time diversity in order to overcome this issue, multi-user diversity (MUD) has been considered in underlay CR systems for opportunistic communications with multiple SUs [48]. Subject to the interference constraint at the PR, the SU with the highest instantaneous SNR is selected for communication. Under this assumption, statistics of the SU transmit SNR in the high power region is studied in [48]. When taking into account the interference introduced by the PU at the secondary receiver, MUD gain of the signal-to-noise-plus-interference ratio (SINR) under cognitive multiple-access channel (MAC), broadcast channel (BC), and parallel-access (PAC) are investigated in [49]. The CDF expressions of the SINR under MAC, BC [50], and PAC [51] are derived to analyze the bit-error rate (BER) performance. Another common assumption in cognitive MUD systems requires that SUs satisfy an average transmit and interference power constraint at the PR [52]. In this scheme, secondary link capacity is shown to scale like $O(M \log\log N)$ as a function of the number of SUs N and available primary spectra M [53, 54].

In most existing cognitive MUD systems, all secondary transmitters scale down their transmit power to meet the interference constraint if the instantaneous peak transmit power causes too much interference. After this potentially continuous power adjustment, the user with the best instantaneous SNR at the secondary receiver is chosen [48, 49, 51]. This scheme requires accurate continuous feedback of the interference channel. In the Chapter 2, we consider an uplink underlay CR system setup

with a single PU and multiple SUs, each equipped with a single antenna [55]. All secondary transmissions obey a pre-determined interference constraint at the PR. The secondary receiver, which is the base station (BS), dynamically updates an index set which contains a list of SUs that satisfy the interference constraint, which creates a random number of SUs. This can be realized with the presence of a feedback channel between PR and BS [56] to inform users whether they are active or passive. For the first time in the literature, we investigate the effect of having a random number of active users on the performance analysis of CR system with MUD. In Chapter 2, we study the asymptotic behavior of ergodic capacity and BER averaged across the fading and the user distribution with large mean number of SUs. We also derive non-asymptotic closed form expressions for average BER under several user distributions. Then we consider the non-homogeneous interference case. Furthermore, a stochastic ordering approach is adopted to compare the system performances under different active user distributions.

1.1.2 Cooperative Cognitive Radio Systems

As we illustrated, the overlay scheme relies on the efficient and accurate sensing ability at the SU. In the underlay scheme, SUs will transmit with limited power in order to satisfy the interference constraint. To overcome this drawback in the underlay setup, besides MUD, the cooperative spectrum sharing system has been considered recently. Cooperation within the PU and the SU networks has been studied in an information theoretic framework in [57, 58]. References [59–61] and the literature therein focus on the scenario that SUs relay their own signals. Recently, the case that when SU assist PU's transmission has been drawn attention to. Physical layer spectrum sharing protocols based on amplify-and-forward (AF) and decode-and-forward (DF) relaying techniques are proposed in [62] and [63] where single transmit/receive

pair of PUs and SUs are considered with outage probability as a performance metric. Reference [64] generalizes to the case of multiple SUs for fixed transmission power with opportunistic SU relays selection [65, 66], and studies numerically the choice of number of potential SU relays. In [67], a dynamic cooperation scheme is proposed where the SU adjusts its transmission power based on how much bandwidth it can occupy to relay PU's signal. This scheme increases the interference tolerance at the PR, and improves PU's rate as well as saves PU's transmission power. In [68], instead of power adaptation, the SU switches its transmission strategy between relaying and its own transmission with imperfect channel knowledge based on game theory. Reference [69] analyzes the stable throughput of the SU from a network layer perspective and shows that having packets relayed by the SU can empty the queue of the PU quickly, thus creating transmitting opportunities for the SU. A dynamic spectrum sharing scheme is proposed in [68] that the SU adjusts between relay and own transmission modes to achieve the data rate improvements for both PU and SU.

In Chapter 3, we consider a cooperative CR system containing a single PU and multiple SUs [70–72]. A subset of size M of a total $N+M$ SUs that have interference less than a certain threshold at the PR will enter the underlay mode, among which MUD are assumed among to enhance SU network's performance. The remaining N SUs whose interference exceed the threshold will amplify and relay the PU's signal to mitigate the limited interference caused by the underlay SUs. AF relaying is assumed due to its practical simplicity and to maintain the PU's privacy by keeping the SU from decoding the PU's signal, and opportunistic relay selection is applied among SU relays to achieve spatial diversity. Opportunistic relay selection based on the highest end-to-end relay gain has been recently studied in the cognitive radio setup [73–76], where the relay cooperation is exclusively among either PU or SU networks. In this dissertation, we assume that one out of N SUs will relay PU's signal in exchange

for the spectrum access, and the average BER and achievable rates of both PU and SU are studied. Hence, as the ratio $t = N/(N+M)$ varies, a trade-off between the primary and secondary network performance is observed. Our novel average overall BER and sum rate metrics capture the combined system performance, and enable optimizing the ratio t in closed form. The optimal ratio reveals the potential number of relays N and underlay SUs M as a function of the average SNR on each fading path and the total number of SUs. Practically, N and M could be random because of the mobility of the users and non-homogeneous interference environment in the cellular. Hence, we also consider the same setup with a random number of users denoted as $\mathcal{N}$ and $\mathcal{M}$, where $t = \mathrm{E}[\mathcal{N}]/\mathrm{E}[\mathcal{M}+\mathcal{N}]$ is optimized.

1.2 Device-to-Device Communication Systems

With the rapid increase of multi-media applications, there have been a phenomenal increase in the high data rate demands and smart devices. Similar to conventional cellular networks, CR systems still suffer from an overloaded receiver having to manage signals from a large number of users. To address this issue, the concept of Device-to-Device (D2D) communications underlaying the cellular network has been proposed in the 3GPP Long Term Evolution (LTE) recently [77,78], and considered as a promising technique to improve the spectrum utilization towards future 5G networks [79].

One fundamental issue in D2D communications is that how to address the co-existence of cellular users (CUs) and D2D users. Underlay D2D schemes where the cellular spectrum is reused by D2D users have been studied intensively in the literature. The main purpose of these works is to control the mutual interference between the cellular and D2D networks [77,80–85]. Power control of D2D users can be used to restrict the interference temperature in the deterministic [80–82], and random (Poisson) networks [83]. Precoding techniques [84, 85] in a MIMO setup are considered to

minimize the interference signal aligned with the cellular signal spaces. Reference [86] extends the study to the massive-MIMO scenario and studies the spectral efficiency with perfect and imperfect channel state information (CSI) at the cellular BS. Overlay schemes where a part of the cellular spectrum is dedicated only for D2D communications have been studied to mitigate the interference between the cellular and the D2D networks. In [87], an uplink D2D communication system is considered where the cellular BS is assumed to act as a re-transmitter of the D2D transmitter (DT) when the CU is idle. Reference [88] allows a DT with a good channel condition to transmit D2D multi-cast data from the BS directly to those D2D users experiencing poor channel conditions.

In-band cooperation between the CU and the D2D networks has been considered to accommodate both CU and D2D users within the same spectrum band. This can be realized via superposition coding, where the DT broadcasts the CU's signal superimposed by its own D2D signal to both the cellular and the D2D receivers. Superposition coding is a non-orthogonal scheme that achieves the capacity on scalar Gaussian broadcast channels [89]. A cooperative overlay D2D scheme is proposed in [90] based on ideas from cognitive radio systems [91, 92], where one D2D user acts as a two-way relay to facilitate the cellular transmission using superposition coding. The single relay selection case in this setup is also considered in [90] but with a numerical approach, without analytical results. Reference [93] extends this study to the full-duplex one-way relay scenario where the power allocation strategy maximizing the D2D link rate is derived, and the residual self-interference is assumed [94–96]. The above literature all assume up to only one pair of D2D users facilitating CU's transmission at the same time, which deteriorates the spectrum utilization for the D2D network. Intuitively, with maximum ratio combining (MRC) at the CU, by increasing the number of D2D pairs relaying the CU's signal, CU's performance can

be improved compared with the single D2D pair scenario. However, this creates peer interference among D2D pairs. For the first time in the literature, we are able to characterize this performance trade-off and show that both CU and D2D users can potentially benefit from multiple D2D pairs by properly balancing the amount of power allocated to relaying the CU's signal against D2D communications.

In Chapter 4, we propose a new downlink cellular system allowing *multiple* D2D pairs, using superposition coding, coexisting with the CU simultaneously [97]. Each active DT acts as a half-duplex one-way relay to decode and forward the CU's signal from the BS with a certain fraction of its transmission power, and communicates with the D2D receiver using the remaining power to superimpose its own signal. Those DTs who can not successfully decode the CU's signal will remain silent during the second half of the transmission block. Four spectrum access policies for single and multiple D2D pairs are studied based on different CSI assumptions. Beyond the existing literature [90, 93] where the CU's signal is perfectly canceled at the D2D receiver, we also study the imperfect interference cancellation case. Closed-form second order approximations of the average achievable rates for both the CU and D2D users in all spectrum access policies are derived. As the number of D2D pairs increases, the CU's achievable rate is improved while causing peer interference to other D2D pairs concurrently. Through our analysis, this trade-off can be characterized analytically by balancing between the number of active D2D pairs and the power allocation factor at each DT. It is shown that, by a proper choice of the number of D2D pairs and the power allocation factor, both CU and the individual D2D users' performance as well as the spectral efficiency can be improved simultaneously up to a maximum number of D2D pairs. Closed-form expressions are derived for this number of D2D pairs as a function of the average interference level. We also generalize the study to random number of DUs case in this setup where the perfect DF scenario at each DT

is not guaranteed for the first time in literature, and stochastic ordering is applied to compare the CU's rates under different DU distributions in the large mean number of DUs regime.

1.3 Main Contributions of This Dissertation

Here we summarize the main contributions of this dissertation.

- For the first time in the literature, we consider the effect of having a random number of active users on the performance analysis of CR system with MUD.
- We consider the non-homogeneous interference case where SUs yield different interference constraints.
- A stochastic ordering approach is adopted to compare the system performances under different active user distributions.
- Opportunistic relaying and MUD are considered in the primary and the secondary network respectively in a cooperative CR system with multiple SUs.
- For both PU and the selected underlay SU, closed form expressions of the average BER and the scaling laws of achievable rate in large number of SUs regime are derived, going beyond the outage performance in [63, 64].
- Novel overall performance metrics are defined to mathematically quantify the trade-off between primary and secondary networks in the average BER and achievable rate sense. We show that our proposed scheme outperforms conventional underlay CR systems.
- Above trade-off studies are generalized to the random number of SUs scenario, which arises due to heterogeneous and mobile environments.

- Multiple D2D communications underlaying cellular networks with DF relaying and superimposition coding at each DT is proposed.
- We show that in the small SNR regime, multiple DUs can be activated simultaneously to improve the system performance as well as achieving better spectrum efficiency.
- Finite order Taylor expansion of the CU and the DU's achievable rates are rigorously proved to be tight in small SNR regime.
- We show that both CU and DU's performance can be improved at the same time with a proper choice of the spectrum access policy for the DUs.
- The study is generalized to the random number of DUs case where the DF relaying is not perfect at each DT.

1.4 Outline of This Dissertation

The remainder of this dissertation is organized as follows. Chapter 2 begins with a system model for a underlay CR system with MUD and random number of SUs. Later in the chapter, ergodic capacity and average BER metrics are derived and ordered using stochastic ordering under different user distributions. In Chapter 3, we focus on a cooperative underlay CR system where SUs relay the PU's signal in return for the spectrum access opportunities. This is then followed by optimizing the total system performance with respect to average channel statistics. Chapter 4 discusses the cooperative D2D communication underlaying a downlink cellular network, and addresses the issue on improving the CU and the DU's performance simultaneously. Chapter 5 draws the conclusion of this dissertation.

Chapter 2

COGNITIVE RADIO SYSTEM WITH RANDOM NUMBER OF SECONDARY USERS

In this chapter, a single primary user (PU) cognitive radio (CR) system with multi-user diversity (MUD) among the secondary users (SUs) is considered where there is an instantaneous interference constraint assumed at the primary receiver (PR). The SU with the highest instantaneous SNR is selected for communication from a set of active SUs who satisfy the interference constraint. The number of active SUs is shown to be binomial, negative binomial, or Poisson-binomial distributed depending on various SU spectrum accessing policies. Outage probability in the slow fading scenario is also studied. This is then followed by a derivation of the scaling law of the ergodic capacity and closed form expressions for BER averaged across the fading, and user distribution in the large mean number of SUs regime. System performance under different user distributions with the same mean value are order in a stochastic ordering sense.

2.1 System Model

We consider an uplink CR system with multiple SUs, a single PU, and one base station (BS) which serves as the receiver to the SUs. Both the BS and users are assumed to have a single antenna.

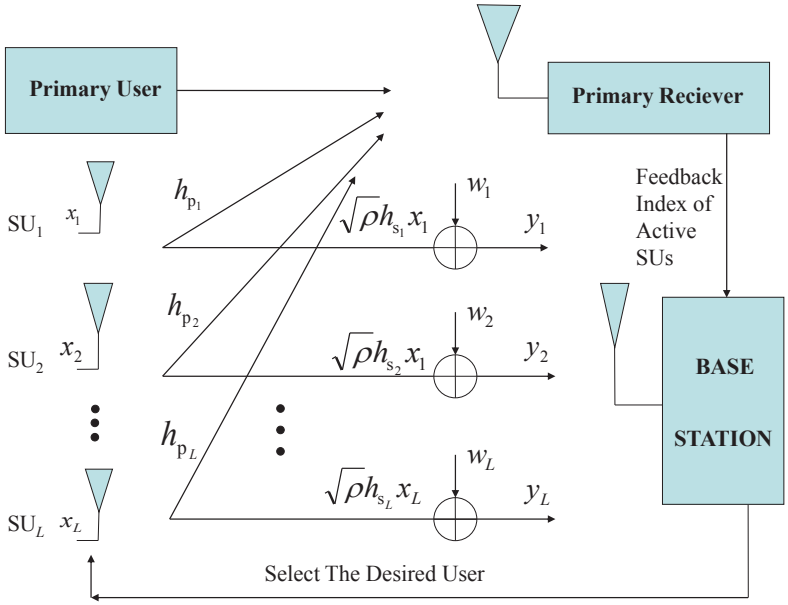

Figure 2.1: System Model of Proposed CR System

As shown in Figure 2.1, we consider a CR system with a total of L SUs where the MUD scheme is applied to the secondary system. A SU is allowed to share the spectrum with a primary link as long as the interference power to the primary receiver is less than a threshold Q for instantaneous interference. The received signal from the i^{th} SU at the BS can be expressed as,

$$y_i = \sqrt{\rho} h_{\mathrm{s}_i} x_i + w_i, \qquad i = 1, 2, \ldots, L, \tag{2.1}$$

where h_{s_i} denotes the channel coefficient from the i^{th} SU to the BS, x_i is the transmitted symbol, w_i is white Gaussian noise (AWGN). Variance of h_{s_i}, x_i, and w_i are normalized. The average received power ρ at the BS is assumed to be identical across SUs. The channel gain of the i^{th} SU at the secondary BS can be expressed as $\gamma_{\mathrm{s}_i} = |h_{\mathrm{s}_i}|^2$, whereas the interference channel gain of the i^{th} SU at the primary

receiver is $\gamma_{\mathrm{p}_i} = |h_{\mathrm{p}_i}|^2$. The channel gain of the selected user is denoted by

$$\gamma_{\mathrm{s}}^* = \max_{\{i|i\in S\}} \{|h_{\mathrm{s}_i}|^2\}, \tag{2.2}$$

where S is a subset of the users that respect the interference constraint. Consequently, SUs either transmit with fixed power ρ, or remain silent, so that a simple transmitter with a fixed power level and one bit feedback is sufficient. In contrast, previous work [48,49,51] assumes that secondary transmit power is adjusted to Q/γ_{p_i} if interference constraint is violated, which requires feedback of instantaneous channel state information (CSI) of the interference channel and a sophisticated transmitter to support infinite power levels.

The distribution of the cardinality of S will be specified when different SU distributions are studied. Since all SUs have i.i.d. fading channels to the secondary BS, the subscript i will be dropped when deriving the cumulative distribution function of γ_{s_i}. Let $\mathcal{N}$ be the cardinality of S. Conditioned on $\mathcal{N} = k$, the CDF of the channel gain of the chosen user can be obtained using order statistics as $F_{\gamma_{\mathrm{s}}}^k(x)$. To obtain the CDF of γ_{s}^* in (2.2) we have

$$F_{\gamma_{\mathrm{s}}^*}(x) = \mathrm{E}_{\mathcal{N}}\left[F_{\gamma_{\mathrm{s}}}^{\mathcal{N}}(x)\right] = \sum_{k=0}^{\infty} \Pr\left[\mathcal{N} = k\right] F_{\gamma_{\mathrm{s}}}^k(x) = U_{\mathcal{N}}(F_{\gamma_{\mathrm{s}}}(x)) \tag{2.3}$$

where $U_{\mathcal{N}}(z) = \sum_{k=0}^{\infty} \Pr\left[\mathcal{N} = k\right] z^k$, $0 \le z \le 1$, is the probability generating function (PGF) of $\mathcal{N}$.

2.2 Mathematical Preliminaries

In this section, we introduce some mathematical preliminaries that will be useful throughout the dissertation.

2.2.1 Completely Monotonic Functions

A non-negative function $\tau(x) : \mathbb{R}^+ \to \mathbb{R}$ is *completely monotonic* (c.m.) if its derivatives alternate in sign [98], i.e.,

$$(-1)^k \frac{d^k \tau(x)}{dx^k} \geq 0, \quad \forall x, \quad k = 1, 2, 3, \ldots. \tag{2.4}$$

We are also interested in positive functions whose first-order derivatives are c.m., which are said to have a completely monotonic derivative (c.m.d.). Due to a well-known theorem by Bernstein [98, pp. 22], an equivalent definition for c.m. function is that it can be expressed as a positive mixture of decaying exponentials:

$$\tau(x) = \int_0^\infty e^{-sx} d\psi(s) \tag{2.5}$$

for some non-decreasing function $\psi(s)$.

2.2.2 Laplace Transform Ordering

In this section we introduce *Laplace transform* (LT) ordering, a kind of stochastic ordering, to compare different user distributions. This stochastic ordering will be useful in comparing error rate and ergodic capacity averaged across user and channel distributions. LT order is a partial ordering on non-negative random variables [99, pp. 233].

Let $\mathcal{X}$ and $\mathcal{Y}$ be non-negative random variables. $\mathcal{X}$ is said to be less than $\mathcal{Y}$ in the LT order (written $\mathcal{X} \leq_{\mathrm{Lt}} \mathcal{Y}$), if $\mathrm{E}[e^{-s\mathcal{X}}] \geq \mathrm{E}[e^{-s\mathcal{Y}}]$ for all $s > 0$. An important theorem found in [98], and [100] is given next:

Theorem 1. *Let $\mathcal{X}$ and $\mathcal{Y}$ be two random variables. If $\mathcal{X} \leq_{\mathrm{Lt}} \mathcal{Y}$, then, $E[\psi(\mathcal{X})] \geq E[\psi(\mathcal{Y})]$ for all c.m. functions $\psi(\cdot)$, provided the expectation exists. Moreover, when $\mathcal{X} \leq_{\mathrm{Lt}} \mathcal{Y}$, $E[\psi(\mathcal{X})] \leq E[\psi(\mathcal{Y})]$ holds for any c.m.d. function $\psi(\cdot)$, provided the expectation exists.*

We will use an equivalent representation of LT ordering of discrete random variables to order the user distribution by the ordering of their PGFs. By defining $z := e^{-s}$, one can rewrite $\mathrm{E}\left[e^{-s\mathcal{X}}\right] \geq \mathrm{E}\left[e^{-s\mathcal{Y}}\right]$ for $z \geq 0$ as $\mathrm{E}\left[z^{\mathcal{X}}\right] \geq \mathrm{E}\left[z^{\mathcal{Y}}\right]$ for $0 \leq z \leq 1$, which is the same as $U_{\mathcal{X}}(z) \geq U_{\mathcal{Y}}(z)$, $0 \leq z \leq 1$, where we recall that $U_{\mathcal{X}}(z) = \mathrm{E}[z^{\mathcal{X}}]$ represents the probability generating function of the discrete random variable $\mathcal{X}$. This representation will be helpful when we compare two user distributions in Section 2.6.

2.2.3 Regular Variation

A function $\psi(s)$ is *regularly varying* with exponent $\mu \neq 0$ at $s = \infty$ if it can be expressed as $\psi(s) = s^{\mu} l(s)$ where $l(s)$ is slowly varying which by definition satisfies $\lim_{s\to\infty} l(\kappa s)/l(s) = 1$ for $\kappa > 0$. So, intuitively, regular captures the notion of polynomial-like behavior asymptotically. Regular (slow) variation of $\psi(s)$ at $s = 0$ is equivalent to regular (slow) variation of $\psi(1/s)$ at ∞. The Tauberian theorem for Laplace transforms, applies to c.m. functions of the form (2.5) and states that $\tau(x)$ is regularly varying at $x = \infty$ if and only if $\psi(s)$ is regularly varying at $s = 0$. The following theorem is from [101, pp. 73]:

Theorem 2. *If a non-decreasing function $\psi(s) \geq 0$ defined on $\mathbb{R}^+$ has a Laplace transform $\tau(x) = \int_0^\infty e^{-sx} d\psi(s)$ for $x \geq 0$, then $\psi(s)$ having variation exponent μ at ∞ (or 0) and $\tau(x)$ having variation exponent $-\mu$ at 0 (or ∞) imply each other.*

2.2.4 Schur-Concave Functions and Majorization

In this section we first introduce the notion of majorization and Shur-convex functions. For any $\boldsymbol{x} = (x_1, ..., x_n) \in \mathbb{R}^n$ and $\boldsymbol{y} = (y_1, ..., y_n) \in \mathbb{R}^n$, let $x_{[1]} \geq \cdots \geq x_{[n]}$ and $y_{[1]} \geq \cdots \geq y_{[n]}$ denote the components of $\boldsymbol{x}$ and $\boldsymbol{y}$ in decreasing order. We say $\boldsymbol{x}$ is majorized by vector $\boldsymbol{y}$, equivalently $\boldsymbol{x} \prec \boldsymbol{y}$ to mean $\sum_{i=1}^{k} x_{[i]} \leq \sum_{i=1}^{k} y_{[i]}$ for all

$k = 1, \ldots, n$, and $\sum_{i=1}^{n} x_{[i]} = \sum_{i=1}^{n} y_{[i]}$. A Schur-concave function g:$\mathbb{R}^n \to \mathbb{R}$ satisfies $g(\boldsymbol{x}) \geq g(\boldsymbol{y})$ whenever $\boldsymbol{x} \prec \boldsymbol{y}$. The following theorem is proved in [102]:

Theorem 3. *Let g be a continuous non-negative function defined on an interval $I \subset \mathbb{R}$. Then*

$$\phi(\boldsymbol{x}) = \prod_{i=1}^{n} g(x_i), \qquad \boldsymbol{x} \in I^n, \tag{2.6}$$

is Schur-concave on I^n if and only if $\log(g)$ *is concave on I.*

2.2.5 Bounds of Probability Generating Function

Following theorem has been proved in [103]:

Theorem 4. *Let $U_{\mathcal{N}}(z)$ be the PGF of a discrete random variable $\mathcal{N}$ with non-negative integer support. If the mean value λ and variance $\sigma^2_{\mathcal{N}}$ exist, then the following inequalities hold for all $0 \leqslant z \leqslant 1$:*

$$1 + (z-1)\lambda \leqslant U_{\mathcal{N}}(z) \leqslant 1 + (z-1)\lambda + \frac{(z-1)^2}{2} m(z) \tag{2.7}$$

where $m(z)/(\sigma^2_{\mathcal{N}} + \lambda^2 - \lambda)$ is another PGF.

2.2.6 Asymptotics

We say $\tau(x) = O(g(x))$ as $x \to \infty$ if and only if there is a positive constant M and a real number x_0 such that $|f(x)| \leq M|g(x)|$ for all $x > x_0$. We say $\tau(x) = o(g(x))$ as $x \to \infty$ that for every positive integer ϵ there exists a constant x_0 such that $|f(x)| \leq \epsilon|g(x)|$ for all $x > x_0$ [104].

2.3 Ergodic Capacity

When h_{s_i} and h_{p_i} both vary rapidly over the duration of a codeword, system is in the so-called fast fading regime. We consider the ergodic capacity of the secondary

system averaged over both fading and user distributions. We then study the asymptotic behavior of ergodic capacity with large mean number of SUs. The expression of the ergodic capacity of a multi-user system with deterministic number of users N and average SNR ρ is given by,

$$\overline{C}(\rho, N) = \int_0^\infty \log(1+\rho x)\, dF_{\gamma_s}^N(x) = \rho \int_0^\infty \frac{1 - F_{\gamma_s}^N(x)}{1+\rho x} dx. \tag{2.8}$$

where $\overline{C}(\rho, N)$ is the ergodic capacity averaged over the fading channel. For the random number of users case, N is a realization of a random variable $\mathcal{N}$, which is the number of users respecting the interference constraint. By using (2.3) the ergodic capacity averaged across the user distribution can be expressed as,

$$\mathrm{E}_{\mathcal{N}}\left[\overline{C}(\rho, \mathcal{N})\right] = \mathrm{E}_{\gamma_s^*}[\log(1+\rho\gamma_s^*)] = \rho \int_0^\infty \frac{1 - U_{\mathcal{N}}(F_{\gamma_s}(x))}{1+\rho x} dx. \tag{2.9}$$

It can be shown that $\overline{C}(\rho, N)$ in (2.8) is a c.m.d. function of N [105]. According to Theorem 1, if two user distributions are LT ordered, so will their ergodic capacities. $\overline{C}(\rho, N)$ is also a concave increasing function of N. Applying the Jensen's inequality [106] and defining $\lambda := \mathrm{E}[\mathcal{N}]$, we have

$$\mathrm{E}_{\mathcal{N}}\left[\overline{C}(\rho, \mathcal{N})\right] \leq \overline{C}(\rho, \lambda). \tag{2.10}$$

Therefore, randomization of N will always deteriorate the average ergodic capacity of a MUD system.

2.3.1 Scaling Laws of Ergodic Capacity

To study how the number of active number of users $\mathcal{N}$ affects the average throughput of the system, we derive the scaling laws of the ergodic capacity for large average number of users λ. Reference [105] considers the Poisson distribution for $\mathcal{N}$ in a non-cognitive context and derives the scaling laws of ergodic capacity as $\lambda \to \infty$.

In this section, we generalize this result to a large family of user distributions and determine conditions under which similar scaling laws hold. Under a Rayleigh fading scenario, γ_{s} is exponentially distributed [107]. Substituting $F_{\gamma_{\mathrm{s}}}(x) = 1-e^{-x}$ into (2.9) and assuming that mean value λ and variance $\sigma_{\mathcal{N}}^2$ of $\mathcal{N}$ exist, we have the following theorem:

Theorem 5. *The ergodic capacity averaged across the fading and user distribution, denoted as* $E_{\mathcal{N}}\left[\overline{C}(\rho,\mathcal{N})\right]$*, has the following scaling law as* $\lambda \to \infty$*,*

$$\begin{aligned} E_{\mathcal{N}}\left[\overline{C}(\rho,\mathcal{N})\right] &= \rho \int_0^{\infty} \frac{1-U_{\mathcal{N}}(1-e^{-x})}{1+\rho x} dx \\ &= \log\left(1+\rho\log(\lambda)\right) + O(1/\sqrt{\log(\lambda)}), \end{aligned} \tag{2.11}$$

provided that $(a)\Pr\left[\mathcal{N}=0\right] = o(1/\log\log\lambda)$ and $(b)\sigma_{\mathcal{N}}^2 = o(\lambda^2)$ as $\lambda \to \infty$.

Proof. See Appendix A. □

Note that if $\mathcal{N}$ is not random (i.e., the number of users is deterministic), then $\mathcal{N} = \lambda$ with probability one, which satisfies both assumption (a) and (b) in Theorem 5. This implies that $\overline{C}(\rho, L) = O(\log\log L)$, as $L \to \infty$, as also observed in [53, Theorem 5]. Theorem 5 can be viewed as a generalization of this result. From a practical point of view, Theorem 5 holds for the user distributions are close to the deterministic case. Conditions (a) and (b) mean that the probability mass function of $\mathcal{N}$ should not spread evenly over its whole support, when mean number of users is large. Instead, it should be centered around the mean value, so that it is close to the deterministic SUs case.

In the secondary network, the feedback load between SUs and the BS will be increased significantly as $\lambda \to \infty$. One approach to reduce the feedback load is to replace the conventional MUD scheme with selective MUD (SMUD) proposed in [108, 109], in which only the qualified SUs with channel gain γ_{s_i} above a threshold

γ_{th} feedback their transmit CSI to BS. At each time slot, BS will select the SU with highest channel gain among all the qualified users. If there are no qualified users, the BS will select randomly among all $\mathcal{N}$ active SUs. Denote the number of SUs that satisfy both interference and feedback constraint as $\mathcal{N}_{\text{SMUD}}$, the ergodic capacity in SMUD scheme $\text{E}_{\mathcal{N}_{\text{SMUD}}}\left[\overline{C}(\rho, \mathcal{N}_{\text{SMUD}})\right]$ for a given γ_{th} can be expressed as,

$$\begin{aligned}\text{E}_{\mathcal{N}_{\text{SMUD}}}\left[\overline{C}(\rho, \mathcal{N}_{\text{SMUD}})\right] &= \text{E}_{\mathcal{N}}\left[\overline{C}(\rho, \mathcal{N}) \cdot (1 - P_o(\rho, \mathcal{N})) + \overline{C}(\rho) \cdot P_o(\rho, \mathcal{N})\right] \\ &= \text{E}_{\mathcal{N}}\left[\overline{C}(\rho, \mathcal{N})\right] - \text{E}_{\mathcal{N}}\left[\overline{C}(\rho, \mathcal{N}) \cdot P_o(\rho, \gamma_{\text{th}}, \mathcal{N}) - \overline{C}(\rho) \cdot P_o(\rho, \gamma_{\text{th}}, \mathcal{N})\right] \qquad (2.12)\end{aligned}$$

where $P_o(\rho, \gamma_{\text{th}}, \mathcal{N})$ is the probability that no SU satisfies feedback threshold γ_{th} among $\mathcal{N}$ SUs, and $\overline{C}(\rho) = \int_0^\infty \log(1 + \rho x) f_{\gamma_{\text{s}}}(x) dx$ is the averaged ergodic capacity of an arbitrary SU across fading. $\text{E}_{\mathcal{N}}\left[\overline{C}(\rho, \mathcal{N})\right]$ in (2.12) is the ergodic capacity in conventional MUD systems and $\text{E}_{\mathcal{N}}\left[\overline{C}(\rho, \mathcal{N}) \cdot P_o(\rho, \gamma_{\text{th}}, \mathcal{N}) - \overline{C}(\rho) \cdot P_o(\rho, \gamma_{\text{th}}, \mathcal{N})\right]$ in (2.12) can be shown to be non-negative, which implies that the conventional MUD scheme outperforms the SMUD scheme. This is reasonable since fewer SUs are involved in the SMUD scheme. In return, the feedback load in SMUD systems is significantly smaller than conventional MUD systems, so that there is a trade-off between the ergodic capacity performance and the feedback load. Furthermore, using equation (2.7) and (2.3), it can be shown that for a given threshold, γ_{th}, and average SNR ρ, $\text{E}_{\mathcal{N}_{\text{SMUD}}}\left[\overline{C}(\rho, \mathcal{N}_{\text{SMUD}})\right]$ scales like $\log(\log(\lambda))$ as $\lambda \to \infty$. The intuition is that as the mean number of SUs increases, outage probability $P_o(\rho, \gamma_{\text{th}}, \mathcal{N})$ decreases since it is more likely that γ_{s^*} is above the feedback threshold. As a result, $\text{E}_{\mathcal{N}}\left[\overline{C}(\rho, \mathcal{N}) \cdot P_o(\rho, \gamma_{\text{th}}, \mathcal{N}) - \overline{C}(\rho) \cdot P_o(\rho, \gamma_{\text{th}}, \mathcal{N})\right]$ becomes negligible as $\lambda \to \infty$. For small and moderate λ, we expect that the threshold γ_{th} will affect the ergodic capacity $\text{E}_{\mathcal{N}_{\text{SMUD}}}\left[\overline{C}(\rho, \mathcal{N}_{\text{SMUD}})\right]$ significantly and the performance/feedback load trade-off will be more apparent in this regime. However, since we are mainly concerned about large λ, we did not pursue the small/moderate λ regime in detail.

2.3.2 Binomial Distributed $\mathcal{N}$

In our proposed CR system, one possible mode of operation to select a desired user can be expressed as follows: choose the user set among L total users which satisfy the interference constraint $S = \{j \in 1, \ldots, L : \gamma_{\mathrm{p}_j} < Q\}$. Then choose the user index in S with the best channel gain γ_{s_i}. In another words, the user with highest γ_{s_i} which also satisfies the interference constraint will be selected. Recall that $\mathcal{N} = |S|$, the cardinality of S, which is the number of users satisfying the interference constraint, termed as successful users. Users will be said to be failures if they are not successful. If the interference test of each user is treated as an independent Bernoulli experiment, $\mathcal{N}$ is a binomial random variable. The success probability p of this binomial random variable can be represented as $F_{\gamma_{\mathrm{p}}}(Q)$, where $F_{\gamma_{\mathrm{p}}}(x)$ is the CDF of $|h_{\mathrm{p}}|^2$ which is i.i.d. across all SUs.

We use Bin(L,p) to denote the binomial distribution with L trials and success probability p. Since $\mathcal{N}$ users are chosen from L total users subject to an interference threshold Q, the random variable $\mathcal{N}$ follows Bin(L,$F_{\gamma_{\mathrm{p}}}(Q)$). Consequently, using (3) and substituting $F_{\gamma_{\mathrm{s}}}(x)$ in to the PGF of Bin(L,$F\gamma_{\mathrm{p}}(Q)$), the CDF of the channel gain of the selected user can be expressed as,

$$\begin{aligned} F_{\gamma_{\mathrm{s}}^*}(x) &= [1 - F_{\gamma_{\mathrm{p}}}(Q) + F_{\gamma_{\mathrm{p}}}(Q)F_{\gamma_{\mathrm{s}}}(x)]^L = [1 - p + p(1 - e^{-x})]^{\frac{\lambda}{p}} \\ &= (1 - pe^{-x})^{\frac{\lambda}{p}} \end{aligned} \tag{2.13}$$

where $p := F_{\gamma_{\mathrm{p}}}(Q)$ and $\lambda := Lp$ is the mean value of random variable $\mathcal{N}$. It can be verified that in this case $\Pr[\mathcal{N} = 0] = \binom{L}{0} p^0 (1-p)^{\frac{\lambda}{p}}$ and $\sigma_{\mathcal{N}}^2 = \lambda(1-p)$, which implies that (a) and (b) in Theorem 5 are satisfied. Therefore, (2.11) holds for the binomial case.

2.3.3 Negative Binomial Distributed $\mathcal{N}$

The number of SUs could follow discrete distributions other than binomial if different modes of operation are adopted. In the binomial case, the primary receiver performs an exhaustive search to find all active SUs among L total users. When L is large, this approach might require a long processing time to form the active SUs set S. We term the processing time as system delay, which is in proportion to the number of SUs which has been checked for interference constraint. An alternative is to decrease the system delay by selecting the desired user from a proper subset among all users whose interference are below the threshold.

For example, the BS can form the set S sequentially as follows. The BS selects all the active users before a predetermined number r failures occurs. In this case, $\mathcal{N}$ is NB distributed with parameter r and p, which is denoted as NB(r,p). There exists a trade-off between the time BS takes to form the set S and the secondary link performance, which can be balanced by the parameter r. In this case, system delay is a random variable and its mean value is in proportion to r.

CDF of the channel gain of the best user selected from a NB random set of users can be written as using (2.3) as:

$$F_{\gamma_{\mathrm{s}}^*}(x) = \frac{1}{(1+e^{-x}u)^r}, \tag{2.14}$$

where $u := F_{\gamma_{\mathrm{p}}}(Q)/(1-F_{\gamma_{\mathrm{p}}}(Q))$, $r := \lambda/u$. Similar to the binomial $\mathcal{N}$, the conditions of Theorem 5 are satisfied since $\Pr[\mathcal{N}=0] = \binom{r-1}{0}p^0(1-p)^r$ and $\sigma^2_{\mathcal{N}} = \lambda/(1-p)$, hence (2.11) also holds in the NB case.

2.3.4 Poisson-Binomial Distribution

In practical systems, SUs might not necessarily suffer an interference probability that is identical across all users. Therefore, the case where SUs have different $F_{\gamma_{\mathrm{p}_i}}(Q)$

is of interest. In this case, the number of active SUs follows a PB distribution, which is mathematically defined as the sum of non identically distributed independent Bernoulli random variables X_i so that

$$\Pr[X_i = 1] = p_i = 1 - \Pr[X_i = 0] > 0, \qquad i = 1, ..., L. \tag{2.15}$$

Let $\mathcal{W} = \sum_{i=1}^{L} X_i$ be the number of the active users among total SUs, then $\mathcal{W}$ will have a PB distribution. It is verified in Appendix C that condition (a) and (b) are also satisfied in this case, so that (2.11) holds. Furthermore, this user distribution will be studied in Section 2.5 and approximated by the Poisson distribution when $F_{\gamma_{\mathrm{p}_i}}(Q)$ is small and all X_i are independent.

2.4 Outage Probability and Average Bit Error Rate

2.4.1 Outage Probability

The randomness of the number of active SUs arise from the selection of a desired SU according to their interference temperature at the primary receiver. Hence, how rapidly $\mathcal{N}$ varies with time depends on the rapidity fading h_{p_i} over the interference channel. When h_{s_i} and h_{p_i} both remain constant over the transmission duration of a codeword, the system is experiencing slow fading. Outage probability is an appropriate metric for slowly varying channels. The expression of the outage probability at average SNR ρ, and a desired transmit rate R is defined as:

$$\mathrm{P}_{\mathrm{out}}(\rho, R) := \Pr\left[\log(1 + \rho\gamma_{\mathrm{s}}^*) < R\right], \tag{2.16}$$

where γ_{s}^* is defined in (2.2). Recalling that $\mathcal{N} = |S|$, the cardinality of the active set S, we can express (2.16) as:

$$\mathrm{P}_{\mathrm{out}}(\rho, R) = \Pr\left[\gamma_{\mathrm{s}}^* < \frac{2^R - 1}{\rho}\right] = U_{\mathcal{N}}\left(F_{\gamma_{\mathrm{s}}}\left(\frac{2^R - 1}{\rho}\right)\right) \tag{2.17}$$

using (2.3). It is clear that by comparing (2.17) for different user distributions, outage probability $\mathrm{P}_{\mathrm{out}}(\rho, R)$ can be ordered at every value of ρ and R based on comparing their PGFs, also known as Laplace transform ordering. A similar property will be observed for the average BER metrics in Sections 2.3 and 2.4.2, by using this LT ordering approach introduced in Section 2.2.2.

2.4.2 Average Bit Error Rate

Average bit error rate is another key performance metric. The error rate at average SNR ρ averaged over the fading and users distribution is given by

$$\mathrm{E}_{\mathcal{N}}\left[\overline{\mathrm{P}}_{\mathrm{e}}(\rho, \mathcal{N})\right] = \mathrm{E}_{\mathcal{N}}\left[\int_0^{\infty} \mathrm{P}_{\mathrm{e}}(\rho x) dF_{\gamma_{\mathrm{s}}}^N(x)\right] \tag{2.18}$$

where $\mathrm{P}_{\mathrm{e}}(\rho x)$ is the instantaneous error rate over an AWGN channel for an instantaneous SNR ρx. $\mathrm{P}_{\mathrm{e}}(\rho x)$ is often approximated to have the form of $\mathrm{P}_{\mathrm{e}}(\rho x) = \alpha e^{-\eta \rho x}$, where α and η can be chosen to capture different modulation schemes. Other variations such as $\mathrm{P}_{\mathrm{e}}(\rho x) = \alpha Q(\sqrt{\eta \rho x})$ is also adopted in literature [110].

To see that $\overline{\mathrm{P}}_{\mathrm{e}}(\rho, N)$ is a c.m. function in N, consider the k^{th} derivative

$$\frac{\partial^k \overline{\mathrm{P}}_{\mathrm{e}}(\rho, N)}{\partial N^k} = \rho \int_0^{\infty} B(\rho x) F_{\gamma_{\mathrm{s}}}^N(x) \left[\log\left(F_{\gamma_{\mathrm{s}}}(x)\right)\right]^k dx, \tag{2.19}$$

where we define $B(x) = -d\mathrm{P}_e(x)/dx$. Since $\mathrm{P}_{\mathrm{e}}(\rho x)$ is decreasing in x for any $\rho > 0$ and $\log\left(F_{\gamma_{\mathrm{s}}}(x)\right) \leq 0$, the derivative in (2.19) alternates in sign as k incremented and satisfies the definition in (2.4). Consequently, $\overline{\mathrm{P}}_{\mathrm{e}}(\rho, N)$ is a c.m. function of N. In Section 2.6, this c.m. property along with Theorem 1 will be used to show that stochastic order on a pair of user distributions can be shown to order the average bit error rate under those user distributions. In particular, $\overline{\mathrm{P}}_{\mathrm{e}}(\rho, N)$ being a c.m. function of N means that (2.19) is negative for $k = 1$ and positive for $k = 2$, and consequently $\overline{\mathrm{P}}_{\mathrm{e}}(\rho, N)$ is a convex decreasing function of N. For the case that the

number of users in the system is random, by applying Jensen's inequality, we have,

$$\mathrm{E}_{\mathcal{N}}\left[\overline{\mathrm{P}}_{\mathrm{e}}(\rho,\mathcal{N})\right] \geq \overline{\mathrm{P}}_{\mathrm{e}}(\rho,\lambda), \tag{2.20}$$

where $\lambda := \mathrm{E}[\mathcal{N}]$. Therefore, randomization of the number of users always deteriorates the average error rate performance of a multiple SUs CR systems. In Section 2.5.2 we will show that the Jensen's inequality in (2.20) is tight for large λ and Poisson $\mathcal{N}$.

2.4.3 Binomial Distributed $\mathcal{N}$

In Section 2.3.2, we derived the CDF of the channel gain of the best user chosen from a binomial distributed random set of users. Here we take derivative of (2.3) with respect to x so that the PDF of the channel gain of the best user in the binomial case can be expressed as:

$$f_{\gamma_{\mathrm{s}}^*}(x) = \frac{dF_{\gamma_{\mathrm{s}}^*}(x)}{dx} = \lambda e^{-x}(1-e^{-x}p)^{\frac{\lambda}{p}-1}, \qquad x>0. \tag{2.21}$$

where we recall that $p := F_{\gamma_{\mathrm{p}}}(Q)$. Assuming the instantaneous error rate has the form $\mathrm{P}_{\mathrm{e}}(\rho x) = \alpha e^{-\eta\rho x}$, substituting (2.21) into (2.18) we get:

$$\mathrm{E}_{\mathcal{N}}\left[\overline{\mathrm{P}}_{\mathrm{e}}(\rho,\mathcal{N})\right] = \int_0^\infty \alpha e^{-\eta\rho x} e^{-x}(1-e^{-x}p)^{\frac{\lambda}{p}-1}dx \quad = \alpha p^{-1-\eta\rho}\lambda\beta\left(p, 1+\eta\rho, \frac{\lambda}{p}\right) \tag{2.22}$$

where the incomplete beta function is defined as $\beta\left(x,a,b\right) = \int_0^x y^{a-1}(1-y)^{b-1}dy$. Note that when $p=1$ in (2.22), every SU satisfies the interference constraints, in which case $\mathcal{N}$ is deterministic. In this specific case, (2.22) equals $\alpha\lambda B(1+\eta\rho,\lambda)$, which can be shown as the average BER under deterministic number of active users. Here $B(1+\eta\rho,\lambda) = \beta\left(1,1+\eta\rho,\lambda\right)$ is the beta function.

2.4.4 Negative Binomial Distributed $\mathcal{N}$

In Section 2.3.3, we derived the CDF of the channel gain of the best user chosen from a NB distributed set of users. The PDF of the channel gain of the best user in the NB case can be expressed as:

$$f_{\gamma_s^*}(x) = \frac{dF_{\gamma_s^*}(x)}{dx} = rue^{-x}(1+ue^{-x})^{-1-r}, \qquad x > 0. \tag{2.23}$$

where r is the parameter of the NB distribution and $u = p/(1-p)$. Assuming that the instantaneous error rate has the form $\mathrm{P_e}(\rho x) = \alpha e^{-\eta\rho x}$, substituting (2.23) into (2.18) we can get:

$$\begin{aligned} \mathrm{E}_{\mathcal{N}}\left[\overline{\mathrm{P}}_{\mathrm{e}}(\rho,\mathcal{N})\right] &= \int_0^\infty \alpha e^{-\eta\rho x} rue^{-x}(1+ue^{-x})^{-1-r}dx \\ &= \frac{ru\alpha}{1+\eta\rho}{}_2F_1\left(1+r, 1+\eta\rho, 2+\eta\rho, -u\right) \end{aligned} \tag{2.24}$$

where ${}_2F_1\left(a,b,c,z\right)$ is Gauss's hyper geometric function. As number of failures r is incremented, average BER performance improves. However, for increased r, the time BS takes to form set S will also be increased, so that one can balance the performance and delay trade off by adjusting the r parameter.

2.5 Non-homogeneous Interference Probability and Poisson Approximation

We have introduced in Section 2.1 that the interference test of each SU is treated as an independent Bernoulli experiment with success probability $F_{\gamma_p}(Q)$. In this section, the interference model will be generalized to the non-i.i.d case, in which the number of active SUs results in a PB distribution following the definition in Section 2.3.4. Since it is mathematically complicated to calculate the ergodic capacity and average BER of the SU system in this case, a Poisson approximation will be utilized to approximate PB distribution.

2.5.1 Poisson Approximation

In this section, we will bound the error between the ergodic capacity under Poisson and PB $\mathcal{N}$ to show that as the PB distribution converges to Poisson distribution, the ergodic capacity $\mathrm{E}_{\mathcal{N}}\left[\overline{C}(\rho,\mathcal{N})\right]$ under PB $\mathcal{N}$ also converges to the ergodic capacity at the Poisson case.

Following the definition in Section 2.3.4 then $\mathcal{W}$ will have a distribution that is approximately Poisson with mean $\lambda = \sum_{i=1}^{L} p_i$. This approximation will hold if $F_{\gamma_{\mathrm{p}_i}}(Q)$ is small and all X_i are independent. We will now make this rigorous and bound the error between the ergodic capacity under a PB user distribution $\mathcal{W}$ and its corresponding Poisson approximated $\mathcal{N}$ [111]. First, consider the following theorem by Le Cam [111]:

Theorem 6. *$X_1, \ldots, X_i$ are independent random variables, each with a Bernoulli distribution of parameter p_i. $Pr[X_i = 1] = p_i$ for all $i = 1, \ldots, L$, i.e. $\mathcal{W} = \sum_{i=0}^{\infty} X_i$ approximately follows a PB distribution. We have*

$$\sum_{k=0}^{\infty} \left| Pr[\mathcal{W} = i] - \frac{e^{-\lambda}\lambda^i}{i!} \right| \leq 2 \sum_{i=1}^{L} {p_i}^2, \qquad i = 1, 2, \ldots, L \tag{2.25}$$

where $\lambda = \sum_{i=1}^{L} p_i$.

Using Theorem 6, we will bound the gap between the ergodic capacity under PB and Poisson distributions, which is denoted as Δ_C. We have:

$$\begin{aligned} \Delta_C &= \left| \mathrm{E}_{\mathcal{W}}\left[\overline{C}(\rho,\mathcal{W})\right] - \mathrm{E}_{\mathcal{N}}\left[\overline{C}(\rho,\mathcal{N})\right] \right| = \left| \sum_{i=1}^{L} \overline{C}(\rho,i) \left(\Pr\left[\mathcal{W} = i\right] - \frac{e^{-\lambda}\lambda^i}{i!} \right) \right| \\ &\leq \sum_{i=1}^{L} \overline{C}(\rho,i) \left| \left(\Pr\left[\mathcal{W} = i\right] - \frac{e^{-\lambda}\lambda^i}{i!} \right) \right| \end{aligned} \tag{2.26}$$

Since $\overline{C}(\rho, i)$ is increasing in i, and $\overline{C}(\rho, L) = O(\log\log L)$ as we mentioned in Section 2.3.1, applying (2.25) we have:

$$\Delta_C = O\left(\log\log L \sum_{i=1}^{L} p_i^2\right) \tag{2.27}$$

where $i = 1, 2, \ldots, L$. As long as $\sum_{i=1}^{L} p_i^2 = o(1/(\log\log L))$, the error between the capacity under PB and Poisson distributions goes to zero as $L \to \infty$.

For a special case consider $p_i = \lambda/L$ for $i = 1, 2, \ldots, L$, in which all the SUs have i.i.d. interference channels, $\mathcal{W}$ follows a binomial distribution. In this case, we have

$$\Delta_C = O\left(\frac{\lambda^2}{L}\log\log L\right) \tag{2.28}$$

Obviously, as $L \to \infty$ and $p \to 0$, Δ_C approaches zero. Consequently, the gap between the binomial and the approximated Poisson capacity is shown to be negligible as total number of users grows large and the interference probability is sufficiently small. This will be illustrated numerically in Section 2.7.

2.5.2 Tightness in the Jensen's Inequality in the Average BER

Since in Section 2.5 we proved that Poisson distribution can be utilized to precisely approximate PB distribution, it is of interest to study the average BER under Poisson $\mathcal{N}$. In Section 2.4.2, we proved that the average BER $\overline{\mathrm{P}}_{\mathrm{e}}(\rho, N)$ is a completely monotonic function of N, which implies the convexity. Applying the Jensen's inequality, we have (2.20).

We now provide sufficient conditions for Jensen's inequality involving $\overline{\mathrm{P}}_{\mathrm{e}}(\rho, N)$ to be asymptotically tight for large λ. Recall that $\overline{\mathrm{P}}_{\mathrm{e}}(\rho, N)$ is the error rate averaged over the channel distribution for deterministic number of users N. To this end, we use [112, Theorem 2.2] which were derived in a networking context for arbitrary *c.m.* functions.

Theorem 7. *Let $\overline{P}_{\mathrm{e}}(\rho, N)$ be c.m. and regularly varying at $N = \infty$ and consider the error rate averaged across the channel and the users $E_{\mathcal{N}}\left[\overline{P}_{\mathrm{e}}(\rho, \mathcal{N})\right]$, where $\mathcal{N}$ is a Poisson distributed random variable with mean λ. Then,*

$$E_{\mathcal{N}}\left[\overline{P}_{\mathrm{e}}(\rho, \mathcal{N})\right] = \overline{P}_{\mathrm{e}}(\rho, \lambda) + O\left(\overline{P}_{\mathrm{e}}(\rho, \lambda)/\lambda\right) \tag{2.29}$$

as $\lambda \to \infty$.

Equation (2.29) shows that as $\lambda \to \infty$, the difference between the error rate averaged across the user distribution and the error rate evaluated at the average number of users vanishes as λ tends to ∞. This implies that for sufficiently large λ the performance of the MUD systems with random number of users will be almost equal to the performance of the MUD systems with a deterministic number of users with the number of users equal to λ.

To apply Theorem 7 we require $\overline{\mathrm{P}}_{\mathrm{e}}(\rho, N)$ to be c.m. and regularly varying. We have already shown in Section 2.4.2 that $\overline{\mathrm{P}}_{\mathrm{e}}(\rho, N)$ is always completely monotonic in N. Next, we provide the conditions under which $\overline{\mathrm{P}}_{\mathrm{e}}(\rho, N)$ is a regularly varying function of N. Consider

$$\overline{\mathrm{P}}_{\mathrm{e}}(\rho, N) = \rho \int_0^\infty B(\rho x) e^{N \log F_{\gamma_{\mathrm{s}}}(x)} dx \tag{2.30}$$

where $B(\cdot)$ is defined as $B(x) = -d\mathrm{P}_e(x)/dx$. Now, setting $u := -\log(F_{\gamma_{\mathrm{s}}}(x))$, and integrating by substitution we have,

$$\overline{\mathrm{P}}_{\mathrm{e}}(\rho, N) = \rho \int_0^\infty \frac{B(\rho F_{\gamma_{\mathrm{s}}}^{-1}(e^{-u}))e^{-u}e^{-uN}du}{f_{\gamma_{\mathrm{s}}}(F_{\gamma_{\mathrm{s}}}^{-1}(e^{-u}))}, \tag{2.31}$$

where $F_{\gamma_{\mathrm{s}}}^{-1}(x)$ is the inverse CDF and $f_{\gamma_{\mathrm{s}}}(x)$ is the PDF of γ_{s}. We now establish the sufficient conditions for $\overline{\mathrm{P}}_{\mathrm{e}}(\rho, N)$ to be a regularly varying function of N:

Theorem 8. *If $\overline{P}_{\mathrm{e}}(\rho, N)$ is c.m. in N, a sufficient condition for it to be regularly varying at $N = \infty$ is that, $t(u) := \rho(B(\rho F_{\gamma_{\mathrm{s}}}^{-1}(e^{-u}))e^{-u})/(f_{\gamma_{\mathrm{s}}}\left(F_{\gamma_{\mathrm{s}}}^{-1}(e^{-u})\right))$ is regularly varying at $u = 0$.*

Proof. By comparing the representation of $\overline{\mathrm{P}}_{\mathrm{e}}(\rho, N)$ in (2.31) with the Bernstein's representation of c.m. functions discussed after (2.4), it can be seen that (2.31) can be represented as the Laplace transform of $t(u)$. Using Theorem 2, the proof follows. □

Theorem 8 shows that for the conclusions of Theorem 7 to hold (i.e., Jensen's inequality to be asymptotically tight), the CDF of the single-user channel $F_{\gamma_{\mathrm{s}}}(x)$, and the error rate expression $\mathrm{P}_{\mathrm{e}}(\rho x)$ have to jointly satisfy the regular variation condition given in Theorem 8. Next, we examine whether this condition holds for commonly assumed instantaneous error rates $\mathrm{P}_{\mathrm{e}}(\rho x)$ with γ_{s} being exponentially distributed. For the case of $\mathrm{P}_{\mathrm{e}}(\rho x) = \alpha e^{-\eta\rho x}$, we have $t(u) = \alpha\rho(1-e^{-u})^{\eta\rho-1}e^{-u}$, which satisfies $\lim_{u\to 0} t(\kappa u)/t(u) = \kappa^{\eta\rho-1}$, therefore proving the regular variation of $t(u)$ at 0. By using Theorem 2 this in turn proves regular variation of $\overline{\mathrm{P}}_{\mathrm{e}}(\rho, N)$ at $N = \infty$. Therefore $\overline{\mathrm{P}}_{\mathrm{e}}(\rho, N)$ is both a c.m. and a regularly varying function of N for this case. Consequently, when $\mathrm{P}_{\mathrm{e}}(\rho x) = \alpha e^{-\eta\rho x}$ and the fading is Rayleigh (i.e. channel gain is exponential), the difference in error rate performance of a MUD system with a random number of users averaged over the number of users distribution and of a deterministic number users approaches zero for sufficiently large λ, as in Theorem 7.

Consider now $\mathrm{P}_{\mathrm{e}}(\rho x) = \alpha Q(\sqrt{\eta\rho x})$, with γ_{s} being exponentially distributed. The error rate can be expressed as,

$$\begin{aligned}
\overline{\mathrm{P}}_{\mathrm{e}}(\rho, N) &= \alpha \int_0^\infty Q\left(\sqrt{\eta\rho x}\right) dF_{\gamma_{\mathrm{s}}}^N(x) \\
&= \alpha\, Q(\sqrt{\eta\rho x}) F_{\gamma_{\mathrm{s}}}^N(x)\big|_0^\infty - \alpha \int_0^\infty F_{\gamma_{\mathrm{s}}}^N(x) dQ(\sqrt{\eta\rho x}) \\
&= 0 - \alpha \int_0^\infty F_{\gamma_{\mathrm{s}}}^N(x) dQ(\sqrt{\eta\rho x}) = \frac{\alpha\sqrt{\eta\rho}}{2\sqrt{2\pi}} \int_0^\infty \frac{e^{N\log\left(1-e^{-x}\right)} e^{-\eta\rho x/2}}{\sqrt{x}} dx, \quad (2.32)
\end{aligned}$$

where the second equality is obtained by integration by parts. Once again, by setting $u = -\log(1-e^{-x})$ we can rewrite (2.32) as,

$$\overline{\mathrm{P}}_{\mathrm{e}}(\rho, N) = \frac{\alpha\sqrt{\eta\rho}}{2\sqrt{2\pi}} \int_0^\infty \exp(-Nu)\,(1-e^{-u})^{\eta\rho/2-1} \frac{e^{-u}}{\sqrt{-\log(1-e^{-u})}} du. \tag{2.33}$$

Thus we have $t(u) = \alpha\sqrt{\eta\rho}(1-e^{-u})^{\eta\rho/2-1}e^{-u}/(2\sqrt{-2\pi\log(1-e^{-u})})$ and it can be shown that $\lim_{u\to 0} t(\kappa u)/t(u) = \kappa^{\eta\rho/2-1}$, therefore once again proving that $\overline{\mathrm{P}}_{\mathrm{e}}(\rho, N)$ is both a c.m. and a regularly varying function of N. Having verified the conditions of Theorem 8 for $\mathrm{P}_{\mathrm{e}}(\rho x) = \alpha Q(\sqrt{\eta\rho x})$ with γ_{s} being exponentially distributed, we conclude the tightness of Jensen's inequality as suggested by Theorem 7.

2.6 Laplace Transform Ordering of User Distributions

We know from Jensen's inequality that a deterministic number of SUs will always outperform a random number of SUs both for average BER and ergodic capacity. Moreover, different random SU distributions can also be ordered among themselves. In this section, we introduce Laplace transform (LT) ordering, a method to compare the effect that different user distributions has on the average error rate, ergodic capacity, or other metrics that are either c.m. or c.m.d. in the number of active users. From [105] we know that ergodic capacity is c.m.d. and averaged BER is c.m.. Consequently, Theorem 1 implies that if the number of users is from a distribution that can be ordered in the LT sense, then both the average error rate and capacity can be ordered at every value of SNR ρ.

Theorem 9. *Let $\mathcal{X}$ denote a Poisson random variable with parameter λ, $\mathcal{Y}$ denotes a binomial random variable with mean value Lp, and $\mathcal{Z}$ denote a NB random variable with mean value $rp/(1-p)$, and $\mathcal{W}$ denote a PB random variable defined in Theorem 6. By assuming equal mean for all distributions, that is $Lp = \lambda = rp/(1-p) = \sum_{i=1}^{L} p_i$,*

we have $U_{\mathcal{Z}}(z) \geq U_{\mathcal{X}}(z) \geq U_{\mathcal{Y}}(z) \geq U_{\mathcal{W}}(z)$*, for* $0 \leq z \leq 1$*. In other words*

$$\mathcal{Z} \leq_{\mathrm{Lt}} \mathcal{X} \leq_{\mathrm{Lt}} \mathcal{Y} \leq_{\mathrm{Lt}} \mathcal{W}. \tag{2.34}$$

Proof. See Appendix B. □

It can be observed that for the extreme case that when parameter $p = 1$, binomial user distribution converges to the deterministic number of users, which dominates any kind of random distributions with the same mean value under LT ordering sense. PB user distribution also subsumes deterministic case when p_i are either 1 or 0. Moreover, due to Theorem 1, if the SU distributions are ordered in LT sence, any c.m. (c.m.d.) performance metric of N will also be ordered. Hence, without calculating or deriving the closed form expression, system performance can be compared after knowing the corresponding user distributions.

2.7 Simulations

An uplink CR system with multiple SUs where both SUs and BS having a single antenna is considered. In this section, using Monte-Carlo simulations, ergodic capacity and averaged BER are simulated to corroborate our analytical results. For all simulations, Rayleigh fading channels are assumed.

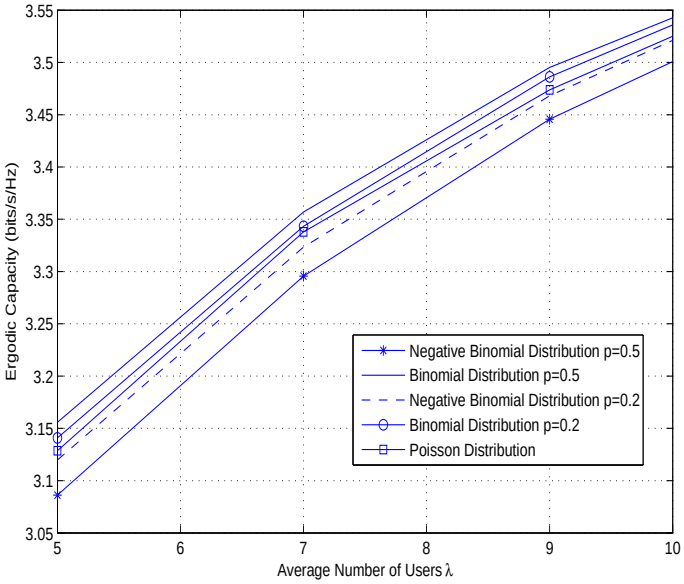

Figure 2.2: Ergodic Capacity Under Different User Distributions.

In Section 2.3.2 and 2.3.3, ergodic capacity performances under binomial and NB user distributions are established. In Figure 2.2, ergodic capacity is plotted versus $\lambda = \mathrm{E}[\mathcal{N}]$ for different user distributions. It can be seen that for a given user distribution, the ergodic capacity improves with average number of users. Also, in Section 2.6, these two distributions are compared with the Poisson distribution in LT ordering sense. In Figure 2.2, for a given λ, binomial user distribution yields better ergodic capacity performance than Poisson, followed by NB user distribution. Furthermore, NB distribution converges to the Poisson distribution as the trial probability $p \to 0$ and stopping parameter $r \to \infty$, and the binomial distribution also converges towards the Poisson distribution as the number of trials goes to infinity and the product Lp remains fixed. It can be seen from Figure 2.2 that for a fixed λ, when the trial probability p varies from 0.5 to 0.2, ergodic capacity of binomial and NB cases converge to the Poisson case.

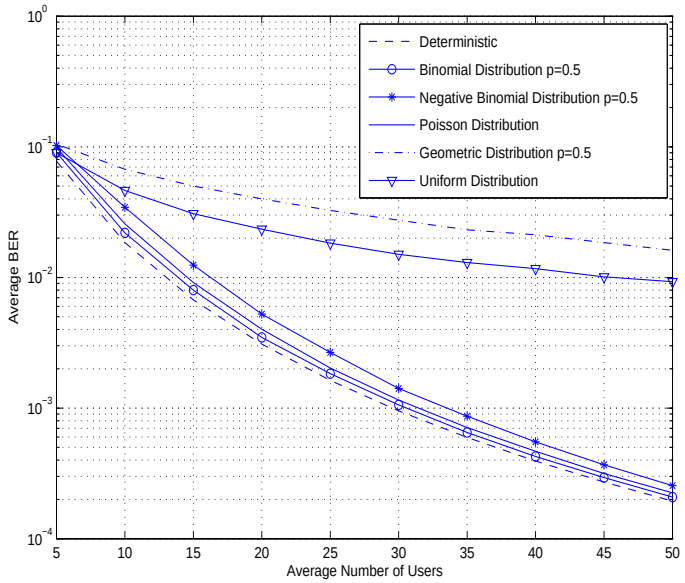

Figure 2.3: Average BER Under Different User Distributions.

In Section 2.4.3 and 2.4.4, we derived closed form expressions for averaged BER under binomial and NB user distributions. It can be observed that any kind of random user distribution will deteriorate the average BER performance compared with the fixed number of users case. As we introduced in Section 2.2.2, $\overline{\mathrm{P}}_{\mathrm{e}}(\rho, N)$ is c.m. in N and if $\mathcal{Z} \leq_{\mathrm{Lt}} \mathcal{X} \leq_{\mathrm{Lt}} \mathcal{Y}$, we have $\mathrm{E}_{\mathcal{Z}}\left[\overline{\mathrm{P}}_{\mathrm{e}}(\rho, \mathcal{Z})\right] \geq \mathrm{E}_{\mathcal{X}}\left[\overline{\mathrm{P}}_{\mathrm{e}}(\rho, \mathcal{X})\right] \geq \mathrm{E}_{\mathcal{Y}}\left[\overline{\mathrm{P}}_{\mathrm{e}}(\rho, \mathcal{Y})\right]$, $\forall \rho$. As shown in Figure 2.3, average BER performances under are plotted against $\lambda = \mathrm{E}[\mathcal{Z}] = \mathrm{E}[\mathcal{X}] = \mathrm{E}[\mathcal{Y}]$. Here, $\mathcal{Z}$ is NB, $\mathcal{X}$ is Poisson, and $\mathcal{Y}$ is binomial distributed. With same mean number of users, average BER under binomial $\mathcal{Y}$ always outperforms Poisson $\mathcal{X}$ and NB $\mathcal{Z}$. Additionally, when λ is fixed, BER performance under binomial and NB cases converge to Poisson case as p is decreased from 0.5 to 0.2. Moreover, BER performance under geometric and uniform $\mathcal{N}$ are simulated to show that more discrete distributions can be ordered in LT ordered sense.

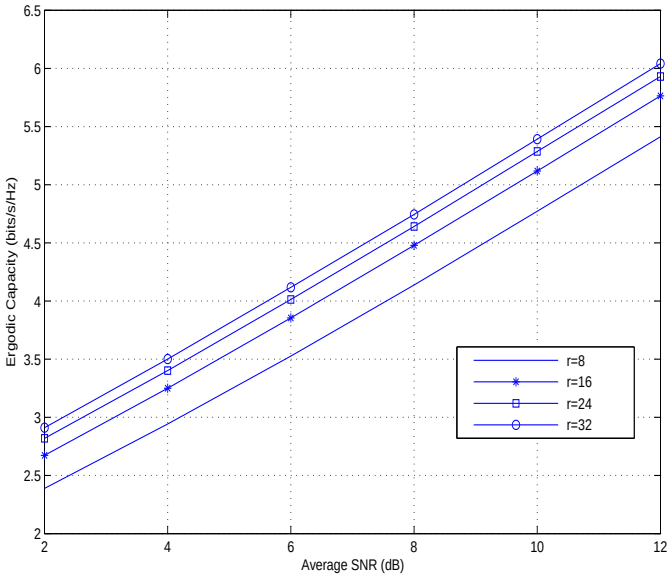

Figure 2.4: Ergodic Capacity of NB $\mathcal{N}$ with Different r.

In Section 2.3.3, we mentioned that in NB case, the trade-off between performance and system delay can be balanced by a choice of the parameter r. As shown in Figure 2.4, for a given average SNR, ergodic capacity under different values of parameter r are simulated. It can be observed that as r increases from 8 to 32, the ergodic capacity performance is increased only approximately 20%. However, the average system delay when $r = 32$ is four times as much as $r = 8$. Hence there are diminishing returns in capacity as the delay parameter is increased.

In Section 2.5, we discussed a non-homogeneous interference setup, which results in a Poisson-binomial $\mathcal{N}$. In Figure 2.5, the average BER of Poisson-binomial $\mathcal{N}$ with different L are plotted versus the mean number of SUs λ, and compared with the average BER of Poisson $\mathcal{N}$. It can be observed that the average BER of Poisson-binomial case is always better than that of the Poisson case, which has been proved mathematically in Section 2.6 in Laplace transform ordering sense. Practically, when $\mathcal{N}$ is PB distributed, interference probability p_i of each SU is no longer identical. One

extreme situation of this PB case is when some SUs violate interference constraint with $p_i = 1$, and the rest of the SUs always satisfy the interference constraint, which is equivalent to the deterministic N case. Another extreme situation is when p_i is identical to each SU, this PB is equivalent to binomial case. Hence, PB case should outperform Poisson case as we observed from the figure. Moreover, we suggested in Section 2.5.1 that PB is a good approximation of Poisson $\mathcal{N}$ for a fixed mean value λ, as $L \to \infty$. It can been seen that as L increases from 20 to 60, the average BER of Poisson-binomial curve approaches the Poisson curve.

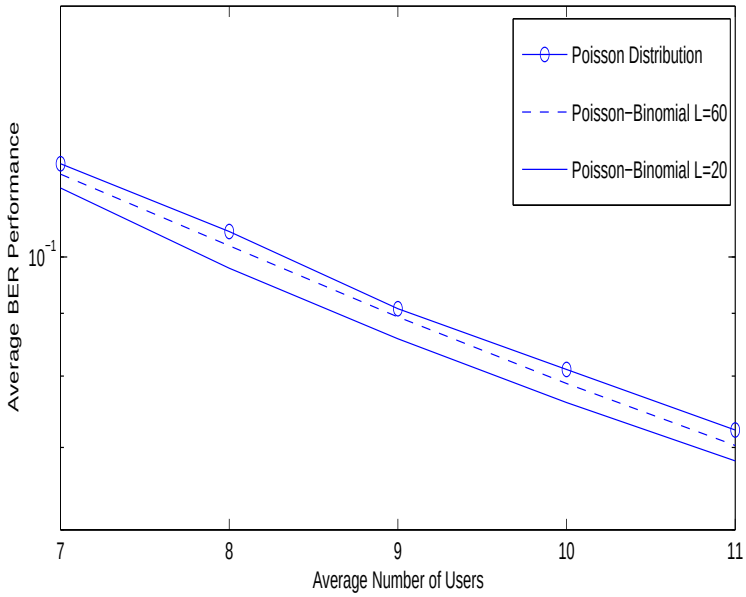

Figure 2.5: Average BER Under PB and Poisson User Distributions.

Chapter 3

FUNDAMENTAL PERFORMANCE TRADE-OFF BETWEEN PU AND SU IN COOPERATIVE COGNITIVE RADIO SYSTEMS

In this chapter, a relay-aided cooperative underlay CR system with an instantaneous interference constraint at the PR is considered. When the PU is active, those SUs whose interference at the PR is above a threshold will amplify-and-forward (AF) PU's signal to enhance its performance, while those SUs below this threshold will proceed with their own transmission in an underlay fashion. Opportunistic relay selection and underlay MUD are applied in the primary and secondary networks respectively. As the number of relay SUs increases, the PU's performance is improved which causes degradation of SU's performance concurrently. With our novel overall average BER and the sum achievable rate metrics, we quantify this fundamental performance trade-off mathematically in the large number of SUs regime. This is then followed by a derivation of the optimal ratio in closed form between the number of relaying and underlay SUs to optimize the overall system performance as a function of statistics of the fading links.

3.1 System Model

3.1.1 Access Strategy

As shown in Figure 3.1, we consider an uplink CR system with $L = M + N$ SUs, a single PU, a primary receiver (PR), and one secondary receiver (SR). The transmitters and receivers are assumed to be equipped with a single antenna.

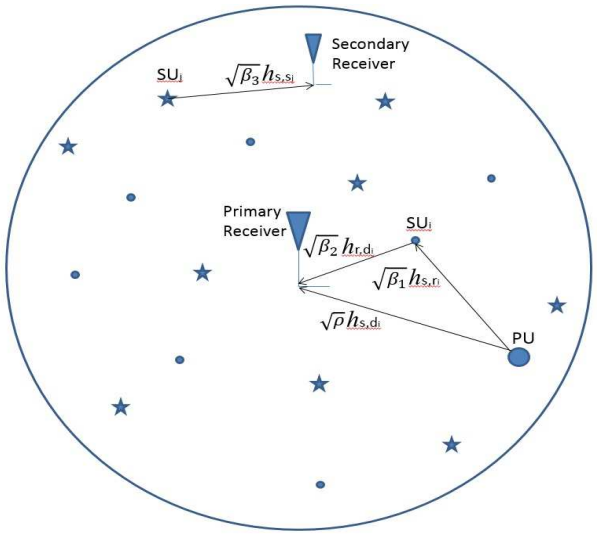

Figure 3.1: System Model of Proposed Cooperative CR System

We assume that at the beginning of each transmission block, SUs will decide their access mode in the transmission phase by estimating their interference temperature at the PR with the knowledge of the interference channel through feedback [113], and comparing with a threshold. M SUs below the threshold will enter the underlay mode and transmit to the SR in a MUD fashion, where only a single SU with the highest transmission SNR will be selected to communicate. N SUs above the interference threshold will serve as relays to the PU in order to compensate for the limited interference caused by the selected underlay SU at the PR. An opportunistic relay technique is applied among N SUs where only the best relay path is selected to relay at each time slot.

Due to the MUD scheme among M underlay SUs and the independence between the SU-SR channel and the SU-PR interference channel, only a single underlay SU will be selected to transmit whose interference temperature satisfies the threshold at the PR. This scheme enables the system to trade off between primary and secondary network performance with flexibility by adjusting the values of N and M. Our novel combined metrics enable us to mathematically quantify the performance trade-off

between the PU and SU networks for the first time in the literature. More specifically, we will show that if the average SNR of the PU to PR channel is poor, large number of relays is preferred to enhance the PU network quality; and when the underlay SUs experience deep fading, more SUs should be included in the MUD.

3.1.2 Description of the Relay Selection

The opportunistic relay selection is implemented at the primary network. A single SU out of the N SUs will be selected, depending on which SU relay provides the largest end-to-end path gain between the PU and the PR. We adopt the cooperative diversity model in [114] so that during the first half of the transmission block, PU broadcasts its signal, and SUs and the PR receive it. In the second half, the selected SU relay the received signal to the PR, and the PR combines two copies using maximum ratio combining (MRC). Similar to [115, 116], we assume that the knowledge of the relay and directed channels have been acquired by the PR.

The received signal at the PR and the i^{th} SU in the first half of the block can be expressed as,

$$y^1_{\mathrm{PR}} = \sqrt{\beta_1} h_{\mathrm{PU,PR}} x_{\mathrm{PU}} + n^1_{\mathrm{PR}}, \tag{3.1}$$

$$y_{\mathrm{SU}_i} = \sqrt{\beta_2} h_{\mathrm{PU,SU}_i} x_{\mathrm{PU}} + n_{\mathrm{SU}_i}, \qquad i = 1, 2, \ldots, N, \tag{3.2}$$

where $h_{\mathrm{PU,PR}}$ and $h_{\mathrm{PU,SU}_i}$ denote the channel coefficients from the PU to the PR and PU to the i^{th} SU, x_{PU} is the transmitted symbol from PU, n^1_{PR} and n_{SU_i} are the additive white Gaussian noise (AWGN) at the PR and i^{th} SU relay in the first half of the block respectively. In the second half of the transmission block, we model the received signal at the PR as:

$$y^2_{\mathrm{PR}} = \sqrt{\beta_3} A h_{\mathrm{SU}_i,\mathrm{PR}} x_{\mathrm{SU}_i} + n^2_{\mathrm{PR}}, \tag{3.3}$$

where $h_{\mathrm{SU}_i,\mathrm{PR}}$ denotes the channel coefficient from the i^{th} SU relay to the PR, x_{SU_i} is the transmitted signal from the i^{th} relay. n^2_{PR} is the AWGN at the PR. In this chapter, all the links are assumed to be Rayleigh fading. $h_{\mathrm{PU,PR}}$, $h_{\mathrm{PU,SU}_i}$, and $h_{\mathrm{SU}_i,\mathrm{PR}}$ are complex Gaussian random variables with zero mean and unit variance. The variances of x_{PU}, x_{SU_i}, n^1_{PR}, n^2_{PR} and n_{SU_i} are normalized to 1. β_i are the average SNR on each fading link. The received SNR of the direct link is $\gamma_{\mathrm{D}} = \beta_1 |h_{\mathrm{PU,PR}}|^2$, and the received SNR on the i^{th} SU relay path can be expressed as $\gamma_{\mathrm{P,S}_i} = \beta_2 |h_{\mathrm{PU,SU}_i}|^2$ and $\gamma_{\mathrm{S}_i,\mathrm{P}} = \beta_3 |h_{\mathrm{SU}_i,\mathrm{PR}}|^2$. $A = \sqrt{1/(\beta_2 \gamma_{\mathrm{P,S}_i} + 1)}$ is the amplification factor at the i^{th} SU, which maintains constant average power output [114]. By using equation (6) in [116], the received SNR of the opportunistic relay is derived as

$$\gamma^*_{\mathrm{R}} = \max_{1 \le i \le N} \frac{\gamma_{\mathrm{P,S}_i} \gamma_{\mathrm{S}_i,\mathrm{P}}}{1 + \gamma_{\mathrm{P,S}_i} + \gamma_{\mathrm{S}_i,\mathrm{P}}}. \tag{3.4}$$

3.1.3 SU's Underlay Transmission

According to the access strategy described in 3.1.1, when M SUs satisfy the interference constraint at the PR, only one SU among all M SUs with the highest received SNR at the SR will be selected to transmit. The received signal at the SR from the j^{th} SU can be expressed as:

$$y_{\mathrm{SR}} = \sqrt{\beta_4} h_{\mathrm{SU}_j,\mathrm{SR}} x_{\mathrm{SU}_j} + n_{\mathrm{SR}}, \qquad j = 1, 2, \ldots, M, \tag{3.5}$$

where $h_{\mathrm{SU}_j,\mathrm{SR}}$ denotes the channel coefficient from the j^{th} SU to the SR, x_{SU_j} is the transmitted symbol, n_{SR} is the AWGN at the SR. $h_{\mathrm{SU}_j,\mathrm{SR}}$ and n_{SR} have the same distribution as $h_{\mathrm{PU,PR}}$ and n^1_{PR} in the primary network. The channel gain of the selected SU is denoted by

$$\gamma^*_{\mathrm{S}} = \beta_4 \max_{1 \le j \le M} |h_{\mathrm{SU}_j,\mathrm{SR}}|^2. \tag{3.6}$$

3.2 Average Bit Error Rate

Average bit error rate (BER) is a key performance metric. In this section, we will derive the average BER of both the PU and SU in closed form respectively. In the primary network, opportunistic relay selection among N SUs is assumed. In the secondary network, MUD is applied where the SU with the highest transmission SNR will be selected to communicate at each time instance. At last, we will define a new metric to capture the overall BER performance of the whole system, and derive the optimal choice of t to minimize the overall system BER.

3.2.1 Average BER of the Primary System

Denoting the received SNR at the PR as γ_{P}, the error rate averaged over the fading with relay selection among N SUs is given by

$$\overline{\mathrm{P}}_{\mathrm{e_P}}(N) = \int_0^\infty \mathrm{P_e}(\rho x) f_{\gamma_{\mathrm{P}}}(x) dx. \tag{3.7}$$

where $\mathrm{P_e}(\rho x)$ is the instantaneous error rate over an AWGN channel for an instantaneous SNR x. $\mathrm{P_e}(\rho x)$ is often approximated to have the form of $\mathrm{P_e}(\rho x) = \alpha e^{-\eta x}$, where α and η can be chosen to capture different modulation schemes. For example, for binary differential phase-shift-keying (DPSK) this is exact with $\alpha = 0.5$ and $\eta = 1$. $f_{\gamma_{\mathrm{P}}}(x)$ is the PDF of the received SNR γ_{P} using MRC at the PR. Since a closed form expression for $f_{\gamma_{\mathrm{P}}}(x)$ is unavailable, we adopt the moment generating function (MGF) approach to study $\overline{\mathrm{P}}_{\mathrm{e_P}}(N)$ [117]. The MGF-based approach for the average BER performance of digital modulations over fading channels allows us to obtain the closed form expression for BER of variety of M-ary modulations such as M-DPSK. Due to the MRC scheme at the PR and the independence between the direct link and

the relay link, we have $\gamma_{\mathrm{P}} = \gamma_{\mathrm{D}} + \gamma_{\mathrm{R}}^*$. This implies that

$$\overline{\mathrm{P}}_{\mathrm{e_P}}(N) = \overline{\mathrm{P}}_{\mathrm{e_D}} \cdot \overline{\mathrm{P}}_{\mathrm{e_R}}(N), \tag{3.8}$$

where $\overline{\mathrm{P}}_{\mathrm{e_D}}$ is the average BER of the direct link at the average SNR β_1, and the $\overline{\mathrm{P}}_{\mathrm{e_R}}(N)$ is the average BER on the opportunistic relay path among N relays. Equation (3.8) is due to the property of MGF that the MGF of γ_{P} equals to the product of two individual MGFs of γ_{D} and γ_{R}^*.

Direct Link From PU to PR

For the direct link, it is simply the average BER over a Rayleigh fading channel with average SNR β_1, which can be obtained as

$$\overline{\mathrm{P}}_{\mathrm{e_D}} = \int_0^\infty \exp(-\eta x)\frac{1}{\beta_1}\exp(-\frac{x}{\beta_1})dx = \frac{\alpha}{1+\eta\beta_1}. \tag{3.9}$$

Opportunistic Relay Selection

As shown in Section 3.1.2, applying the opportunistic relay among N SUs, the received SNR at the PR can be expressed as (3.4). To derive $\overline{\mathrm{P}}_{\mathrm{e_R}}(N)$, the PDF of γ_{R}^* is needed. Due to its intractability, common upper bounds on γ_{R}^*, which are harmonic mean and min-max bounds, are studied.

Harmonic Mean Upper Bound The harmonic mean of $\gamma_{\mathrm{P,S}_i}$ and $\gamma_{\mathrm{S}_i,\mathrm{P}}$

$$\gamma_{\mathrm{HM}} = \frac{\gamma_{\mathrm{P,S}_i}\gamma_{\mathrm{S}_i,\mathrm{P}}}{\gamma_{\mathrm{P,S}_i} + \gamma_{\mathrm{S}_i,\mathrm{P}}}, \tag{3.10}$$

can be used to tightly upper bound γ_{R}^* in (3.4) by simply removing the 1 on the denominator as

$$\gamma_{\mathrm{R}}^* = \max_{1\le i\le N} \frac{\gamma_{\mathrm{P,S}_i}\gamma_{\mathrm{S}_i,\mathrm{P}}}{1+\gamma_{\mathrm{P,S}_i} + \gamma_{\mathrm{S}_i,\mathrm{P}}} \le \max_{1\le i\le N} \gamma_{\mathrm{HM}} = \gamma_{\mathrm{HM}}^*. \tag{3.11}$$

The right hand side of the inequality in (3.11) is the maximum among all the harmonic means of the SNRs on the two hops of a relay path. the left hand side is the maximum of the end-to-end SNR gains among all possible relay paths. This upper bound is a widely adopted approximation where the PDF and CDF of the individual relay path SNR γ_{HM} has been derived in [118]. After the best relay selection, γ^*_{HM} is the received SNR of the opportunistic relay path, which is mathematically intractable. However, using asymptotic extreme value theory, the maximum of N i.i.d. random variables whose complementary CDF has an exponential tail, can be shown to be Gumbel distributed as $N \to \infty$ [119]. Hence, the CDF and PDF of γ^*_{HM} can be captured in the large N regime as [66]:

$$F_{\gamma^*_{\mathrm{HM}}}(x) \approx \exp\left(-\exp\left(-\frac{x-\alpha_N}{c}\right)\right), \tag{3.12}$$

and

$$f_{\gamma^*_{\mathrm{HM}}}(x) \approx \frac{1}{c}\exp\left(-\frac{x-\alpha_N}{c}+\exp\left(-\frac{x-\alpha_N}{c}\right)\right). \tag{3.13}$$

where

$$c = \frac{\beta_2\beta_3}{(\sqrt{\beta_2}+\sqrt{\beta_3})^2} \tag{3.14}$$

$$\alpha_N = \frac{\log(N)+O(\log(\sqrt{\log(N)}))}{c} \tag{3.15}$$

Assuming that the instantaneous error rate has the form $\mathrm{P_e}(\rho x) = \alpha e^{-\eta x}$, substituting $\mathrm{P_e}(\rho x)$ and (3.13) into (3.7) and obtain the average BER of the PU with harmonic mean upper bound as:

$$\begin{aligned}\overline{\mathrm{P}}^{\mathrm{HM}}_{\mathrm{e_P}}(N) &= \overline{\mathrm{P}}_{\mathrm{e_D}} \cdot \overline{\mathrm{P}}^{\mathrm{HM}}_{\mathrm{e_R}}(N) \\ &= \frac{1}{1+\eta\beta_1}\alpha\int_0^\infty \frac{1}{c}\exp\left(-\frac{x-\alpha_N}{c}+\exp-\left(\frac{x-\alpha_N}{c}\right)\right)\mathrm{P_e}(\rho x)dx. \end{aligned} \tag{3.16}$$

After a change of variables, the average BER of the relay assisted PU with MRC at the PR is derived by carrying out the integral in (3.16) [120, eqn. (13)]

$$\overline{\mathrm{P}}_{\mathrm{e_P}}^{\mathrm{HM}}(N) = \alpha^2 \exp(-\eta\alpha_N c)\frac{1}{1+\eta\beta_1}\gamma(\eta c+1, \exp(\alpha_N)), \tag{3.17}$$

where $\gamma(\cdot,\cdot)$ is the lower incomplete gamma function defined as $\gamma(x,y) = \int_0^x t^{y-1}e^{-t}dt$ [121]. Equation (3.17) provides a tight upper bound on the average BER performance. It shows that as long as the individual links in the proposed system experience Rayleigh fading, the average BER is in the form of (3.17) with different parameters.

Min-Max Upper Bound An alternative upper bound on γ_{R}^* is the min-max upper bound introduced in [122] that maximize the minimum SNR on the relay path

$$\gamma_{\mathrm{R}}^* \leq \max_{1\leq i\leq N} \min\{\gamma_{\mathrm{P,S}_i}, \gamma_{\mathrm{S}_i,\mathrm{P}}\} = \gamma_{\mathrm{MM}}^*. \tag{3.18}$$

In this bound, the minimum of the link qualities of both relay hops are obtained, and then the maximum among these N minimum values is the desired opportunistic relay path SNR. This method captures each of the two relay hops as a bottle neck.

The random variable $\min\{\gamma_{\mathrm{P,S}_i}, \gamma_{\mathrm{S}_i,\mathrm{P}}\}$ is shown to be exponentially distributed with $\rho = \frac{\beta_2\beta_3}{\beta_2+\beta_3}$. Hence, the CDF and the PDF of γ_{MM}^* can be expressed as:

$$F_{\gamma_{\mathrm{MM}}^*}(x) = (1-\exp(-\rho x))^N, \tag{3.19}$$

and

$$f_{\gamma_{\mathrm{MM}}^*}(x) = N\rho\exp(-\rho x)(1-\exp(-\rho x))^{N-1}. \tag{3.20}$$

Assuming that the instantaneous error rate has the form $\mathrm{P_e}(\rho x) = \alpha e^{-\eta x}$, substituting $\mathrm{P_e}(\rho x)$ and (3.20) into (3.7) and obtain the average BER of the PU with min-max upper bound as:

$$\overline{\mathrm{P}}_{\mathrm{e_P}}^{\mathrm{MM}}(N) = \overline{\mathrm{P}}_{\mathrm{e_D}} \cdot \overline{\mathrm{P}}_{\mathrm{e_R}}^{\mathrm{MM}}(N) = \frac{\alpha^2}{1+\eta\beta_1} NB(N, 1+\eta\rho) \tag{3.21}$$

where $B(\cdot,\cdot)$ is the beta function defined as $B(x,y) = \int_0^1 t^{x-1}(1-t)^{y-1}dt$. It can be shown that $\gamma^*_{\mathrm{HM}} \leq \gamma^*_{\mathrm{MM}}$ which implies that the harmonic mean upper bound is always tighter than the min-max upper bound at every value of β_2 and β_3, and will converge to each other as $\beta_2 \gg \beta_3$ or $\beta_2 \ll \beta_3$. In Section 3.2.3, we will minimize the BER performance of the overall system analytically for both harmonic mean and min-max cases with respect to $N/(N+M)$, and verify that the solutions in two cases will coincide when $\beta_2 \gg \beta_3$ or $\beta_2 \ll \beta_3$, corresponding to that one of the relay hop is much stronger than another on the path. For example, the relay SU is close to either PU or the PR.

3.2.2 Average BER of the Underlay SU Transmission

As we described in the system model, when N SUs relay the PU's signal, M SUs above the interference constraint will operate in the underlay transmission mode in a MUD fashion. The CDF and PDF of the channel gain of the selected underlay SU with average SNR β_4 can be obtained as

$$F_{\gamma^*_{\mathrm{S}}}(x) = \left(1 - \exp\left(-\frac{x}{\beta_4}\right)\right)^M \tag{3.22}$$

and

$$f_{\gamma^*_{\mathrm{S}}}(x) = \frac{M}{\beta_4}\exp\left(-\frac{x}{\beta_4}\right)\left(1 - \exp\left(-\frac{x}{\beta_4}\right)\right)^{M-1}. \tag{3.23}$$

Assuming that the instantaneous error rate has the form $\mathrm{P_e}(\rho x) = \alpha e^{-\eta x}$, average BER performance of the selected underlay SU can be obtained as

$$\overline{\mathrm{P}}_{\mathrm{es}}(M) = \alpha M B(M, 1+\eta\beta_4) \tag{3.24}$$

3.2.3 Optimal Ratio of t for Average BER

In our proposed cooperative CR system, when N SUs are above the interference constraint, opportunistic relay over N SUs is utilized to improve the PU's BER per-

formance. On the other hand, MUD scheme is applied among M underlay SUs. Consequently, the PU and SU's average BER performance can be balanced by adjusting the value of N and M. To recall that we defined a ratio parameter $t \triangleq N/(N+M)$, and we will show that there exists an optimal value of t to maximize the overall average BER performance of both PU and SU.

The overall average BER $\overline{\mathrm{P}}_{\mathrm{e_{all}}}(N,M)$ is defined as the product of PU's average BER $\overline{\mathrm{P}}_{\mathrm{e_P}}(N)$ and SU's average BER $\overline{\mathrm{P}}_{\mathrm{e_S}}(M)$. Assuming that the instantaneous error rate has the form $\mathrm{P_e}(\rho x) = \alpha e^{-\eta x}$, $\overline{\mathrm{P}}_{\mathrm{e_{all}}}(N,M)$ is equivalent to the average BER of the summed SNR $\gamma_{\mathrm{P}} + \gamma_{\mathrm{S}}^{*}$, which characterizes the overall performance of the proposed system. In this section, we study the trade-off between the PU and SU's average BER performance in closed form, and obtain the overall BER expressions $\overline{\mathrm{P}}^{\mathrm{HM}}_{\mathrm{e_{all}}}(N,M)$ and $\overline{\mathrm{P}}^{\mathrm{MM}}_{\mathrm{e_{all}}}(N,M)$ for both harmonic mean and min-max upper bounds respectively as

$$\begin{aligned}\overline{\mathrm{P}}^{\mathrm{HM}}_{\mathrm{e_{all}}}(N,M) &= \overline{\mathrm{P}}^{\mathrm{HM}}_{\mathrm{e_P}}(N) \cdot \overline{\mathrm{P}}_{\mathrm{e_S}}(M) \\ &= \alpha^3 \frac{\exp(-\eta\alpha_N c)\gamma(\eta c+1, \exp(\alpha_N))MB(M, 1+\eta\beta_4)}{1+\eta\beta_1}, \end{aligned} \tag{3.25}$$

and

$$\overline{\mathrm{P}}^{\mathrm{MM}}_{\mathrm{e_{all}}}(N,M) = \overline{\mathrm{P}}^{\mathrm{MM}}_{\mathrm{e_P}}(N) \cdot \overline{\mathrm{P}}_{\mathrm{e_S}}(M) = \alpha^3 \frac{NB(N, 1+\eta\rho)MB(M, 1+\eta\beta_4)}{1+\eta\beta_1}. \tag{3.26}$$

When the PU is active, an increase in N, or equivalently t, will result in a decrease of $\overline{\mathrm{P}}^{\mathrm{HM}}_{\mathrm{e_P}}(N)$ and $\overline{\mathrm{P}}^{\mathrm{MM}}_{\mathrm{e_P}}(N)$, and increase of $\overline{\mathrm{P}}_{\mathrm{e_S}}(M)$. The behavior of $\overline{\mathrm{P}}^{\mathrm{HM}}_{\mathrm{e_{all}}}(N,M)$ and $\overline{\mathrm{P}}^{\mathrm{MM}}_{\mathrm{e_{all}}}(N,M)$ in terms of t can be studied in the high M and N regime, and we have the following theorem:

Theorem 10. *The overall BER performance of the proposed system applying the harmonic mean upper bound denoted as $\overline{P}^{\mathrm{HM}}_{\mathrm{e_{all}}}(N,M)$, and the min-max upper bound denoted as $\overline{P}^{\mathrm{MM}}_{\mathrm{e_{all}}}(N,M)$ can be minimized at*

$$t^{*}_{\mathrm{HM}} = \frac{c}{c+\beta_4} \tag{3.27}$$

and

$$t^*_{\mathrm{MM}} = \frac{\rho}{\rho + \beta_4}, \tag{3.28}$$

when M and N are large, $\rho = \frac{\beta_2\beta_3}{\beta_2+\beta_3}$ is the average end to end SNR of the relay path, and $c = \frac{\beta_2\beta_3}{(\sqrt{\beta_2}+\sqrt{\beta_3})^2}$.

Proof. See Appendix D. □

Recalling that $t = N/(N+M)$ is the fraction of SUs acting as relays to the total number SUs. Theorem 10 provides the optimal relationship between N and M as a function of the average SNR on each fading link. By knowing the statistics of each fading link, we can derive how far the system average BER performance is away from the optimal scenario. t^*_{HM} and t^*_{MM} are monotonically increasing functions of c and ρ, and decreasing functions of β_4. This means that when c and ρ are small and β_4 is large, SUs tend to proceed with their own transmission since the underlay SUs experience high quality channels. On the other hand, more SUs will relay PU's signal when c and ρ are large and β_4 is small. In Appendix D, it has been shown that $\overline{\mathrm{P}}^{\mathrm{HM}}_{\mathrm{e_{all}}}(N,M)$ and $\overline{\mathrm{P}}^{\mathrm{MM}}_{\mathrm{e_{all}}}(N,M)$ are positive logarithmically convex functions of t, which implies that $\overline{\mathrm{P}}^{\mathrm{HM}}_{\mathrm{e_{all}}}(N,M)$ and $\overline{\mathrm{P}}^{\mathrm{MM}}_{\mathrm{e_{all}}}(N,M)$ are convex of t over $0 \leq t \leq 1$. Moreover, it can be shown that $\overline{\mathrm{P}}^{\mathrm{HM}}_{\mathrm{e_{all}}}(N,M)$ and $\overline{\mathrm{P}}^{\mathrm{MM}}_{\mathrm{e_{all}}}(N,M)$ are decreasing when $t < t^*_{\mathrm{HM}}$ and $t < t^*_{\mathrm{MM}}$, and increasing when $t > t^*_{\mathrm{HM}}$ and $t > t^*_{\mathrm{MM}}$. Hence, the maximal value of $\overline{\mathrm{P}}^{\mathrm{HM}}_{\mathrm{e_{all}}}(N,M)$ and $\overline{\mathrm{P}}^{\mathrm{MM}}_{\mathrm{e_{all}}}(N,M)$ can only be achieved either at $t = 0$ or $t = 1$. When $t = 1$, all L SUs will relay the PU's transmission and the proposed cooperative underlay CR system is equivalent to the cooperative CR system introduced in [67]. When $t = 0$, all L SUs will operate in the underlay mode, so that the proposed system reduces to a conventional underlay CR system. Consequently, our CR system outperforms both the existing cooperative CR system and the underlay CR system in the average BER sense when N and M are large.

It can be derived that $c \approx \rho$ when $\beta_2 \gg \beta_3$ or $\beta_2 \ll \beta_3$. This indicates that $\overline{\mathrm{P}}_{\mathrm{e_{all}}}^{\mathrm{HM}}(N, M)$ and $\overline{\mathrm{P}}_{\mathrm{e_{all}}}^{\mathrm{MM}}(N, M)$ can be minimized at the same value of t, which coincide with the fact that $\gamma_{\mathrm{HM}}^{*} \approx \gamma_{\mathrm{MM}}^{*}$ when $\beta_2 \gg \beta_3$ or $\beta_2 \ll \beta_3$ as we described in Section 3.2.1. Also, when $\beta_i = \beta$ for $i = 1, \ldots, 4$, which corresponds to homogeneous fading links, $t_{\mathrm{MM}}^{*} = 1/3$. This means that the optimal number SU relays is one third of the total number SUs given the average SNR values β_2, β_3 and β_4. We will see in the next section that the sum achievable rate criterion will also yield a similar result. Another interpretation of the min-max upper bound is that if the decode-and-forward scheme is applied among SU relays, γ_{MM}^{*} is the equivalent SNR value of the relay path if both hops are not in outage. Hence the min-max case is of interest.

3.3 Achievable Rate

3.3.1 Scaling Laws for Achievable rates of the PU and Underlay SU

When $h_{\mathrm{PU,PR}}$, $h_{\mathrm{PU,SU}_i}$, $h_{\mathrm{SU}_i,\mathrm{PR}}$ and $h_{\mathrm{SU}_j,\mathrm{SR}}$ vary rapidly over the duration of a codeword, the system is in the so-called fast fading regime. We consider the achievable rate of both PU and the selected SU averaged over channel fading. When the PU's transmission exists, N SUs serve as relays to the PU and M SUs communicate with the SR using MUD. In the primary network, it has been shown in [114] that the achievable rate of the relay assisted PU can be expressed as

$$\overline{\mathrm{C}}_{\mathrm{P}}(N) = \frac{1}{2} \int_0^{\infty} \log\left(1 + x\right) f_{\gamma_{\mathrm{P}}}(x) dx, \tag{3.29}$$

where $\overline{\mathrm{C}}_{\mathrm{P}}(N)$ is the achievable rate of the PU and $\gamma_{\mathrm{P}} = \gamma_{\mathrm{D}} + \gamma_{\mathrm{R}}^{*}$. The factor $1/2$ is due to the fact that PU only transmit at the first half of the transmission phase. When the number of SU relays N is large, we show in Appendix E that for both harmonic

mean and min-max cases,

$$\overline{\mathrm{C}}_{\mathrm{P}}(N) = \frac{1}{2}\log(\log(N)) + o(\log(\log(N))). \tag{3.30}$$

In the secondary network, the achievable rate of the selected SU with MUD can be expressed as

$$\overline{\mathrm{C}}_{\mathrm{S}}(M) = \int_0^\infty \log(1+x)\, f_{\gamma_{\mathrm{S}}^*}(x)dx. \tag{3.31}$$

Similar to (3.30), the scaling laws for $\overline{\mathrm{C}}_{\mathrm{S}}(M)$ as $M \to \infty$ can be obtained using previously derived expressions for non-cooperative point-to-point systems [55] as

$$\overline{\mathrm{C}}_{\mathrm{S}}(M) = \log(\log(M)) + O\left(\frac{1}{\sqrt{\log(M)}}\right). \tag{3.32}$$

3.3.2 Optimal Ratio of t for Achievable Rate

As we described in Section 3.2.3, the trade-off between the PU and the selected underlay SU performance also exists when the metric of interest is the achievable rate. We define $t = N/(N+M)$ and

$$\overline{\mathrm{C}}_{\mathrm{all}}(N, M) = \overline{\mathrm{C}}_{\mathrm{P}}(N) + \overline{\mathrm{C}}_{\mathrm{S}}(M) \tag{3.33}$$

as the sum rate of the proposed system to capture the overall rate performance of the whole system. $\overline{\mathrm{C}}_{\mathrm{all}}(N, M)$ characterizes the total rate that the whole network can support at a certain time instance. In this section, we will adjust the value of t to balance between the primary and secondary network performance in the achievable rate sense, and then aim to maximize the sum rate $\overline{\mathrm{C}}_{\mathrm{all}}(N, M)$ as a function of t in the large number of SUs regime. Combining (3.30) with (3.32) we have

$$\overline{\mathrm{C}}_{\mathrm{all}}(N, M) = \frac{1}{2}\log(\log(N)) + \log(\log(M)) + o(\log(\log(N))) \quad + O\left(\frac{1}{\sqrt{\log(M)}}\right), \tag{3.34}$$

and obtain the following theorem:

Theorem 11. *When the number of SUs N and M are large, the sum rate of the proposed system $\overline{C}_{\text{all}}(N, M)$ is concave in t over $0 \leq t \leq 1$, and can be maximized at $t^* = 1/3$.*

Proof. See Appendix E. □

The optimal ratio $t^* = 1/3$ coincides with the results in Theorem 10 based on the error probability when we have homogeneous fading links in the network. This implies that both total average BER and sum achievable rate can be jointly optimized at the same time. $\overline{\text{C}}_{\text{all}}(N, M)$ can be shown to increase when $t < t^*$ and decrease $t > t^*$, hence the maximum value of $\overline{\text{C}}_{\text{all}}(N, M)$ can only be achieved either at $t = 0$ or $t = 1$. $t = 0$ and $t = 1$ stand for conventional cooperative and underlay CR systems respectively. Consequently, our proposed system outperforms both the existing cooperative CR system and the underlay CR system in the achievable rate sense when N and M are large. Moreover, we can generalize $\overline{\text{C}}_{\text{all}}(N, M)$ to any weighted linear combinations of $\overline{\text{C}}_{\text{P}}(N)$ and $\overline{\text{C}}_{\text{S}}(M)$, which can be maximized using the same method as Theorem 11 applying harmonic mean or min-max upper bound on the opportunistic relay selection.

3.4 Cooperative Underlay CR Systems with Random Number of SUs

In Section 3.2 and 3.3, the average BER and achievable rate of the relay-aided cooperative underlay CR system is investigated for fixed number of SUs N and M. Practically, due to the mobility of the users and interference heterogeneity in different parts of the environment, the number of SUs need not to be deterministic. We now assume that $\mathcal{L}$ SUs are located randomly but uniformly inside the cell. The number of SUs $\mathcal{N}$ and $\mathcal{M}$ are a pair of i.i.d. random variables with mean value λt and $\lambda(1-t)$. In this case, the overall BER and sum achievable rate defined in (3.25) and (3.33) are

averaged over the user distributions, and can be expressed as

$$\mathrm{E}_{\mathcal{N},\mathcal{M}}[\overline{\mathrm{P}}_{\mathrm{e_{all}}}(\mathcal{N},\mathcal{M})] = \mathrm{E}_{\mathcal{N}}[\overline{\mathrm{P}}_{\mathrm{e_P}}(\mathcal{N})] \cdot \mathrm{E}_{\mathcal{M}}[\overline{\mathrm{P}}_{\mathrm{e_S}}(\mathcal{M})] \tag{3.35}$$

and

$$\mathrm{E}_{\mathcal{N},\mathcal{M}}[\overline{\mathrm{C}}_{\mathrm{all}}(\mathcal{N},\mathcal{M})] = \mathrm{E}_{\mathcal{N}}[\overline{\mathrm{C}}_{\mathrm{P}}(\mathcal{N})] + \mathrm{E}_{\mathcal{M}}[\overline{\mathrm{C}}_{\mathrm{S}}(\mathcal{M})] \tag{3.36}$$

respectively, where $\mathcal{N} + \mathcal{M} = \mathcal{L}$. In this section, we will show that as $\lambda \to \infty$, both $\mathrm{E}_{\mathcal{N},\mathcal{M}}[\overline{\mathrm{P}}_{\mathrm{e_{all}}}(\mathcal{N},\mathcal{M})]$ and $\mathrm{E}_{\mathcal{N},\mathcal{M}}[\overline{\mathrm{C}}_{\mathrm{all}}(\mathcal{N},\mathcal{M})]$ can be optimized at the same value of t as their deterministic counterparts derived in Theorems 10 and 11.

3.4.1 Overall BER in Poisson User Distribution

Whether a SU is under or above the interference constraint at the PR can be modeled as a Bernoulli random variable. When the number of SUs is large and each user is active (interference at the PR is below the threshold) with small and mutually independent probability, the number of active users is well approximated as Poisson distribution [105]. For the overall average BER case, when the harmonic mean and min-max upper bounds are applied in the high λ regime, $\mathrm{E}_{\mathcal{N},\mathcal{M}}[\overline{\mathrm{P}}_{\mathrm{e_{all}}}(\mathcal{N},\mathcal{M})]$ can be lower bounded and denoted as $\mathrm{E}^{\mathrm{HM}}_{\mathcal{N},\mathcal{M}}[\overline{\mathrm{P}}_{\mathrm{e_{all}}}(\mathcal{N},\mathcal{M})]$ and $\mathrm{E}^{\mathrm{MM}}_{\mathcal{N},\mathcal{M}}[\overline{\mathrm{P}}_{\mathrm{e_{all}}}(\mathcal{N},\mathcal{M})]$. Similar to Theorem 10, $\mathrm{E}^{\mathrm{HM}}_{\mathcal{N},\mathcal{M}}[\overline{\mathrm{P}}_{\mathrm{e_{all}}}(\mathcal{N},\mathcal{M})]$ and $\mathrm{E}^{\mathrm{MM}}_{\mathcal{N},\mathcal{M}}[\overline{\mathrm{P}}_{\mathrm{e_{all}}}(\mathcal{N},\mathcal{M})]$ can be minimized over $0 \le t \le 1$ and the following Theorem can be obtained:

Theorem 12. *When $\mathcal{M}$ and $\mathcal{N}$ are Poisson distributed with mean value $\lambda(1-t)$ and λt, the overall BER of the proposed CR system $E^{\mathrm{HM}}_{\mathcal{N},\mathcal{M}}[\overline{P}_{\mathrm{e_{all}}}(\mathcal{N},\mathcal{M})]$ and $E^{\mathrm{MM}}_{\mathcal{N},\mathcal{M}}[\overline{P}_{\mathrm{e_{all}}}(\mathcal{N},\mathcal{M})]$ averaged across both fading and user distributions can be minimized at*

$$t^*_{\mathrm{HM}} = \frac{c}{c+\beta_4} \tag{3.37}$$

and

$$t^*_{\mathrm{MM}} = \frac{\rho}{\rho + \beta_4} \tag{3.38}$$

when $\lambda \to \infty$*, and* $\rho = \frac{\beta_2\beta_3}{\beta_2+\beta_3}$ *is the average end to end SNR on the relay path, and* $c = \frac{\beta_2\beta_3}{(\sqrt{\beta_2}+\sqrt{\beta_3})^2}$.

Proof. Due to Jensen's inequality,

$$\begin{aligned} \mathrm{E}^{\mathrm{MM}}_{\mathcal{N},\mathcal{M}}[\overline{\mathrm{P}}_{\mathrm{e_{all}}}(\mathcal{N},\mathcal{M})] &= \mathrm{E}_{\mathcal{N}}[\overline{\mathrm{P}}^{\mathrm{MM}}_{\mathrm{e_P}}(\mathcal{N})] \cdot \mathrm{E}_{\mathcal{M}}[\overline{\mathrm{P}}_{\mathrm{e_S}}(\mathcal{M})] \\ &\geq \overline{\mathrm{P}}^{\mathrm{MM}}_{\mathrm{e_P}}(\mathrm{E}[\mathcal{N}]) \cdot \overline{\mathrm{P}}_{\mathrm{e_S}}(\mathrm{E}[\mathcal{M}]) \end{aligned} \tag{3.39}$$

It has been proved in (D.2) that,

$$\overline{\mathrm{P}}^{\mathrm{MM}}_{\mathrm{e_P}}(N) = \alpha B(N, 1+\eta\rho) \to \alpha\Gamma(1+\eta\rho)N^{-\eta\rho}, \tag{3.40}$$

as $N \to \infty$, which can be verified to be regularly varying at $N \to \infty$ with parameter $\eta\rho$. It has been shown in equation (19) in [55] that $\overline{\mathrm{P}}^{\mathrm{MM}}_{\mathrm{e_P}}(N)$ is a completely monotonic function of N. Similarly, $\overline{\mathrm{P}}_{\mathrm{e_S}}(M)$ is also regularly varying at $M \to \infty$ with parameter $\eta\beta_4$, and completely monotonic of M. Using the result of equation (29) in [55], the equality in (3.39) is achieved as $\lambda \to \infty$ when $\mathcal{N}$ and $\mathcal{M}$ are Poisson distribution. Hence, minimizing $\mathrm{E}^{\mathrm{MM}}_{\mathcal{N},\mathcal{M}}[\overline{\mathrm{P}}_{\mathrm{e_{all}}}(\mathcal{N},\mathcal{M})]$ with $\mathrm{E}[\mathcal{L}] = \lambda$ is equivalent to minimizing $\overline{\mathrm{P}}^{\mathrm{MM}}_{\mathrm{e_{all}}}(N, M)$ with $M = \lambda(1-t)$ and $N = \lambda t$. The rest of the proof follows Appendix D, that $\mathrm{E}^{\mathrm{MM}}_{\mathcal{N},\mathcal{M}}[\overline{\mathrm{P}}_{\mathrm{e_{all}}}(\mathcal{N},\mathcal{M})]$ is convex on t and can be minimized at $t = t^*_{\mathrm{MM}}$. Similarly, $\mathrm{E}^{\mathrm{HM}}_{\mathcal{N},\mathcal{M}}[\overline{\mathrm{P}}_{\mathrm{e_{all}}}(\mathcal{N},\mathcal{M})]$ can be shown to be minimized at $t = t^*_{\mathrm{HM}}$ following the same procedure, which completes the proof. □

3.4.2 Sum Achievable Rate in General User Distributions

In this section, we extend Poisson $\mathcal{M}$ and $\mathcal{N}$ to a large class of user distribution $\mathbb{C}$ and show that as $\lambda \to \infty$, $\mathrm{E}_{\mathcal{N},\mathcal{M}}[\overline{\mathrm{C}}_{\mathrm{all}}(\mathcal{N},\mathcal{M})]$ can be maximized over $0 \leq t \leq 1$.

Theorem 13. *Assuming that $\mathcal{M}$ and $\mathcal{N}$ are positive random variables with mean values $\lambda(1-t)$ and λt, and variances $\sigma^2_{\mathcal{M}}$ and $\sigma^2_{\mathcal{N}}$, the sum achievable rate of the PU and the selected underlay SU $E_{\mathcal{N},\mathcal{M}}[\overline{C}_{\text{all}}(\mathcal{N},\mathcal{M})]$ averaged across fading and user distributions can be maximized at $t = t^*$, provided that: $(a) Pr[\mathcal{M}=0] = o(1/\log\log\lambda(1-t))$, $Pr[\mathcal{N}=0] = o(1/\log\log\lambda t)$; $(b)\sigma^2_{\mathcal{M}} = o(\lambda(1-t)^2)$, $\sigma^2_{\mathcal{N}} = o(\lambda t^2)$ as $\lambda \to \infty$. And $t^* \to 1/3$ as $\lambda \to \infty$.*

Proof. See Appendix F. □

This theorem implies that the random SUs case has the same optimal t^* solution as its deterministic counterpart when $\lambda \to \infty$ proved in Theorem 11. Moreover, it is shown in Appendix F that $\mathrm{E}_{\mathcal{N},\mathcal{M}}[\overline{\mathrm{C}}_{\text{all}}(\mathcal{N},\mathcal{M})]$ is concave in t, hence $\mathrm{E}_{\mathcal{N},\mathcal{M}}[\overline{\mathrm{C}}_{\text{all}}(\mathcal{N},\mathcal{M})]$ $\leq \overline{\mathrm{C}}_{\text{all}}(N,M)$ due to the Jensen's inequality.

3.5 Simulations

In this section, we generate i.i.d. fading coefficients as random variables and use Monte-Carlo simulations to plot averaged BER derived in (3.25) and (3.26), and achievable rate derived in (3.34) to corroborate our analytical results. For all simulations, Rayleigh fading channels are assumed.

In Section 3.1.1, the access strategy of the proposed underlay cooperative CR system is illustrated. By adjusting the value of N, the performance of PU and selected underlay SU can be balanced. In Figure 3.2, the average BER performance of the PU and the selected SU in cooperative and conventional underlay scheme are simulated versus the user ratio t. It can be observed that in the cooperative scheme, as the ratio t increases, the BER performance of the PU improves due to increasing number of SU relays. The BER performance of the underlay SU will deteriorate in this case since the number of potential SUs in the MUD scheme is decreased in the secondary network.

The trade-off between the PU and the selected SU's average BER performance is therefore illustrated in Figure 2.

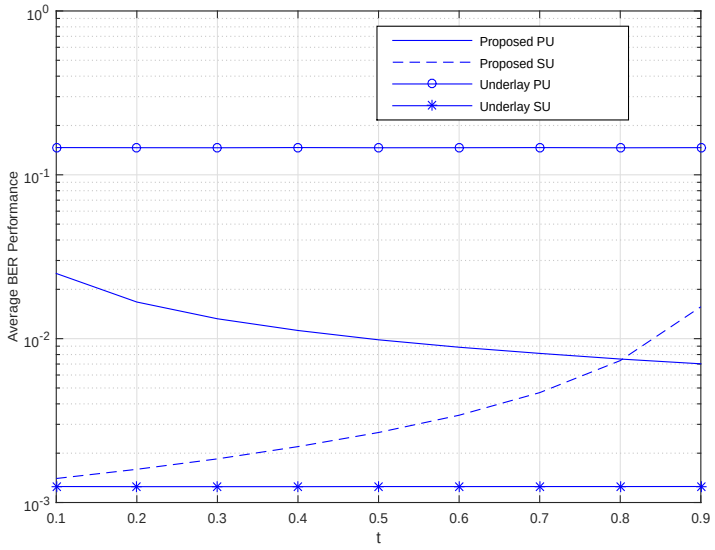

Figure 3.2: Average BER of the Proposed and Conventional Underlay CR Systems.

In Section 3.2.3, we define the overall average BER metric $\overline{\mathrm{P}}_{\mathrm{e_{all}}}(N, M)$ to capture the system performance of both PU and selected underlay SU when M and N are deterministic, and $\mathrm{E}_{\mathcal{N},\mathcal{M}}[\overline{\mathrm{P}}_{\mathrm{e_{all}}}(\mathcal{N}, \mathcal{M})]$ when M and N are random. It has been shown in Theorem 10 that $\overline{\mathrm{P}}^{\mathrm{HM}}_{\mathrm{e_{all}}}(N, M)$ and $\overline{\mathrm{P}}^{\mathrm{MM}}_{\mathrm{e_{all}}}(N, M)$ are both convex functions of t, and can be minimized at $t = c/(c+\beta_4)$ and $t = \rho/(\rho+\beta_4)$ respectively. In Figure 3.3, the overall average BER expressions $\overline{\mathrm{P}}^{\mathrm{HM}}_{\mathrm{e_{all}}}(N, M)$ and $\overline{\mathrm{P}}^{\mathrm{MM}}_{\mathrm{e_{all}}}(N, M)$ as well as their random counterparts $\mathrm{E}^{\mathrm{HM}}_{\mathcal{N},\mathcal{M}}[\overline{\mathrm{P}}_{\mathrm{e_{all}}}(\mathcal{N}, \mathcal{M})]$ and $\mathrm{E}^{\mathrm{MM}}_{\mathcal{N},\mathcal{M}}[\overline{\mathrm{P}}_{\mathrm{e_{all}}}(\mathcal{N}, \mathcal{M})]$ are plotted versus t. In the deterministic case, the total number of SUs $L = 100$, and average SNR of each fading link is normalized to 1. In the random case, $\mathcal{N}$ and $\mathcal{M}$ are assumed to be Poisson distributed with mean value $100t$ and $100(1-t)$. For the harmonic mean upper bound case, according to equation (3.27) and (3.37), $\overline{\mathrm{P}}^{\mathrm{HM}}_{\mathrm{e_{all}}}(N, M)$ and $\mathrm{E}^{\mathrm{HM}}_{\mathcal{N},\mathcal{M}}[\overline{\mathrm{P}}_{\mathrm{e_{all}}}(\mathcal{N}, \mathcal{M})]$ should be both minimized at $c/(c+\beta_4) = (1/4)/(1/4+1) = 1/5$, which can be verified from our numerical results. Similarly, for the min-max upper bound case, $\overline{\mathrm{P}}^{\mathrm{MM}}_{\mathrm{e_{all}}}(N, M)$

and $\mathrm{E}^{\mathrm{MM}}_{\mathcal{N},\mathcal{M}}[\overline{\mathrm{P}}_{\mathrm{e_{all}}}(\mathcal{N},\mathcal{M})]$ should be minimized at $\rho/(\rho+\beta_4) = (1/2)/(1/2+1) = 1/3$, which can be verified by our simulations either. Moreover, the random SUs curves are slightly above the deterministic case, which is due to the fact that by Jensen's inequality, any kind of randomization of the number of SUs will deteriorate the average BER performance.

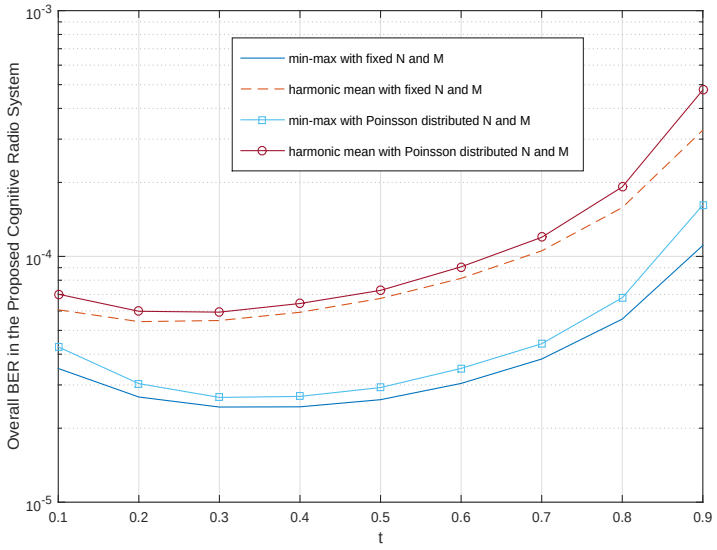

Figure 3.3: Minimize the Overall Average BER.

In Section 3.2.3, we showed that $\overline{\mathrm{P}}^{\mathrm{HM}}_{\mathrm{e_{all}}}(N,M)$ and $\overline{\mathrm{P}}^{\mathrm{MM}}_{\mathrm{e_{all}}}(N,M)$ can be minimized at the same value of t when $\beta_2 \gg \beta_3$ or $\beta_2 \ll \beta_3$. In Figure 3.4, $\overline{\mathrm{P}}^{\mathrm{HM}}_{\mathrm{e_{all}}}(N,M)$ and $\overline{\mathrm{P}}^{\mathrm{MM}}_{\mathrm{e_{all}}}(N,M)$ are simulated with different values of β_3 where $\beta_2 = 1$. It can be observed that as β_3 increases, $\overline{\mathrm{P}}^{\mathrm{HM}}_{\mathrm{e_{all}}}(N,M)$ approaches $\overline{\mathrm{P}}^{\mathrm{MM}}_{\mathrm{e_{all}}}(N,M)$ due to the fact that $\gamma^*_{\mathrm{HM}} \to \gamma^*_{\mathrm{MM}}$. Moreover, when $\beta_3 = 50$, $\overline{\mathrm{P}}^{\mathrm{HM}}_{\mathrm{e_{all}}}(N,M)$ and $\overline{\mathrm{P}}^{\mathrm{MM}}_{\mathrm{e_{all}}}(N,M)$ are both minimized at $t \approx 1/2$ since $c \to \rho \approx \beta_2$ when $\beta_2 \ll \beta_3$.

In Section 3.4.2, we derive the scaling laws for the achievable rate of the PU $\mathrm{E}_{\mathcal{N}}[\overline{\mathrm{C}}_{\mathrm{P}}(\mathcal{N})]$ as $\lambda \to \infty$ in (F.3). We provide an upper bound and a lower bound on $\mathrm{E}_{\mathcal{N}}[\overline{\mathrm{C}}_{\mathrm{P}}(\mathcal{N})]$, and show that both bounds will converge as $\mathrm{E}[\mathcal{N}] = \lambda t \to \infty$. In Figure 3.5, $\overline{\mathrm{C}}_{\mathrm{P}}(N)$ are simulated and compared with both bounds as $\lambda \to \infty$. It can

be shown that the upper bound and lower bound will converge to each other as λ increases, and that the upper bound is tighter.

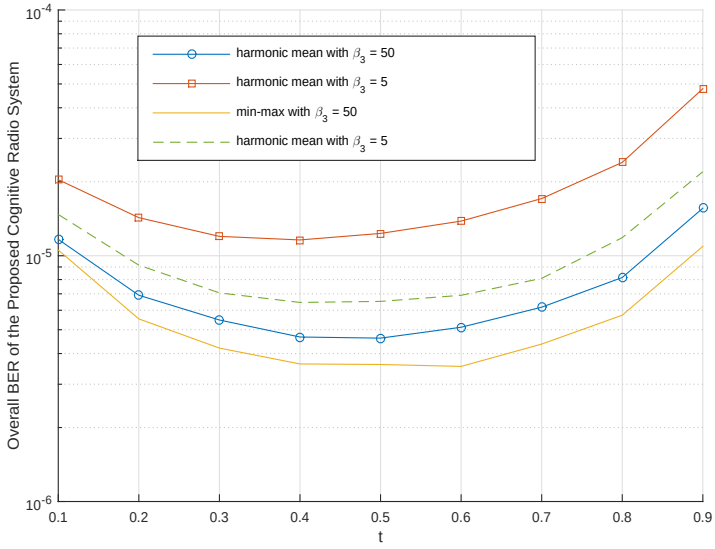

Figure 3.4: Minimize the Overall Average BER when $\beta_3 \gg \beta_2$.

Similar to the overall BER case, we define sum rate of the proposed system $\overline{\mathrm{C}}_{\mathrm{all}}(N, M)$ in Section 3.3 as a metric to study the sum achievable rate of the PU and the selected underlay SU. In Theorem 11 we show that $\overline{\mathrm{C}}_{\mathrm{all}}(N, M)$ is a concave function of t and can be maximized at some t^* when N and M are large. We show in Theorem 13 that when $\mathcal{N}$ and $\mathcal{M}$ are random, similar optimal t^* can be obtained. In Figure 3.6, sum rates $\overline{\mathrm{C}}_{\mathrm{all}}(N, M)$ and $\mathrm{E}_{\mathcal{N},\mathcal{M}}[\overline{\mathrm{C}}_{\mathrm{all}}(\mathcal{N}, \mathcal{M})]$ of both deterministic and random number of SUs are simulated, and compared with the scaling law specified in (F.5). In the simulation, $L = \mathrm{E}[\mathcal{L}] = \lambda = 100$, and the average SNR of all the fading links are normalized to 1. $\mathcal{N}$ and $\mathcal{M}$ are assumed to be Poisson distributed. It can be observed that when λ is large, sum rates in both random and deterministic cases can be maximized simultaneously at the same t^*. We have solved $t^* = 0.3444$ numerically which is very close to $1/3$ as we derived in Theorem 10 and 11 when the

min-max upper bound is applied. The minor difference between 0.3444 and 1/3 is due to the insufficiently large L and λ.

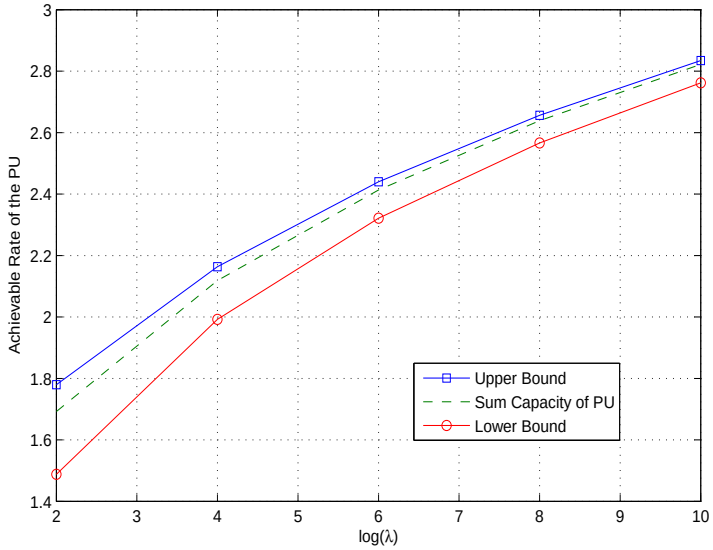

Figure 3.5: Convergence of Upper and Lower Bounds on $\mathrm{E}_{\mathcal{N}}\left[\overline{C}(\rho,\mathcal{N})\right]$ as $\lambda \to \infty$.

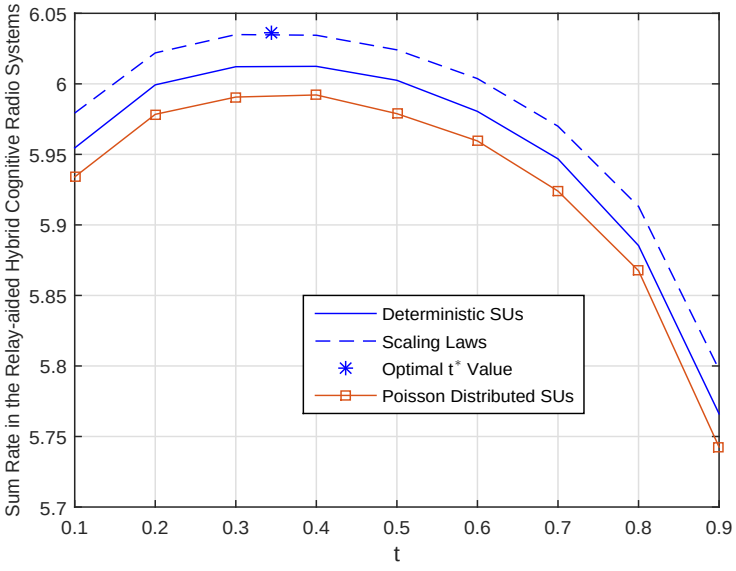

Figure 3.6: Achievable Rate under Deterministic and Poisson User Distributions.

Chapter 4

MULTIPLE D2D USERS UNDERLAYING CELLULAR NETWORKS WITH SUPERPOSITION CODING

In this chapter, a cooperative D2D communication system underlaying a downlink cellular network with multiple D2D pairs is considered. Each individual DT allocates its transmission power to decode-and-forward (DF) CU's traffic while superimposing its own D2D signal. In the small SNR regime, various spectrum accessing policies involving one or multiple DUs are proposed depending on different CSI assumptions at the cellular BS. We provide accurate second order approximations for the average achievable rates of both the CU and the in individual DU for various spectrum accessing policies. We show that by adding multiple DUs, both the CU's and the individual DU's rates can be improved simultaneously. Here are some remarks on notations and definitions. $\tau(x) = o(g(x))$ as $x \to 0$ means that $\limsup_{x\to 0} |\tau(x)/g(x)| = 0$. Notation $:=$ means *by definition*. Throughout the dissertation, two D2D users in communications act as a DT and a DR, and form a D2D pair. D2D users' average achievable rate means the achievable rate averaged over fading on the channel between the DT and its corresponding DR.

4.1 System Model

In Fig. 4.1, we illustrate cooperative D2D users underlaying a downlink cellular user. The system consists of a BS, a CU, and D2D transmitter DT_i and receiver DR_i pairs, $i = 1, \ldots, M$. Only two pairs of D2D users are shown here. Since the cellular system operates in a frequency division multiple access (FDMA) mode in which each sub-band contains one CU, we focus on the case of a single CU, following the existing

literature [90, 93]. When the direct link between the BS and CU is too weak for the CU to decode the cellular signal, D2D pairs are activated as relays to facilitate the BS's transmission to the CU over the CU's sub-band. Due to the proximity between the DT_i and the DR_i, direct transmissions between M D2D pairs will be established to transmit with their own traffic. Receiving CSI is assumed at the CU and D2D users. Each active DT_i will decode the CU's signal in the first transmission phase and forward it to both the CU and the DR_i by superimposing with its own D2D signal x_{D_i}. All links experience Rayleigh fading, and the channel coefficients over $\mathrm{BS} \rightarrow \mathrm{DT_i}$, $\mathrm{BS} \rightarrow \mathrm{DR_i}$, $\mathrm{DT}_i \rightarrow \mathrm{CU}$, $\mathrm{DT}_i \rightarrow \mathrm{DR}_i$, and $\mathrm{DT}_j \rightarrow \mathrm{DR}_i$ are denoted by h_{BT_i}, h_{BR_i}, h_{TC_i} and h_{TR_i}, and $h_{\mathrm{int}_{ij}}$ which are complex Gaussian random variables with zero mean (please see also Fig. 4.1). The direct link channels h_{TC_i} and h_{TR_i} have variance μ, and the interference channels $h_{\mathrm{int}_{ij}}$ have variance β. We also denote $\gamma = |h|^2$ with the associated subscripts for the channel gain. The transmitted signal at the BS, and DT_i are denoted as x_{C} and x_{D_i}. $\mathrm{DT}_i \rightarrow \mathrm{DR}_i$ is the i^{th} D2D pair of interest when studying the D2D users' performance.

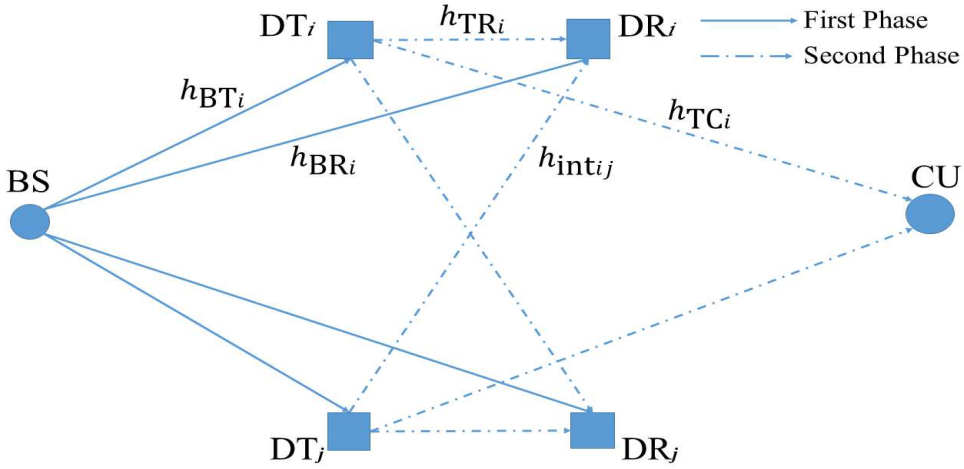

Figure 4.1: System Model of Cooperative D2D Communications with M D2D pairs.

In the first transmission phase, the BS broadcasts its signal x_{C}. The received signal at the DT_i and DR_i are denoted by y_{BT_i} and y_{BR_i} respectively as follows:

$$\begin{aligned} y_{\mathrm{BT}_i} &= \sqrt{P_{\mathrm{B}}}\, h_{\mathrm{BT}_i}\, x_{\mathrm{C}} + n_{\mathrm{BT}_i}, \\ y_{\mathrm{BR}_i} &= \sqrt{P_{\mathrm{B}}}\, h_{\mathrm{BR}_i}\, x_{\mathrm{C}} + n_{\mathrm{BR}_i}, \qquad i = 1, 2, \ldots, M, \end{aligned} \tag{4.1}$$

where P_{B} is the transmit power from the BS, n_{BT_i} and n_{BR_i} are additive white complex Gaussian noise samples with zero mean and unit variance, and the transmitted symbols are normalized to satisfy $\mathbb{E}[|x_{\mathrm{C}}|^2] = \mathbb{E}[|x_{\mathrm{D}_i}|^2] = 1$. After reception in the first transmission phase, x_{C} is decoded at the DT_i for further transmission and also decoded at the DR_i for interference cancellation purposes. At the CU, a global power allocation factor α will be calculated considering the average rate requirement for the CU and D2D users, and shared among all DT_i through feedback from the CU. This value of α only depends on the channel statistics, and not the channel realizations. If the decoding of x_{C} at the DT_i is successful, DT_i will forward x_{C} with power αP_{D} and embed its own D2D signal x_{D_i} with power $(1-\alpha)P_{\mathrm{D}}$, where α is the power allocation factor and P_{D} is the transmitting power at each DT_i. Hence the signal to be transmitted at each DT_i is given as $\left(\sqrt{\alpha P_{\mathrm{D}}}x_{\mathrm{C}} + \sqrt{(1-\alpha)P_{\mathrm{D}}}x_{\mathrm{D}_i}\right)$.

In the second phase, the received signal at the CU, and the DR_i without interference cancellation are given by

$$y_{\mathrm{CU}} = \sum_{i=1}^{M} \left(\sqrt{\alpha P_{\mathrm{D}}}x_{\mathrm{C}} + \sqrt{(1-\alpha)P_{\mathrm{D}}}x_{\mathrm{D}_i}\right) h_{\mathrm{TC}_i} + n_{\mathrm{TC}_i}, \tag{4.2}$$

$$\begin{aligned} y_{\mathrm{TR}_i} = &\left(\sqrt{\alpha P_{\mathrm{D}}}x_{\mathrm{C}} + \sqrt{(1-\alpha)P_{\mathrm{D}}}x_{\mathrm{D}_i}\right) h_{\mathrm{TR}_i} \\ &+ \sum_{j=1, j\neq i}^{M} \left(\sqrt{\alpha P_{\mathrm{D}}}x_{\mathrm{C}} + \sqrt{(1-\alpha)P_{\mathrm{D}}}x_{\mathrm{D}_j}\right) h_{\mathrm{int}_{ij}} + n_{\mathrm{TR}_i}. \end{aligned} \tag{4.3}$$

After reception in the second phase at the CU, the desired signal x_{C} will be decoded from y_{CU}. Moreover, when h_{BR_i} is good enough in (4.1), DR_i can decode x_{C} successfully at the end of the first phase, and remove the interference terms containing x_{C}

from y_{TR_i} in order to decode x_{D_i} in (4.4) correctly. This is referred as the perfect interference cancellation scenario, in which the received signal y_{TR_i} in (4.3) is reduced to

$$y_{\mathrm{TR}_i} = \sqrt{(1-\alpha)P_{\mathrm{D}}}x_{\mathrm{D}_i}h_{\mathrm{TR}_i} + \sum_{j=1, j\neq i}^{M} \sqrt{(1-\alpha)P_{\mathrm{D}}}x_{\mathrm{D}_j}h_{\mathrm{int}_{ij}} + n_{\mathrm{TR}_i}. \tag{4.4}$$

All existing cooperative D2D literature assumes perfect interference cancellation at the DR_i and does the performance analysis of the CU based on (4.4). However this requires that both γ_{BT_i} and γ_{BR_i} should be sufficiently large for each active D2D pair, which potentially reduces the total number of active D2D pairs. In this chapter, we consider both perfect and imperfect interference cancellation scenarios, and show that the CU and the D2D users' performance can be improved simultaneously in both cases.

4.1.1 Access Policy of D2D Users

In this section, four different D2D spectrum access policies which differ in the CSI knowledge they require are discussed. The corresponding received SNR expressions at the CU and the DR_i are provided. Following the existing literature [90, 93], each DT_i transmits if x_{C} can be decoded successfully, and remains silent otherwise.

Cooperative D2D communications with a single pair of D2D users and perfect interference cancellation at the DR_i has been studied in the existing literature [90,93], and is considered in this chapter as a performance benchmark, and referred as Policy-I.

Policy-I: Single D2D Pair

In Policy-I, an arbitrary pair of D2D users will be included in the cellular network. This scheme will be compared with more advanced spectrum sharing schemes. In (4.2)

with $M = 1$, $\sqrt{\alpha P_{\mathrm{D}}}x_{\mathrm{C}}$ is the desired signal and $\sqrt{(1-\alpha)P_{\mathrm{D}}}x_{\mathrm{D}_j}$ is the interference term in the superimposed signal x_{D_i}. The equivalent received SNR for Policy-I at the CU can be derived as

$$\gamma_{\mathrm{C}}^{\mathrm{I}} = \frac{P_{\mathrm{D}}\alpha}{P_{\mathrm{D}}(1-\alpha) + \frac{1}{\gamma_{\mathrm{TC}_i}}}. \tag{4.5}$$

When DR_i is able to cancel x_{C} perfectly in the second transmission phase, the received SNR at DR_i can be derived from (4.4) with $M = 1$ where $\sqrt{(1-\alpha)P_{\mathrm{D}}}x_{\mathrm{D}_i}$ is the desired signal and we have

$$\gamma_{\mathrm{D}_i}^{\mathrm{I}} = (1-\alpha)P_{\mathrm{D}}\gamma_{\mathrm{TR}_i}, \qquad \text{perfect cancellation.} \tag{4.6}$$

When DR_i can not cancel x_{C} perfectly, it can be observed from (4.3) that DR_i suffers from interference signal $\sqrt{\alpha P_{\mathrm{D}}}x_{\mathrm{C}}$ from the CU, and we obtain the received SNR at DR_i in this case as

$$\gamma_{\mathrm{D}_i}^{\mathrm{I}} = \frac{(1-\alpha)P_{\mathrm{D}}\gamma_{\mathrm{TR}_i}}{\alpha P_{\mathrm{D}}\gamma_{\mathrm{TR}_i} + 1}, \qquad \text{imperfect cancellation.} \tag{4.7}$$

Since CU's received SNR $\gamma_{\mathrm{C}}^{\mathrm{I}}$ is increasing in the D2D relay channel gain γ_{TC_i}, small γ_{TC_i} results in a significant degradation of the CU's performance. An intuitive extension of Policy-I without requiring extra transmit channel knowledge is to involve multiple D2D pairs without specific selection, and use MRC at the CU in order to improve CU's achievable rate. This spectrum access scheme leads to the Policy-II.

Policy-II: M D2D Pairs

When the DT_i-CU channel is weak, a single D2D pair assisted cellular network might not be sufficient to decode x_{C} reliably. To address this issue, we propose Policy-II in which multiple D2D pairs are involved in relaying CU's signal, and will show in the following sections that it is possible to improve both the CU and the individual

D2D users' performance, hence the spectral efficiency simultaneously. Assuming that the transmitting CSI are not available at the BS, all M D2D pairs will be activated to underlay the cellular network. It can be observed from (4.2) that the CU obtains M relayed copies containing $\sqrt{\alpha P_{\mathrm{D}}}x_{\mathrm{C}}$ using MRC. Therefore the received SNR for Policy-II at the CU can be derived from (4.2)

$$\gamma_{\mathrm{C}}^{\mathrm{II}} = \frac{P_{\mathrm{D}}\alpha}{P_{\mathrm{D}}(1-\alpha) + \frac{1}{\sum_{i=1}^{M}\gamma_{\mathrm{TC}_i}}}, \tag{4.8}$$

where we notice that $\sum_{i=1}^{M}\gamma_{\mathrm{TC}_i}$ is the D2D relay SNR. Analogous to Policy-I, the D2D users' received SNR can be derived from (4.4) and (4.3) for the perfect interference and imperfect interference cancellation scenarios, respectively. Additionally, each DT_j creates peer interference at the DR_i for $i \neq j$, which results in the interference term $\sum_{j=1,j\neq i}^{M} h_{\mathrm{int}_{ij}}\sqrt{(1-\alpha)P_{\mathrm{D}}}x_{\mathrm{D}_j}$ in (4.3). Therefore, D2D users' received SNR for Policy-II is given by

$$\gamma_{\mathrm{D}_i}^{\mathrm{II}} = \begin{cases} \dfrac{(1-\alpha)P_{\mathrm{D}}\gamma_{\mathrm{TR}_i}}{\sum_{j=1,j\neq i}^{M}(1-\alpha)P_{\mathrm{D}}\gamma_{\mathrm{int}_{ij}}+1} & \text{perfect cancellation} \\ \dfrac{(1-\alpha)P_{\mathrm{D}}\gamma_{\mathrm{TR}_i}}{\alpha P_{\mathrm{D}}\gamma_{\mathrm{TR}_i}+\sum_{j=1,j\neq i}^{M}P_{\mathrm{D}}\gamma_{\mathrm{int}_{ij}}+1} & \text{imperfect cancellation.} \end{cases} \tag{4.9}$$

In Policy-II, we include all M D2D pairs to improve the D2D relay SNR. When the BS has instantaneous CSI of relay channels γ_{TC_i}, selection diversity can be exploited where a subset of D2D pairs with better relay channels can be selected out of the whole set of D2D users. This leads to Policy-III and IV as follows.

Policy-III: Selection of the Best D2D Pair

In Policy-II, the received signal at the DR_i contains $M-1$ peer interference terms from the DT_j. To avoid the peer interference, only a single D2D pair that maximizes the CU's performance can be selected to relay and transmit if BS has the transmitting CSI of γ_{TC_i}. Let $\gamma_{\mathrm{TC}_{(i)}}$ denotes the k^{th} greatest order statistics among γ_{TC_i}. Compared

with Policy-I, the relay SNR is increased due to the multi-user diversity scheme, therefore the received SNR at the CU can be expressed as

$$\gamma_{\mathrm{C}}^{\mathrm{III}} = \frac{P_{\mathrm{D}}\alpha}{P_{\mathrm{D}}(1-\alpha) + \frac{1}{\gamma_{\mathrm{TC}_{(M)}}}} \tag{4.10}$$

where $\gamma_{\mathrm{TC}_{(M)}} := \max_{1\leq i\leq M} \gamma_{\mathrm{TC}_i}$. Since only a single pair of D2D users is selected, there exists no peer interference at the DR_i. Hence the D2D users' received SNR is equivalent to Policy-I and we obtain as

$$\gamma_{\mathrm{D}_i}^{\mathrm{III}} = \gamma_{\mathrm{D}_i}^{\mathrm{I}}. \tag{4.11}$$

Policy-IV: Best r D2D Pairs

Analogous to Policy-II and III, instead of only a single pair of D2D users, best r D2D pairs can be activated to transmit in order to improve the CU's performance compared with Policy-III. The CU's received SNR in this case can be expressed as

$$\gamma_{\mathrm{C}}^{\mathrm{IV}} = \frac{P_{\mathrm{D}}\alpha}{P_{\mathrm{D}}(1-\alpha) + \frac{1}{\sum_{k=M-r+1}^{M} \gamma_{\mathrm{TC}_{(i)}}}}, \tag{4.12}$$

where $\sum_{k=M-r+1}^{M} \gamma_{\mathrm{TC}_{(i)}}$ is the sum of the r largest order statistics among all γ_{TC_i}. Since multiple D2D pairs are involved, each DR_i suffers from peer interference which can be controlled by the value of r. Therefore, the D2D users' received SNR can be obtained by replacing M with r in (4.9) as

$$\gamma_{\mathrm{D}_i}^{\mathrm{IV}} = \begin{cases} \dfrac{(1-\alpha)P_{\mathrm{D}}\gamma_{\mathrm{TR}_i}}{\sum_{j=1,j\neq i}^{r}(1-\alpha)P_{\mathrm{D}}\gamma_{\mathrm{int}_{ij}} + 1}, & \text{perfect cancellation} \\ \dfrac{(1-\alpha)P_{\mathrm{D}}\gamma_{\mathrm{TR}_i}}{\alpha P_{\mathrm{D}}\gamma_{\mathrm{TR}_i} + \sum_{j=1,j\neq i}^{r} P_{\mathrm{D}}\gamma_{\mathrm{int}_{ij}} + 1}, & \text{imperfect cancellation.} \end{cases} \tag{4.13}$$

4.2 Average Achievable Rates and the Rate Trade-off

In this section, the achievable rates of both the CU and the individual D2D users for all four policies are investigated. It will be observed that CU's performance is

improved as more D2D pairs are involved in the system. However, this deteriorates the individual D2D users' achievable rate simultaneously due to the coexistence of peer interference sources. This achievable rate trade-off can be balanced with the judicious choice of the power allocation factor α. To compare the average achievable rates across all policies, both the CU and the individual D2D users' performance have to be jointly considered. In Section 4.2.1 and 4.2.2, a tight approximation of the CU and D2D users' rates are provided. In Section 4.2.3, we adjust α to ensure that the CU's average achievable rates are the same over all policies, and to get a fair comparison of the individual D2D achievable rates for the different policies. Both perfect and imperfect interference cancellation scenarios at the DR_i are studied. We show in Section 4.2.3 that there is a maximum number of D2D users that can be accommodated for policies with multiple D2D users (Policy-II and IV), while maintaining the same average CU rate as Policy-I.

4.2.1 Average Achievable Rate of the Cellular User

Each individual relay channel instantaneous SNR γ_{TC_i} is assumed to be exponentially distributed with mean μ due to the Rayleigh fading model. The average achievable rate of the CU in Policy-I is defined as

$$\overline{R}_{\mathrm{C}}^{\mathrm{I}}(\mu) := \mathbb{E}\left[\log(1+\gamma_{\mathrm{C}}^{\mathrm{I}})\right] = \mathbb{E}\left[\log\left(1+\frac{P_{\mathrm{D}}\alpha}{P_{\mathrm{D}}(1-\alpha)+\frac{1}{\gamma_{\mathrm{TC}_i}}}\right)\right]. \tag{4.14}$$

In the existing literature [123, 124], expectations of the form $\mathbb{E}[\log(1+\mathcal{X})]$ are expanded using Taylor series at the mean value of $\mathcal{X}$ with the N^{th} order Taylor series, where the remainder is simply ignored to obtain an approximation. For the computation of (4.14) this presents challenges. Firstly, this approach requires the moments of $\gamma_{\mathrm{C}}^{\mathrm{I}}$ in (4.5) which are hard to compute and work with. Moreover the Taylor expansion

of $\log(1+x)$ does not converge for all x, and the remainder goes to infinity faster than all its lower order terms at the high SNR regime.

In contrast, in this chapter, we expand $\overline{R}_{\mathrm{C}}^{\mathrm{I}}(\mu)$ using Taylor series at the mean value of γ_{TC_i}, and show that the series is tight at the small μ regime. This involves working with the function $\log(1+\frac{1}{1+\frac{1}{x}})$ rather than $\log(1+x)$. Later in this section, the study is generalized to CU's achievable rates in other policies, which are compared with the Policy-I as a benchmark. The reason that small μ is of interest is that this is the regime where improvements over Policy-I are most possible. For example, instead of small μ, if μ is large, then CU's achievable rates for all four policies achieve their common upper-bound $\log(1+\alpha/(1-\alpha))$, which results in no improvement over Policy-I as $\mu \to \infty$.

Expanding the average achievable rate of the cellular link in Policy-I at the mean value of γ_{TC_i} using Taylor series with remainder and taking expectation we have

$$\overline{R}_{\mathrm{C}}^{\mathrm{I}}(\mu) = \log\left(1+\frac{P_{\mathrm{D}}\alpha}{P_{\mathrm{D}}(1-\alpha)+\frac{1}{\mu}}\right) + \sum_{n=1}^{N} \mathbb{E}\left[(\gamma_{\mathrm{TC}_i}-\mu)^n\right] \frac{1}{n!} \frac{\partial^n \log\left(1+\frac{P_{\mathrm{D}}\alpha}{P_{\mathrm{D}}(1-\alpha)+\frac{1}{\mu}}\right)}{\partial \mu^n} + \mathbb{E}[R_N(\gamma_{\mathrm{TC}_i})], \tag{4.15}$$

which can be further simplified as seen next:

Theorem 14. *CU's average achievable rate $\overline{R}_{\mathrm{C}}^{\mathrm{I}}(\mu)$ in Policy-*I *can be expressed as*

$$\overline{R}_{\mathrm{C}}^{\mathrm{I}}(\mu) = \log\left(1+\frac{P_{\mathrm{D}}\alpha}{P_{\mathrm{D}}(1-\alpha)+\frac{1}{\mu}}\right) - \sum_{n=2}^{N}(-\mu)^n(n-1)!\left(\frac{P_{\mathrm{D}}^n}{(1+P_{\mathrm{D}}\mu)^n} - \frac{P_{\mathrm{D}}^n(1-\alpha)^n}{(1+P_{\mathrm{D}}(1-\alpha)\mu)^n}\right)\sum_{i=0}^{n}\frac{1}{i!} + o(\mu^N), \tag{4.16}$$

as $\mu \to 0$.

Proof. See Appendix G. □

Theorem 14 shows that the remainder can be neglected as $\mu \to 0$ as long as $\mathbb{E}[\gamma_{\mathrm{TC}_i}^{N+1}] = o(\mu^N)$, which indicates that the Taylor series of $\overline{R}_{\mathrm{C}}^{\mathrm{I}}(\mu)$ in (4.15) can be truncated at any finite order N, and remains tight for sufficiently small μ. Since $\mathbb{E}[\gamma_{\mathrm{TC}_i} - \mu] = 0$, the first order term with $n = 1$ in (4.15) is guaranteed to be 0 regardless of the distribution of γ_{TC_i} and the value of μ. Furthermore, it implies that the higher order terms in (4.16) with $N > 1$ can be neglected at the small μ regime. Notice that the first term in (4.16) is what is obtained by Jensen's inequality by using the convexity of $\log\left(1 + \frac{1}{1+\frac{1}{x}}\right)$, with respect to x.

For simplicity, we retain the second order term in (4.16) with $N = 2$ in order to tightly approximate $\overline{R}_{\mathrm{C}}^{\mathrm{I}}(\mu)$ for small values of μ as follows:

$$\overline{R}_{\mathrm{C}}^{\mathrm{I}}(\mu) = \log\left(1 + \frac{P_{\mathrm{D}}\alpha}{P_{\mathrm{D}}(1-\alpha) + \frac{1}{\mu}}\right) - \frac{\alpha P_{\mathrm{D}}^2(2 + 2(1-\alpha)P_{\mathrm{D}}\mu - \alpha)\mu^2}{(P_{\mathrm{D}}\mu + 1)^2((1-\alpha)P_{\mathrm{D}}\mu + 1)^2} + o(\mu^2). \tag{4.17}$$

Using the second order approximation, we can express the average achievable rate in terms of the first and second order moments of the relay channel gains γ_{TC_i} at the CU regardless of its distribution, for small SNRs μ. It will be seen in the simulations (Section 4.4) that the second order approximation is quite accurate not just for small μ, but for all values of μ. This approximation is useful when we study the system performance in various access policies where the mean and variance of the equivalent relay gains at the CU are available.

In Policy-II, $\sum_{i=1}^{M} \gamma_{\mathrm{TC}_i} \sim \mu\chi^2(2M)$ is distributed as chi-square with $2M$ degrees of freedom with mean value $M\mu$. Since the n^{th} order moment of $\sum_{i=1}^{M} \gamma_{\mathrm{TC}_i}$ is equivalent to the n^{th} order derivative of its moment generating function (MGF) $M(t)$ with respect to t at $t = 0$, we have

$$\mathbb{E}\left[\left(\sum_{i=1}^{M} \gamma_{\mathrm{TC}_i}\right)^n\right] = \left.\frac{\partial^n M(t)}{\partial t^n}\right|_{t=0} = \left.\frac{\partial^n (1-\mu t)^{-M}}{\partial t^n}\right|_{t=0} = \mu^n \prod_{k=0}^{n-1}(M+k), \tag{4.18}$$

which satisfies the condition $\mathbb{E}\left[\left(\sum_{i=1}^{M}\gamma_{\mathrm{TC}_i}\right)^{N+1}\right] = o(\mu^N)$. Hence similar to Theorem 14, the CU's achievable rate can be expanded around $\mathbb{E}\left[\sum_{i=1}^{M}\gamma_{\mathrm{TC}_i}\right]$ tightly using finite order Taylor series.

Notice that

$$\mathbb{E}\left[\sum_{i=1}^{M}\gamma_{\mathrm{TC}_i}\right] = M\mu \tag{4.19}$$

$$\mathrm{var}\left[\sum_{i=1}^{M}\gamma_{\mathrm{TC}_i}\right] = M\mu^2, \tag{4.20}$$

and substituting into (4.17), the second order approximation of the achievable rate for the CU in Policy-II can be expressed as

$$\begin{aligned}\overline{R}_{\mathrm{C}}^{\mathrm{II}}(\mu, M) &:= \mathbb{E}\left[\log\left(1+\frac{P_{\mathrm{D}}\alpha}{P_{\mathrm{D}}(1-\alpha)+\frac{1}{\sum_{i=1}^{M}\gamma_{\mathrm{TC}_i}}}\right)\right] \\ &= \log\left(1+\frac{P_{\mathrm{D}}\alpha}{P_{\mathrm{D}}(1-\alpha)+\frac{1}{M\mu}}\right) - \frac{\alpha P_{\mathrm{D}}^2(2+2(1-\alpha)P_{\mathrm{D}}M\mu-\alpha)M\mu^2}{(P_{\mathrm{D}}M\mu+1)^2((1-\alpha)P_{\mathrm{D}}M\mu+1)^2} + o(\mu^2).\end{aligned} \tag{4.21}$$

It can be observed from (4.21) that the CU's achievable rate in Policy-II outperforms that of Policy-I since $M\mu > \mu$. However the D2D users have more interference in Policy-II. This trade-off is controlled by α, and the selection of which will be discussed in Section 4.2.3 to fairly compare both policies.

Theorem 14 can be adapted to Policy-III and IV as well. For the sake of simplicity, we focus on the second order approximation. In Policy-III, with selection diversity, the relay channel gain $\gamma_{\mathrm{TC}_{(M)}}$ yields the largest order statistic among M i.i.d. random variables γ_{TC_i}, and it can be shown in [125] that

$$\mathbb{E}[\gamma_{\mathrm{TC}_{(M)}}] = \mu\sum_{i=1}^{M}\frac{1}{i} \tag{4.22}$$

$$\mathrm{var}[\gamma_{\mathrm{TC}_{(M)}}] = \mu^2\sum_{i=1}^{M}\frac{1}{i^2}. \tag{4.23}$$

Substituting the mean and variance into (4.17), we obtain the second order approximation of the achievable rate for the CU in Policy-III

$$\overline{R}_{\mathrm{C}}^{\mathrm{III}}(\mu, M) := \mathbb{E}\left[\log\left(1+\frac{P_{\mathrm{D}}\alpha}{P_{\mathrm{D}}(1-\alpha)+\frac{1}{\gamma_{\mathrm{TC}_{(M)}}}}\right)\right] = \log\left(1+\frac{P_{\mathrm{D}}\alpha}{P_{\mathrm{D}}(1-\alpha)+\frac{1}{\mu\sum_{i=1}^{M}\frac{1}{i}}}\right)$$
$$-\frac{\alpha P_{\mathrm{D}}^2(2+2(1-\alpha)P_{\mathrm{D}}\mu\sum_{i=1}^{M}\frac{1}{i}-\alpha)(\mu^2\sum_{i=1}^{M}\frac{1}{i^2})}{(P_{\mathrm{D}}\mu\sum_{i=1}^{M}\frac{1}{i}+1)^2((1-\alpha)P_{\mathrm{D}}\mu\sum_{i=1}^{M}\frac{1}{i}+1)^2}+o(\mu^2). \tag{4.24}$$

In contrast to Policy-II, CU's achievable rate in Policy-III is less since M as $\mu\sum_{i=1}^{M}\frac{1}{i} < \mu M$. However, the D2D user performance is improved due to no peer interference at the DR_i.

In Policy-IV, $\sum_{k=M-r+1}^{M}\gamma_{\mathrm{TC}_{(i)}}$ is the sum of the largest k order statistics drawn from M i.i.d. exponential parent random variables γ_{TC_i}. The k^{th} order statistic, $\gamma_{\mathrm{TC}_{(i)}}$, can be expressed as a linear function of independent exponential random variables $\{\mathcal{Y}_i\}$ each with mean value μ [125, 126] as

$$\gamma_{\mathrm{TC}_{(i)}} = \sum_{i=1}^{k}\frac{\mathcal{Y}_i}{M-i+1}, \tag{4.25}$$

so that

$$\mathbb{E}\left[\sum_{k=M-r+1}^{M}\gamma_{\mathrm{TC}_{(i)}}\right] = \mathbb{E}\left[\sum_{k=M-r+1}^{M}\sum_{i=1}^{k}\frac{\mathcal{Y}_i}{M-i+1}\right] = \mathbb{E}\left[\sum_{i=1}^{r}\mathcal{Y}_i + r\sum_{i=r+1}^{M}\frac{\mathcal{Y}_i}{i}\right] \tag{4.26}$$
$$= r\mu\left(1+\sum_{i=r+1}^{M}\frac{1}{i}\right). \tag{4.27}$$

Analogously the variance of $\sum_{k=M-r+1}^{M}\gamma_{\mathrm{TC}_{(i)}}$ can be obtained as

$$\mathrm{var}\left[\sum_{k=M-r+1}^{M}\gamma_{\mathrm{TC}_{(i)}}\right] = \mathrm{var}\left[\sum_{i=1}^{r}\mathcal{Y}_i + r\sum_{i=r+1}^{M}\frac{\mathcal{Y}_i}{i}\right] = r\mu^2 + r^2\mu^2\sum_{i=r+1}^{M}\frac{1}{i^2}. \tag{4.28}$$

Substituting the mean and variance of $\sum_{k=M-r+1}^{M} \gamma_{\mathrm{TC}_{(i)}}$ into (4.17), we obtain the second order approximation of the achievable rate for the CU in Policy-IV

$$\begin{aligned}
\overline{R}_{\mathrm{C}}^{\mathrm{IV}}(\mu, r, M) &:= \mathbb{E}\left[\log\left(1 + \frac{P_{\mathrm{D}}\alpha}{P_{\mathrm{D}}(1-\alpha) + \frac{1}{\sum_{k=M-r+1}^{M}\gamma_{\mathrm{TC}_{(i)}}}}\right)\right] \\
&= \log\left(1 + \frac{P_{\mathrm{D}}\alpha}{P_{\mathrm{D}}(1-\alpha) + \frac{1}{r\mu + r\mu\sum_{i=r+1}^{M}\frac{1}{i}}}\right) \\
&- \frac{\alpha P_{\mathrm{D}}^2\left(2 + 2(1-\alpha)P_{\mathrm{D}}r\mu\left(1 + \sum_{i=r+1}^{M}\frac{1}{i}\right) - \alpha\right) r\mu^2\left(1 + \sum_{i=r+1}^{M}\frac{1}{i^2}\right)}{\left(P_{\mathrm{D}}r\mu\left(1 + \sum_{i=r+1}^{M}\frac{1}{i}\right) + 1\right)^2\left((1-\alpha)P_{\mathrm{D}}r\mu\left(1 + \sum_{i=r+1}^{M}\frac{1}{i}\right) + 1\right)^2} + o(\mu^2)
\end{aligned} \tag{4.29}$$

In equation (4.29) when $r = 1$, only the single best D2D pair is selected and Policy-IV is equivalent to Policy-III. When $r = M$, all M D2D pairs are involved and Policy-IV is equivalent to Policy-II. This implies that CU's achievable rate in Policy-IV is traded off against the D2D users' performance by the value of r.

As already mentioned, the second order approximation overlaps with true value of the achievable rate not just in the small μ regime. When μ is large, the CU's average achievable rate converges to $\log(1 + \alpha/(1-\alpha))$ and our approximations still remain tight since the average achievable rate is bounded.

4.2.2 Average Achievable Rate for D2D Links

The average achievable rate for an individual D2D pair can be categorized into two scenarios: single and multiple D2D pairs. In Policy-I and III, where there is only a single D2D pair is involved and no peer interference at the DR_i, the average achievable rate of an individual D2D user can be obtained as

$$\overline{R}_{\mathrm{D}}^{\mathrm{I}}(\mu) = \overline{R}_{\mathrm{D}}^{\mathrm{III}}(\mu) := \mathbb{E}\left[\log\left(1 + P_{\mathrm{D}}(1-\alpha)\gamma_{\mathrm{TR}_i}\right)\right] = P_{\mathrm{D}}(1-\alpha)\frac{e^{\frac{1}{\mu}}\Gamma(0, \frac{1}{\mu})}{\mu}, \tag{4.30}$$

where $\Gamma(a, z) = \int_z^\infty t^{a-1}e^{-t}dt$ is the upper incomplete gamma function, which is difficult to work with. To get a second-order approximation, observe that the second

term in (4.30) can be expanded around the mean value of γ_{TR_i} to obtain

$$\overline{R}_{\mathrm{D}}^{\mathrm{I}}(\mu) = \overline{R}_{\mathrm{D}}^{\mathrm{III}}(\mu) = \log(1 + P_{\mathrm{D}}(1-\alpha)\mu) - \frac{\mu^2 P_{\mathrm{D}}^2 (1-\alpha)^2}{\left(1 + (1-\alpha)P_{\mathrm{D}}\mu\right)^2} + o(\mu^2), \tag{4.31}$$

for small μ, in which the Taylor series remainder is quantified as $o(\mu^2)$ similar to Theorem 14. We will use the second order approximation when studying the performance trade-off between the cellular and D2D networks.

In Policy-II, the desired D2D pair coexists with $M-1$ peer interference components. The received SNR at DR_i is given by

$$\gamma_{\mathrm{D}_i}^{\mathrm{II}} = \frac{P_{\mathrm{D}}(1-\alpha)\gamma_{\mathrm{TR}_i}}{P_{\mathrm{D}}(1-\alpha)\mathcal{Z} + 1}, \tag{4.32}$$

where γ_{TR_i} is exponentially distributed with mean value μ, and $\mathcal{Z} := \sum_{j=1, j\neq i}^{M} \gamma_{\mathrm{int}_{ij}}$ is chi-squared with $2M-2$ degrees of freedom with mean value $\beta(M-1)$. Similar to (4.31), we can expand $\overline{R}_{\mathrm{D}}^{\mathrm{II}}(\mu, M)$ at the mean values of γ_{TR_i} and $\mathcal{Z}$ to study the asymptotic behavior of $\overline{R}_{\mathrm{D}}^{\mathrm{II}}(\mu, M)$ as a function of M for small μ and β. The following theorem address this multi-variate scenario.

Theorem 15. *D2D users' average achievable rate $\overline{R}_{\mathrm{D}}^{\mathrm{II}}(\mu, M)$ in Policy-*II *can be expanded using finite N-order Taylor series at $\mathbb{E}[\gamma_{\mathrm{TR}_i}] = \mu$ and $\mathbb{E}[\mathcal{Z}] = (M-1)\beta$. When $N = 2$, the second order approximation of $\overline{R}_{\mathrm{D}}^{\mathrm{II}}(\mu, M)$ is expressed as*

$$\begin{aligned}
\overline{R}_{\mathrm{D}}^{\mathrm{II}}(\mu, M) &:= \mathbb{E}\left[\log\left(1 + \frac{P_{\mathrm{D}}(1-\alpha)\gamma_{\mathrm{TR}_i}}{P_{\mathrm{D}}(1-\alpha)\mathcal{Z} + 1}\right)\right] \\
&= \log\left(1 + \frac{P_{\mathrm{D}}(1-\alpha)\mu}{P_{\mathrm{D}}(1-\alpha)(M-1)\beta + 1}\right) + \frac{P_{\mathrm{D}}^2(1-\alpha)^2\mu^2}{(1 + P_{\mathrm{D}}(1-\alpha)((M-1)\beta + \mu))^2} \\
&\quad + \frac{(M-1)P_{\mathrm{D}}^3(1-\alpha)^3\beta^2\mu(2 + P(1-\alpha)(2(M-1)\beta + \mu))}{(1 + P_{\mathrm{D}}(M-1)(1-\alpha)\beta)^2(1 + P_{\mathrm{D}}(1-\alpha)((M-1)\beta + \mu))^2} + o(\mu^2).
\end{aligned} \tag{4.33}$$

where $\mu, \beta \to 0$, and β is related to μ through a proportionality constant.

Proof. The proof involves expanding $\log\left(1 + \frac{P_{\mathrm{D}}(1-\alpha)\gamma_{\mathrm{TR}_i}}{P_{\mathrm{D}}(1-\alpha)\mathcal{Z}+1}\right)$ using a multivariate Taylor series around the mean values of γ_{TR_i} and $\mathcal{Z}$. Please see Appendix H for details. □

In Policy-IV, the second order approximation of individual D2D users' rates $\overline{R}_{\mathrm{D}}^{\mathrm{IV}}(\mu, r)$ can be derived similar to Theorem 15 by substituting M with r in (4.33).

4.2.3 Average Achievable Rate Trade-off between the CU and the D2D User

Due to the superposition coding scheme, CU and D2D users transmit simultaneously, hence their performance have to be jointly considered. In this section, we aim to show that Policy-II, III and IV all potentially outperform the existing benchmark Policy-I in the sense of both CU's and individual D2D users' performance.

To achieve a fair comparison between the different policies, we adjust the power allocation factor α in order to maintain the CU's performance the same for all policies and compare the D2D users' performance. CU's performance is improved due to multiple active D2D relays in Policy-II and IV, and the selection diversity in the Policy-III. Hence, each DT_i can reduce its α in forwarding x_{C}, and allocate the saved power to transmit its own signal x_{D_i} in order to compensate for the interference caused by the peer DT_j. We are able to show that both the CU and the D2D users' achievable rate performance has large potential to improve simultaneously compared to Policy-I, whether the CU's interference can be canceled by DR_i perfectly or not.

Perfect Interference Cancellation

In this section, we assume that x_{C} received from the CU is successfully decoded by DR_i at the end of the first transmission phase, hence gets canceled when decoding x_{D_i}. Assuming that μ is small, ignoring the high order terms and solving $\overline{R}_{\mathrm{C}}^{\mathrm{I}}(\mu) = \overline{R}_{\mathrm{C}}^{\mathrm{II}}(\mu, M)$ from equations (4.17) and (4.21), the relationship between power allocation factors α_{I} and α_{II} in two policies can be characterized as

$$\alpha_{\mathrm{II}} = \frac{P_{\mathrm{D}} + \frac{1}{M\mu}}{P_{\mathrm{D}} + \frac{1}{\mu}} \alpha_{\mathrm{I}}. \tag{4.34}$$

Since $\overline{R}_{\mathrm{D}}^{\mathrm{II}}(\mu, M)$ is decreasing in α_{II} and $\alpha_{\mathrm{II}} \leq \alpha_{\mathrm{I}}$, to maintain the same achievable rate for the CU, the relay power on x_{D_i} in Policy-II can be increased to overcome the cumulative peer interference at each DR_i.

When the DT_i transmits with power allocation factor α_{II} in (4.34), the achievable rate $\overline{R}_{\mathrm{C}}^{\mathrm{II}}(\mu, M)$ is maintained the same as $\overline{R}_{\mathrm{C}}^{\mathrm{I}}(\mu)$, and we can obtain the maximum number of D2D pairs M numerically that Policy-II outperforms Policy-I by substituting (4.34) into (4.33) and solving $\overline{R}_{\mathrm{D}}^{\mathrm{II}}(\mu, M) \geq \overline{R}_{\mathrm{D}}^{\mathrm{I}}(\mu)$. Assuming that μ is small and β is related to μ through a proportionality constant, the maximum M can be expressed in closed form as

$$M \leq \frac{-B \pm \sqrt{B^2 - 4AC}}{2A} \tag{4.35}$$

where

$$A = 2P\beta(\alpha_{\mathrm{I}} - 1), \tag{4.36}$$

$$B = \alpha_{\mathrm{I}} + \alpha_{\mathrm{I}}^2 \mu P_{\mathrm{D}} - \alpha_{\mathrm{I}} \beta P_{\mathrm{D}} - 2\alpha_{\mathrm{I}} \mu P_{\mathrm{D}} + \beta P_{\mathrm{D}}, \tag{4.37}$$

$$C = -2\alpha_{\mathrm{I}} + \alpha_{\mathrm{I}}^2. \tag{4.38}$$

Further assuming that $\mu \ll 1/P_{\mathrm{D}}$, (4.35) can be reduced to

$$M \leq 1 \quad \text{or} \quad M \leq \frac{\alpha_{\mathrm{I}}(\beta P_{\mathrm{D}} - \alpha_{\mathrm{I}} \beta P_{\mathrm{D}} + 1)}{(1 - \alpha_{\mathrm{I}})\beta P_{\mathrm{D}}}. \tag{4.39}$$

We can conclude from (4.39) that as long as $\frac{\alpha_{\mathrm{I}}(\beta P_{\mathrm{D}} - \alpha_{\mathrm{I}} \beta P_{\mathrm{D}} + 1)}{(1 - \alpha_{\mathrm{I}})\beta P_{\mathrm{D}}} \geq 2$, referred as the power dominant region, the interference at DR_i caused by other peer DTs can be compensated by allocating more power on its desired signal x_{D_i}, equivalently decreasing the power allocation factor α_{II} according to (4.34). In contrast, when $\frac{\alpha_{\mathrm{I}}(\beta P_{\mathrm{D}} - \alpha_{\mathrm{I}} \beta P_{\mathrm{D}} + 1)}{(1 - \alpha_{\mathrm{I}})\beta P_{\mathrm{D}}} < 2$, referred as the interference dominant region, the CU and the individual D2D users' performance can not be improved at the same time due to the large number of peer interference sources. This will be verified in Section 4.4 numerically. In (4.39), M

can be shown to be decreasing in β, which implies that when the peer interference channel $\gamma_{\mathrm{int}_{ij}}$ is strong comparing with the D2D channel γ_{TR_i}, few D2D pairs are preferred from the individual D2D users' rates perspective, and vice versa. On the other hand, when the equality in (4.39) holds, the sum rate of all active D2D users has a multiplexing gain of M compared with the single active D2D pair case, hence improves the spectral efficiency significantly.

Similarly, in Policy-III and IV, substituting mean values of $\gamma_{\mathrm{TC}_{(M)}}$ and $\gamma_{\mathrm{TC}_{r:M}}$ into (4.34), we obtain

$$\alpha_{\mathrm{III}} = \frac{P_{\mathrm{D}} + \frac{1}{\mu \sum_{i=1}^{M} \frac{1}{i}}}{P_{\mathrm{D}} + \frac{1}{\mu}} \alpha_{\mathrm{I}} \tag{4.40}$$

and

$$\alpha_{\mathrm{IV}} = \frac{P_{\mathrm{D}} + \frac{1}{r\mu + r\mu \sum_{i=r+1}^{M} \frac{1}{i}}}{P_{\mathrm{D}} + \frac{1}{\mu}} \alpha_{\mathrm{I}} \tag{4.41}$$

respectively to ensure that the CU performance for all policies are the same so that we can focus on the D2D user performance. Since there is no peer interference in Policy-III, $\overline{R}_{\mathrm{D}}^{\mathrm{III}}(\mu)$ is always increasing in M, which is preferred when the average interference channel gain β is large. However, since only a single D2D pair is selected, the spectrum is not utilized efficiently, and it may cause fairness issues among the D2D users. For Policy-IV, the maximum r on $\overline{R}_{\mathrm{D}}^{\mathrm{IV}}(\mu, r) \geq \overline{R}_{\mathrm{D}}^{\mathrm{I}}(\mu)$ can be derived analogously to (4.39) by substituting (4.41) into (4.33).

Imperfect Interference Cancellation

When x_{C} can not be perfectly decoded and removed from the DR_i's received signal, the DR_i suffers not only the possible peer interference from the DT_j as well as the interference while decoding x_{D_i}. In this scenario, we will show that the similar achievable rate trade-off can also be observed and the maximum value of M will be derived.

In Policy-II, when both peer interference and CU's interference exist, the received SNR at the DR_i is given by

$$\gamma_{\mathrm{D}_i}^{\mathrm{II}} = \frac{(1-\alpha)P_{\mathrm{D}}\gamma_{\mathrm{TR}_i}}{\alpha P_{\mathrm{D}}\gamma_{\mathrm{TR}_i} + P_{\mathrm{D}}\mathcal{Z} + 1}. \tag{4.42}$$

Similar to Theorem 15, we obtain the second order approximation of $\overline{R}_{\mathrm{D}}^{\mathrm{II}}(\mu, M)$ as

$$\begin{aligned}\overline{R}_{\mathrm{D}}^{\mathrm{II}}(\mu, M) &= \log\left(1 + \frac{(1-\alpha)P_{\mathrm{D}}\mu}{\alpha P_{\mathrm{D}}\mu + P_{\mathrm{D}}\beta(M-1)+1}\right) \\ &- \frac{P_{\mathrm{D}}(1-\alpha)(1+P_{\mathrm{D}}(M-1)\beta)\mu^2(1+\alpha+P_{\mathrm{D}}(M-1)\beta+P_{\mathrm{D}}(M-1)+2P_{\mathrm{D}}\alpha\mu)}{(1+P_{\mathrm{D}}(M-1)\beta+P_{\mathrm{D}}\mu)^2(1+P_{\mathrm{D}}(M-1)\beta+P_{\mathrm{D}}\alpha\mu)^2} \\ &+ \frac{P_{\mathrm{D}}^3(1-\alpha)(M-1)\beta^2(2+P_{\mathrm{D}}(2(M-1)\beta(1+\alpha)\mu))}{(1+P_{\mathrm{D}}(M-1)\beta+P_{\mathrm{D}}\mu)^2(1+P_{\mathrm{D}}(M-1)\beta+P_{\mathrm{D}}\alpha\mu)^2} + o(\mu^2).\end{aligned} \tag{4.43}$$

Due to the fact that the CU's achievable rate is not affected by introducing this interference, (4.34) still holds in this case. We can substitute (4.34) into (4.43) and solve $\overline{R}_{\mathrm{D}}^{\mathrm{II}}(\mu, M) \geq \overline{R}_{\mathrm{D}}^{\mathrm{I}}(\mu)$ numerically to observe the maximum M that Policy-II outperforms Policy-I. Further assuming that μ is small and β is related to μ through a proportionality constant, the maximum M can be obtained in closed form as

$$M \leq \max\left\{\frac{-B+\sqrt{B^2-4AC}}{2A}, \frac{-B-\sqrt{B^2-4AC}}{2A}\right\} = \frac{-B-\sqrt{B^2-4AC}}{2A} \tag{4.44}$$

where

$$A = 2P\beta(\alpha_{\mathrm{I}} - 1) < 0, \tag{4.45}$$

$$B = \alpha_{\mathrm{I}} + \beta P_{\mathrm{D}} - \alpha_{\mathrm{I}}\beta P_{\mathrm{D}} > 0, \tag{4.46}$$

$$C = -\alpha_{\mathrm{I}} - \alpha_{\mathrm{I}}\mu + \alpha_{\mathrm{I}}^2\mu < 0. \tag{4.47}$$

For Policy-IV, the maximum r that enables $\overline{R}_{\mathrm{D}}^{\mathrm{IV}}(\mu, r)$ outperforming $\overline{R}_{\mathrm{D}}^{\mathrm{I}}(\mu)$ can be derived analogously to (4.44) by substituting (4.41) into (4.43) and solving $\overline{R}_{\mathrm{D}}^{\mathrm{IV}}(\mu, r) \geq \overline{R}_{\mathrm{D}}^{\mathrm{I}}(\mu)$ numerically. These maximum values on M and r under both perfect and imperfect interference cancellation scenarios will be verified numerically in Section

4.4. It can be observed that the perfect interference cancellation does not necessarily accommodate more D2D pairs than the imperfect case, since unlike the peer interference terms, this interference of the CU deteriorates the D2D users' performance in all policies.

Notice that this performance trade-off can be studied for general fading distributions other than Rayleigh fading [127, 128], and a general SNR expression. For instance, with the assumption of proximity between D2D pairs, the DT_i-DR_i channel can yield Rician fading. Analogously to Theorem 14 and 15, we can expand $\overline{R}_{\mathrm{D}}^{\mathrm{I}}(\mu)$ and $\overline{R}_{\mathrm{D}}^{\mathrm{II}}(\mu, M)$ where γ_{TR_i} is non-central gamma distribution with two degrees of freedom and the non-central parameter depending the power of the line of sight (LoS) component. We do not pursue this here due to space limitations.

4.3 Cooperative D2D System with Random Number of D2D Pairs

Practically, the DUs could be on and off with a certain probability, or moving in and out the cellular network coverage randomly. Hence at each time instant, the active number of DUs is usually a random number characterized by a certain positive discrete distribution. In this section, we start with deriving the scaling laws of the CU's rate in Policy-III, following by comparing the system performance in different DU distributions through stochastic ordering.

*4.3.1 Scaling Laws of the CU's Average Achievable Rates in Policy-*III

Theorem 16. *In Policy-*III*, the number of D2D pairs is a Poisson random variable $\mathcal{M}$ with mean value λ, the achievable rate of the CU averaged across fading and user distribution has the following scaling laws as $\lambda \to \infty$:*

$$\mathbb{E}_{\mathcal{M}}[\overline{R}_{\mathrm{C}}^{\mathrm{III}}(\mu, \mathcal{M})] = \log(1 + \frac{P_{\mathrm{D}}\alpha}{P_{\mathrm{D}}(1-\alpha) + \frac{1}{\mu \log(\lambda)}}) + O\left(\frac{\alpha}{P_{\mathrm{D}}(1-\alpha)^2 \log(\lambda)}\right).$$

Proof. Defining $y := e^{-x/\mu}$ and integrating by substitution,

$$\begin{aligned}
\mathbb{E}_{\mathcal{M}}[\overline{R}_{\mathrm{C}}^{\mathrm{III}}(\mu,\mathcal{M})] &= \int_0^\infty \log(1+\frac{P_{\mathrm{D}}\alpha}{P_{\mathrm{D}}(1-\alpha)+\frac{1}{x}})d(1-\exp(-\lambda e^{-\frac{x}{\mu}})) \\
&= P_{\mathrm{D}}\alpha\int_0^1 \frac{1-e^{-\lambda y}}{(1-\mu P_{\mathrm{D}}(1-\alpha)\log(y))^2(1+\frac{P_{\mathrm{D}}\alpha}{P_{\mathrm{D}}(1-\alpha)-\frac{1}{\mu\log(y)}})}\left(\frac{\mu}{y}\right)dy \\
&= P_{\mathrm{D}}\alpha\int_0^{\frac{\log\lambda}{\lambda}} \frac{1-e^{-\lambda y}}{h(y)g(y)}\left(\frac{\mu}{y}\right)dy + P_{\mathrm{D}}\alpha\int_{\frac{\log\lambda}{\lambda}}^1 \frac{1-e^{-\lambda y}}{h(y)g(y)}\left(\frac{\mu}{y}\right)dy \qquad (4.48)
\end{aligned}$$

where $g(y) = 1+\frac{P_{\mathrm{D}}\alpha}{P_{\mathrm{D}}(1-\alpha)-\frac{1}{\mu\log(y)}}$ and $h(x) = (1-\mu P_{\mathrm{D}}(1-\alpha)\log(y))^2$. For the first term after the third equality in (4.48), we have the following inequalities:

$$\begin{aligned}
0 &< P_{\mathrm{D}}\alpha\int_0^{\frac{\log\lambda}{\lambda}} \frac{1-e^{-\lambda y}}{h(y)g(y)}\left(\frac{\mu}{y}\right)dy \\
&< P_{\mathrm{D}}\alpha\int_0^{\frac{\log\lambda}{\lambda}} \frac{\lambda y}{h(\log(\lambda)/\lambda)g(\log(\lambda)/\lambda)}\left(\frac{\mu}{y}\right)dy \qquad (4.49) \\
&= \frac{P_{\mathrm{D}}\alpha\mu\log(\lambda)}{(1+\mu P_{\mathrm{D}}(1-\alpha)(\log(y)-\log(\log(\lambda))))^2(1+\frac{P_{\mathrm{D}}\alpha}{P_{\mathrm{D}}(1-\alpha)+\frac{\mu}{\log(y)-\log(\log(y))}})} \qquad (4.50)
\end{aligned}$$

The right hand side in (4.49) holds because the denominator of the integrand is replaced with its lower limit. It can be seen that the upper bound after the equality in (4.50) yields $O\left(\frac{\alpha}{P_{\mathrm{D}}(1-\alpha)^2\log(\lambda)}\right)$ and has limit 0 as $\lambda\to\infty$. This implies that the first term in (4.48) should have limit 0. The second term in (4.48) has the upper and lower bounds given by,

$$\begin{aligned}
P_{\mathrm{D}}\alpha\int_{\frac{\log\lambda}{\lambda}}^1 \frac{1-\frac{1}{\lambda}}{h(y)g(y)}\left(\frac{\rho}{y}\right)dy &< P_{\mathrm{D}}\alpha\int_{\frac{\log\lambda}{\lambda}}^1 \frac{1-\exp(e^{-\lambda y})}{h(x)g(x)}\left(\frac{\mu}{y}\right)dy \\
&< P_{\mathrm{D}}\alpha\int_{\frac{\log\lambda}{\lambda}}^1 \frac{1-e^{-\lambda}}{h(y)g(y)}\left(\frac{\mu}{y}\right)dy \qquad (4.51)
\end{aligned}$$

in which the lower and upper bounds are obtained by bounding the numerator. Carrying out the integral, the upper and lower bounds in (4.51) turn out to be

$$(1-1/\lambda)\log\left(1+\frac{P_{\mathrm{D}}\alpha}{P_{\mathrm{D}}(1-\alpha)+\frac{1}{\log(\lambda)-\log(\log(\lambda))}}\right) \qquad (4.52)$$

and

$$\left(1-e^{-\lambda}\right)\log\left(1+\frac{P_{\mathrm{D}}\alpha}{P_{\mathrm{D}}(1-\alpha)+\frac{1}{\log(\lambda)-\log(\log(\lambda))}}\right) \tag{4.53}$$

respectively. In (4.52),

$$\lim_{\lambda\to\infty}\frac{1}{\lambda}\log\left(1+\frac{P_{\mathrm{D}}\alpha}{P_{\mathrm{D}}(1-\alpha)+\frac{1}{\log(\lambda)-\log(\log(\lambda))}}\right)=0 \tag{4.54}$$

and in (4.53),

$$\lim_{\lambda\to\infty}e^{-\lambda}\log\left(1+\frac{P_{\mathrm{D}}\alpha}{P_{\mathrm{D}}(1-\alpha)+\frac{1}{\log(\lambda)-\log(\log(\lambda))}}\right)=0. \tag{4.55}$$

Hence, both (4.52) and (4.53) converge to $\log\left(1+\frac{P_{\mathrm{D}}\alpha}{P_{\mathrm{D}}(1-\alpha)+\frac{1}{\log(\lambda)}}\right)$. Considering (4.50) and (4.51), and we complete the proof. □

4.3.2 Laplace Transform Ordering of the Average Achievable Rates

Theorem 17. *In the Policy-*II, III*, assuming that the number of D2D pairs are positive discrete random variables $\mathcal{M}$ and $\mathcal{N}$ with same mean value λ, by assuming $\mathcal{M}\geq_{\mathrm{LT}}\mathcal{N}$, we have $\mathbb{E}_{\mathcal{M}}[\overline{R}_{\mathrm{C}}^{\mathrm{II}}(\mu,\mathcal{M})]\geq E_{\mathcal{N}}[E[R_{\mathrm{C}}^{\mathrm{II}}(\mu,\mathcal{N})]]$, and $\mathbb{E}_{\mathcal{M}}[\overline{R}_{\mathrm{C}}^{\mathrm{III}}(\mu,\mathcal{M})]\geq E_{\mathcal{N}}[E[R_{\mathrm{C}}^{\mathrm{III}}(\mu,\mathcal{N})]]$ at all SNR values.*

Proof. $\frac{1}{x}$ and $\frac{1}{1+x}$ are c.m. in x, so that their compound function $\frac{1}{1+\frac{1}{x}}$ is c.m.d. in x [129, P20]. Since $\log(1+x)$ is c.m.d. in x, hence $\log(1+\frac{1}{1+\frac{1}{x}})$ is c.m.d. in x. Assuming that $\mathcal{M}\geq_{\mathrm{LT}}\mathcal{N}$, in Policy-II it can be shown that [129, P273]

$$\sum_{i=1}^{\mathcal{M}}\gamma_{\mathrm{TC}_i}\geq_{\mathrm{LT}}\sum_{i=1}^{\mathcal{N}}\gamma_{\mathrm{TC}_i} \tag{4.56}$$

and

$$\gamma_{3_{(\mathcal{M})}}\geq_{\mathrm{LT}}\gamma_{3_{(\mathcal{N})}}. \tag{4.57}$$

Using Theorem 1 we have $\mathbb{E}_{\mathcal{M}}[\overline{R}_{\mathrm{C}}^{\mathrm{II}}(\mu,\mathcal{M})]\geq \mathrm{E}_{\mathcal{N}}[\mathrm{E}[R_{\mathrm{C}}^{\mathrm{II}}(\mu,\mathcal{N})]]$, and $\mathbb{E}_{\mathcal{M}}[\overline{R}_{\mathrm{C}}^{\mathrm{III}}(\mu,\mathcal{M})]\geq \mathrm{E}_{\mathcal{N}}[\mathrm{E}[R_{\mathrm{C}}^{\mathrm{III}}(\mu,\mathcal{N})]]$, which complete the proof. □

The achievable rates averaged across $\mathcal{M}$ and $\mathcal{N}$ following their corresponding order in the Laplace transform ordering sense. With the same average total transmission power consumed at all DT_i over the same fading channels, the order of achievable rates of the CU will be determined by the DU distributions. For example, when $\mathcal{N}$ is geometric distributed in Policy-II, the PDF of $\sum_{i=1}^{\mathcal{N}} \gamma_{\mathrm{TC}_i}$ can be obtain as

$$f(y) = \sum_{n=1}^{\infty} \frac{y^{n-1}}{\mu^n (n-1)!} e^{-\frac{y}{\mu}} (1-\frac{1}{\lambda})^{n-1} \frac{1}{\lambda} = \frac{1}{\mu\lambda} e^{-\frac{y}{\mu}} e^{\frac{(1-\frac{1}{\lambda}y)}{\mu}} = \frac{1}{\mu\lambda} e^{-\frac{y}{\mu\lambda}}, \tag{4.58}$$

which implies that $\sum_{i=1}^{\mathcal{N}} \gamma_{\mathrm{TC}_i}$ is an exponential random variable with parameter $\mu\lambda$. Hence $\mathrm{E}_{\mathcal{N}}[\mathrm{E}[R_{\mathrm{C}}^{\mathrm{II}}(\mu, \mathcal{N})]]$ can be considered as the achievable rate of a single pair of DT_i-DR_i averaged over a Rayleigh fading channel with parameter $\lambda\mu$. When $\mathcal{M} = \lambda$, $\mathbb{E}_{\mathcal{M}}[\overline{R}_{\mathrm{C}}^{\mathrm{II}}(\mu, \mathcal{M})]$ is equivalent to the achievable rates average over a Nakagami-m fading channel with parameter (λ, μ). From Theorem 17 we obtain that $\mathbb{E}_{\mathcal{M}}[\overline{R}_{\mathrm{C}}^{\mathrm{II}}(\mu, \mathcal{M})] \geq \mathrm{E}_{\mathcal{N}}[\mathrm{E}[R_{\mathrm{C}}^{\mathrm{II}}(\mu, \mathcal{N})]]$. Moreover, since the deterministic number is greater than any of its random counterpart in the Laplace transform ordering sense [105], among all fading channels with the same diversity order, the achievable rate of CU averaged over fading and user distributions is upper bounded by that of the Nakagami-m fading channel.

4.4 Simulations

In this section, we generate i.i.d. fading coefficients as random variables and use Monte-carlo simulations to plot average achievable rates derived in Section 4.2 and 4.3 to corroborate our analytical results. For all simulations, Rayleigh fading channels are assumed.

In Section 4.2.1, we provide the second order approximation of the average achievable rates of the CU in Policies-II,III, and IV, and showed that these approximations are tight in the small μ regime. In Fig. 4.2 and 4.3, (4.17), (4.21), (4.24) and (4.29) are depicted versus the total number of D2D paris M when $\mu = -10$dB, and $\mu = 5$dB,

respectively, and $\alpha = 0.8$ is the same for all policies. It can be observed that the approximate rates completely overlap with the Monte Carlo simulation results of when $\mu = -10$dB, and are tight even when $\mu = 5$ dB. In Policy-IV, the number of active D2D pairs is always $r = 2$. Multiple D2D pairs are selected in Policy-II, while only a single D2D pair without selection is involved in Policy-I. Notice that all policies in Fig. 4.2 and 4.3 use the same α to illustrate the accuracy of our approximations.

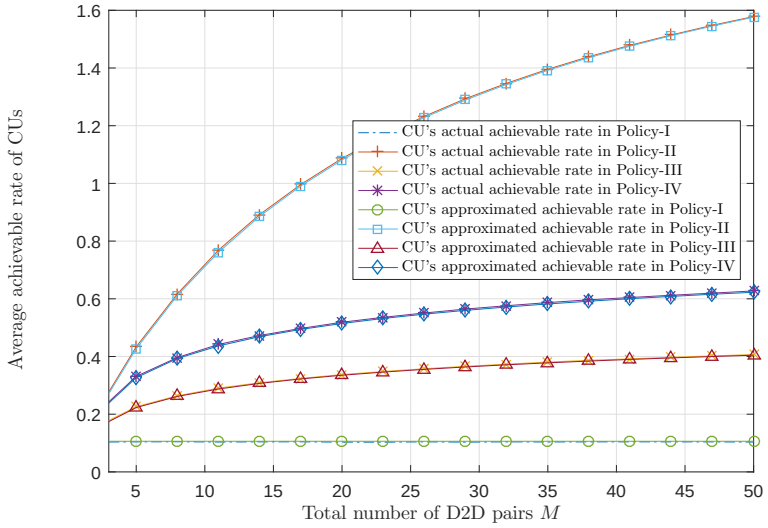

Figure 4.2: CU's Approximated Rates in All Policies with $\mu = -10$dB.

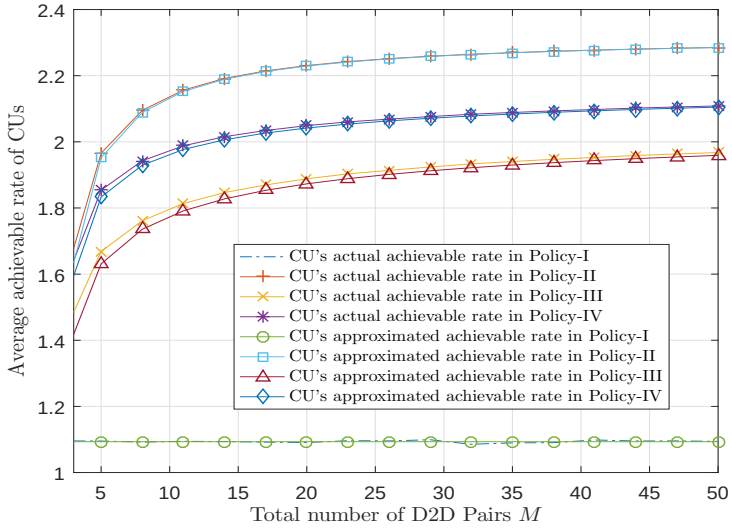

Figure 4.3: CU's Approximated Rates in All Policies with $\mu = 5$dB

The sum rate gains are simulated versus the active number of DUs in Figure 4.4. Comparing with the single D2D pair scheme, by a proper choice of the active DUs, the sum rates of the system can be improved significantly.

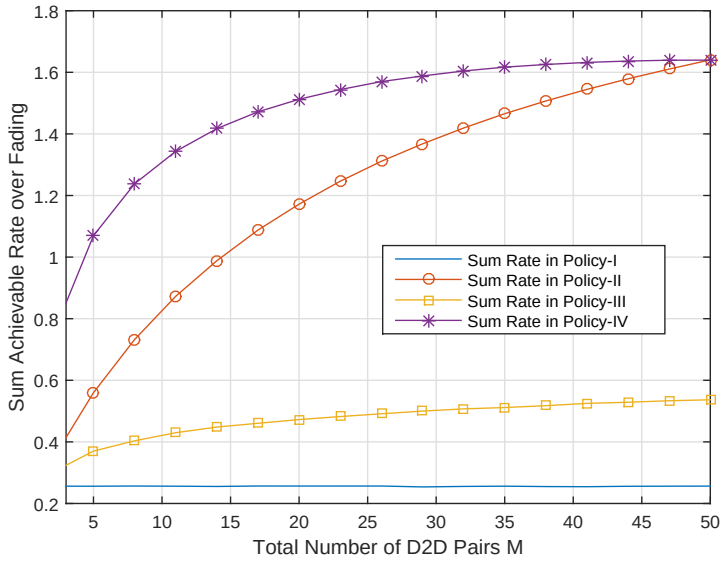

Figure 4.4: Sum Rate Gain of Different Policies with $\mu = -10$dB.

In Section 4.2.3, we observe the rate trade-off between cellular and D2D networks by balancing the number of D2D pairs and power allocation factors under both perfect and imperfect interference cancellation scenarios. In Fig. 4.5 and 4.6, the achievable rates of an individual D2D user in the four policies are compared, where perfect interference cancellation is assumed at each DR_i. α value is adjusted to maintain the same CU's performance over all policies, to make the D2D performance comparison fair. In Fig. 4.5, we assume that $\mu = 0.3$ and $\beta = 0.1$, which is corresponding to the weak peer interference scenario. In Fig. 4.5, we set $\mu = \beta = 0.3$ and $\alpha_{\mathrm{I}} = 0.8$ which corresponds to the moderate peer interference scenario since usually the D2D link should be stronger than the interference channel due to the proximity. In Fig. 4.5 and 4.6, the total number of D2D pairs $M = 50$ is fixed, and the number of selected D2D pairs $r = 2$ in Policy-IV. Our formula in (4.39) predicts maximum values of

M in two scenarios to be 40 and 14, which can be verified by Fig. 4.5 and 4.6. When M is large, Policy-III is preferred, however it requires perfect instantaneous channel knowledge at the BS. Comparing with the single D2D pair case, Policies-II,III,IV have large potential to improve both the CU and the D2D performance simultaneously. Moreover, it can be observed that D2D users' rates in Policy-II is not necessarily monotonic in M. As M increases, more power is allocated on the D2D signal in order to compensate the peer interference from the other $M-1$ D2D transmitters. When M grows larger, the peer interference becomes dominant, hence the D2D users' rates then decreases with M.

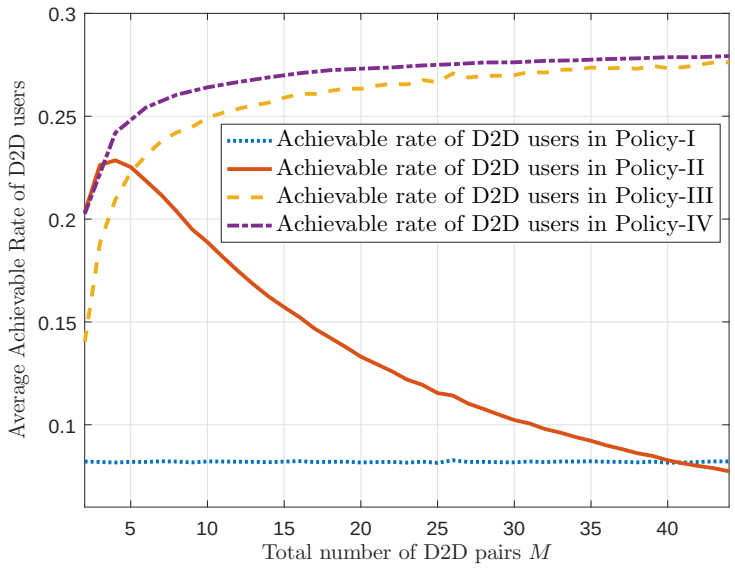

Figure 4.5: D2D Rates with Perfect Interference Cancellation at DR_i and Small Peer Interference at DT_i.

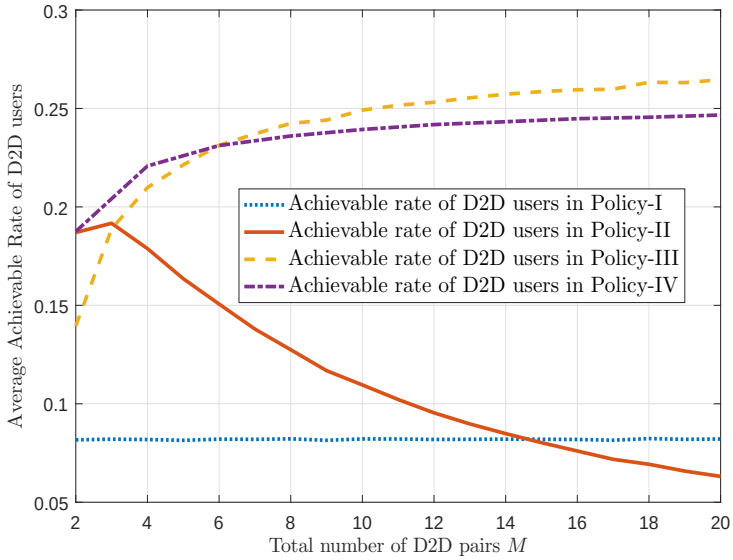

Figure 4.6: D2D Rates with Perfect Interference Cancellation at DR_i and Moderate Peer Interference at DT_i.

Similar achievable rate trade-off and the maximum M are also observed with imperfect interference cancellation, which are depicted numerically in Fig. 4.7 and 4.8. α value is adjusted to maintain the same CU's performance over all policies, to make the D2D performance comparison fair. Comparing with Fig. 4.5 and 4.6, it can be observed that D2D rates in all policies deteriorate due to the interference from the CU. However, the maximum values of M are not necessarily smaller than the perfect interference scenario.

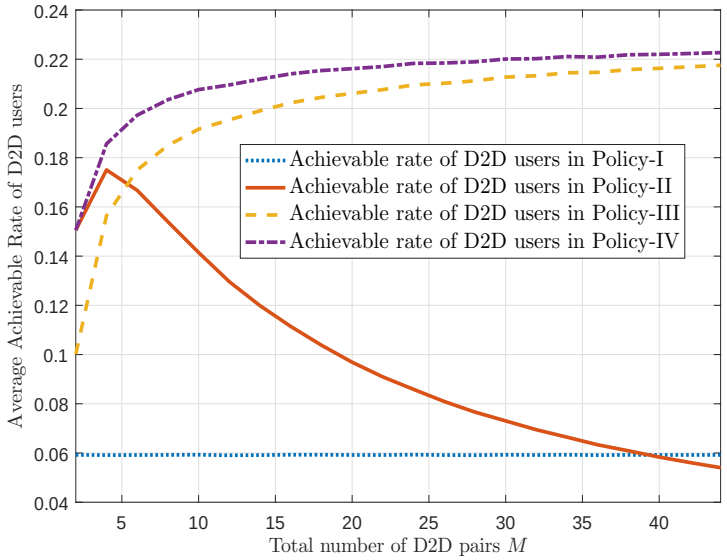

Figure 4.7: D2D Rates with Imperfect Interference Cancellation at DR_i and Small Peer Interference at DT_i.

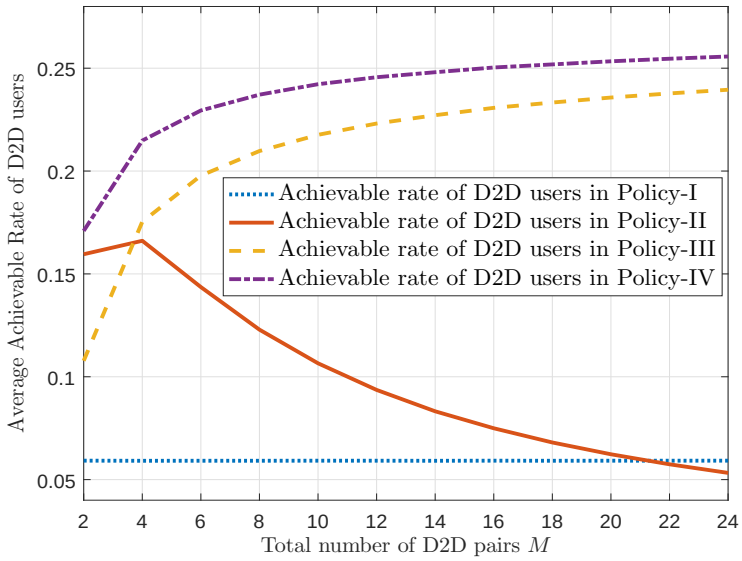

Figure 4.8: D2D Rates with Imperfect Interference Cancellation at DR_i and Moderate Peer Interference at DT_i.

In Fig. 4.9 and 4.10, D2D users' rates in Policy-IV are plotted versus the number of selected D2D pairs r, where $M = 50$ is fixed. α value is adjusted to maintain the same CU's performance for both policies. It can be seen that D2D users' rates is

decreasing in r due to the increasing of the peer interference at DR_i from other $r-1$ D2D transmitters. Similar to other policies, D2D users' rates is deteriorated by the imperfect interference cancellation of x_{C} at the DR_i.

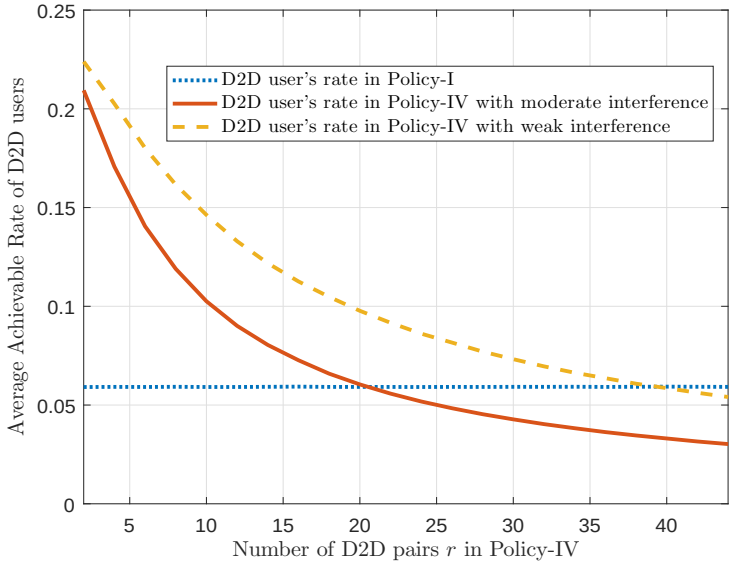

Figure 4.9: D2D Users' Rates in Policy-IV with Perfect Interference Cancellation at DT_i.

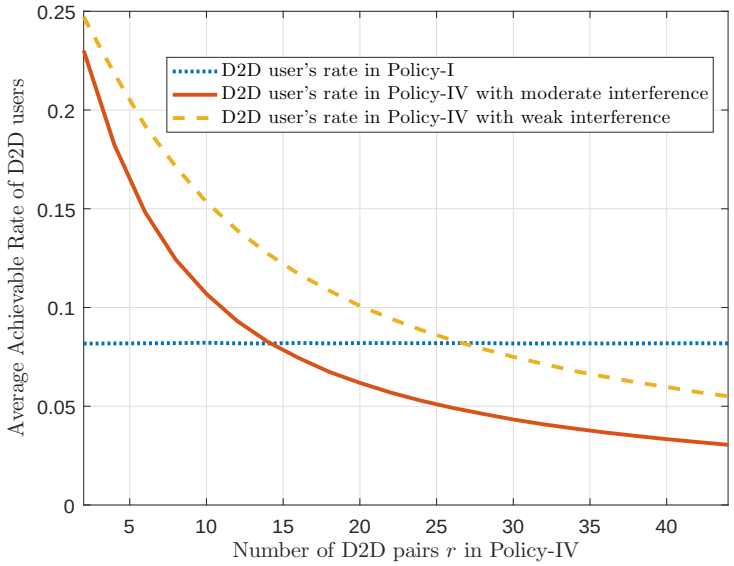

Figure 4.10: D2D Users' Rates in Policy-IV with Imperfect Interference Cancellation at DT_i.

In Section 4.3.1, the scaling laws of $\mathbb{E}_{\mathcal{M}}[\overline{R}_{\mathrm{C}}^{\mathrm{III}}(\mu, \mathcal{M})]$ is derived as $\lambda \to \infty$. Monte-carlo simulation and $\log(1 + \frac{P_{\mathrm{D}}\alpha}{P_{\mathrm{D}}(1-\alpha)+\frac{1}{\mu \log(\lambda)}})$ are plotted versus λ when $\mathcal{M}$ is Poisson distributed. It can be seen from Figure 4.11 that the gap between random number of DUs and the corresponding deterministic counterpart vanishes as $\lambda \to \infty$.

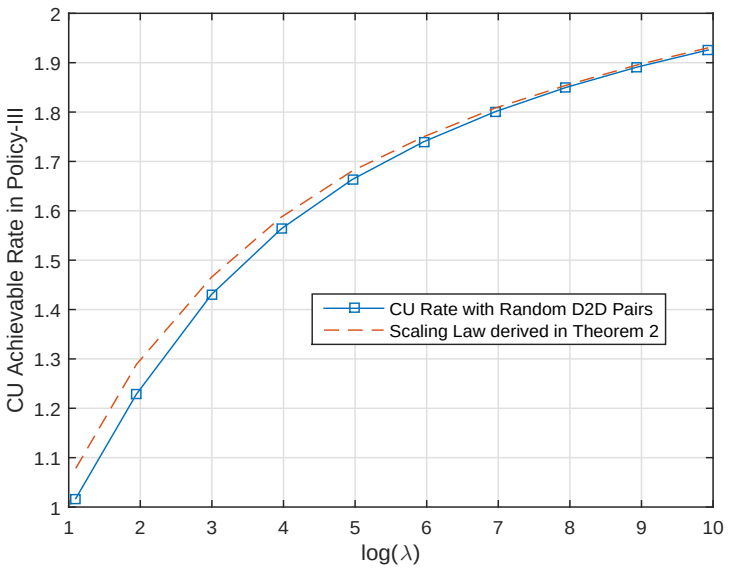

Figure 4.11: Scaling Laws of CU's Rate in Policy-III.

$\mathbb{E}_{\mathcal{M}}[\overline{R}_{\mathrm{C}}^{\mathrm{II}}(\mu, \mathcal{M})]$ and $\mathbb{E}_{\mathcal{M}}[\overline{R}_{\mathrm{C}}^{\mathrm{III}}(\mu, \mathcal{M})]$ are depicted in Figure 4.12 and 4.13 under several positive discrete user distributions. The Laplace transform order of Poisson, negative binomial and geometric distributions has been shown in [55]. For a given user distribution, $\mathbb{E}_{\mathcal{M}}[\overline{R}_{\mathrm{C}}^{\mathrm{II}}(\mu, \mathcal{M})]$ and $\mathbb{E}_{\mathcal{M}}[\overline{R}_{\mathrm{C}}^{\mathrm{III}}(\mu, \mathcal{M})]$ improve as λ increases. It can be observed that $\mathbb{E}_{\mathcal{M}}[\overline{R}_{\mathrm{C}}^{\mathrm{II}}(\mu, \mathcal{M})]$ and $\mathbb{E}_{\mathcal{M}}[\overline{R}_{\mathrm{C}}^{\mathrm{III}}(\mu, \mathcal{M})]$ follow the Laplace transform order of their corresponding user distributions, which collaborate our analysis in Theorem 17.

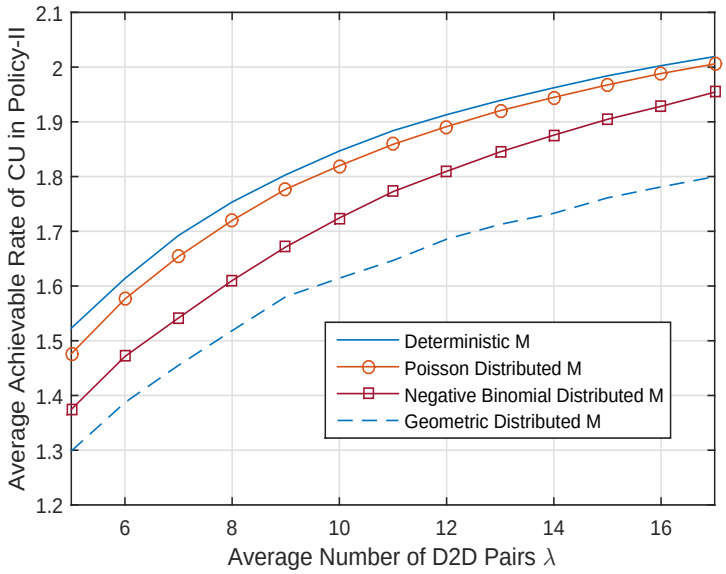

Figure 4.12: CU Rates Averaged Across Fading and Different User Distributions in Policy-II.

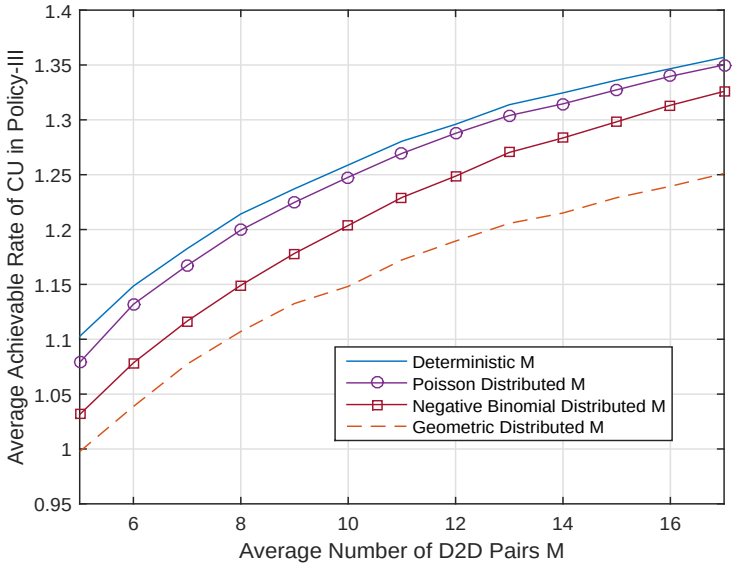

Figure 4.13: CU Rates Averaged Across Fading and Different User Distributions in Policy-III.

Chapter 5

CONCLUSIONS

In this dissertation, we study the system performance in the underlay CR systems, and the cooperative D2D communications underlaying a downlink cellular network. The aim is to investigate how overall system performance benefits from the cooperation.

An underlay CR system with single PU and multiple SUs is analyzed when the number of active SUs is random. Three performance metrics are considered: outage probability, ergodic capacity, and average BER. Stochastic ordering approach is applied in this topic. The scaling laws of the ergodic capacity for large mean number of users are studied in Theorem 5. The closed form expression of outage probability is related directly to the probability generating function of the number of active users (2.17). The closed form non-asymptotic expressions for the averaged BER under binomial, and NB active users are also derived using equation (2.18). A non-homogeneous interference scenario is also considered where the number of active SUs follows PB distribution. In this case, Poisson approximation is applied to study the ergodic capacity performance. Furthermore, all three metrics are proved to be ordered when their corresponding user distributions are Laplace transform ordered in Theorem 9.

A relay-aided cooperative underlay CR system with a single PU and multiple SUs is studied where opportunistic relay and MUD are applied in primary and secondary networks respectively. The closed form expressions for the average BER and scaling laws for achievable rates of both the PU and the selected SU are derived. A performance trade-off between the PU and the selected SU is observed for large number of SUs. The novel combined average BER and sum rate of the system are defined to capture the performance trade-off between PU and the underlay SU analytically.

Both metrics are optimized with respect to the ratio $t = N/(N+M)$ in Theorems 10 and 11 when the number of SUs is deterministic. It can be observed that when the system has homogeneous fading links, the optimal ratio in the BER and achievable rate yield the same result for the optimal ratio $t^* = 1/3$. Similar results when the number of users are random are derived in Theorem 12 and 13.

A cooperative system allowing multiple D2D pairs underlaying a downlink cellular network is considered. Each DT decodes and forwards the BS's information by superimposing its own D2D signal. Second order approximation of the CU as well as the D2D users' achievable rates are derived using Taylor series expansions. In Section 4.2.3 we illustrate the achievable rate trade-off between the CU and the D2D networks. We show that by a proper choice of the active D2D pairs and power allocation factor α, both the CU and the individual D2D users' achievable rate can be improved simultaneously, compared with the single D2D relay assisted scheme. The maximum number of D2D pairs allowed simultaneously in Policy-II and IV are derived in terms of the channel statistics and the power allocation factor. We also generalize the study to random number of DUs scenario where the DF is not perfect at each DT, by deriving the scaling laws of CU's rate in Policy-III in Theorem 16 for large mean number of DUs. Later in Section 4.3.2, CU's achievable rates averaged over fading and different user distributions are compared using stochastic ordering tool.

References

[1] V. Valenta, R. mars anda andlek, G. Baudoin, M. Villegas, M. Suarez, and F. Robert, "Survey on spectrum utilization in Europe: Measurements, analyses and observations," in *Proc. Fifth Int. Conf. Cog. Radio Oriented Wireless Netw. Commun. (CROWNCOM),*, June 2010, pp. 1 –5.

[2] D. Cabric, S. Mishra, and R. Brodersen, "Implementation issues in spectrum sensing for cognitive radios," in *Asilomar Conf. Sig., Systems and Computers, Conf.*, vol. 1, Nov. 2004, pp. 772 – 776 Vol.1.

[3] T. Yucek and H. Arslan, "A survey of spectrum sensing algorithms for cognitive radio applications," *IEEE Commun. Surveys Tut.*, vol. 11, no. 1, pp. 116–130, First 2009.

[4] J. Mitola and G. Maguire, "Cognitive radio: making software radios more personal," *IEEE Pers. Commun.*, vol. 6, no. 4, pp. 13–18, 1999.

[5] M. Mchenry, "Frequency agile spectrum access technologies," *FCC Workshop Cog. Radio*, May 2003.

[6] J. Kim, Y. Shin, T. W. Ban, and R. Schober, "Effect of spectrum sensing reliability on the capacity of multiuser uplink cognitive radio systems," *IEEE Trans. Veh. Technol.*, vol. 60, no. 9, pp. 4349 –4362, Nov. 2011.

[7] J.-H. Baek, H.-J. Oh, and S.-H. Hwang, "Improved reliability of spectrum sensing using energy detector in cognitive radio system," in *10th Int. Conf. Adv. Commun. Technol. (ICACT)*, vol. 1, Feb. 2008, pp. 575 –578.

[8] A. Goldsmith, S. Jafar, I. Maric, and S. Srinivasa, "Breaking spectrum gridlock with cognitive radios: An information theoretic perspective," *Proc. IEEE*, vol. 97, no. 5, pp. 894–914, 2009.

[9] Y. Zou, Y.-D. Yao, and B. Zheng, "Cooperative relay techniques for cognitive radio systems: Spectrum sensing and secondary user transmissions," *IEEE Commun. Mag.*, vol. 50, no. 4, pp. 98 –103, Apr. 2012.

[10] T. Do and B. Mark, "Exploiting multiuser diversity for spectrum sensing in cognitive radio networks," in *IEEE Radio Wireless Commun. Symp. (RWS)*, Jan. 2010, pp. 228 –231.

[11] H. Urkowitz, "Energy detection of unknown deterministic signals," *Proc. IEEE*, vol. 55, no. 4, pp. 523–531, Apr. 1967.

[12] A. Ghasemi and E. S. Sousa, "Collaborative spectrum sensing for opportunistic access in fading environments," in *First IEEE Int. Symp. New Frontiers Dynamic Spectr. Access Netw. (DySPAN)*, Nov. 2005, pp. 131–136.

[13] H. Tang, "Some physical layer issues of wide-band cognitive radio systems," in *First IEEE Int. Symp. New Frontiers Dynamic Spectr. Access Netw. (DySPAN)*, Nov. 2005, pp. 151–159.

[14] N. Hoven, R. Tandra, and A. Sahai, "Some fundamental limits on cognitive radio," in *Proc. Allerton Conf. Commun., Control, and Comput.*, 2005.

[15] J. Lunden, V. Koivunen, A. Huttunen, and H. V. Poor, "Spectrum sensing in cognitive radios based on multiple cyclic frequencies," in *Proc. Int. Conf. Cognitive Radio Oriented Wireless Netw. Commun. (CROWNCOM),*, Aug. 2007, pp. 37–43.

[16] K. Maeda, A. Benjebbour, T. Asai, T. Furuno, and T. Ohya, "Recognition among OFDM-based systems utilizing cyclostationarity-inducing transmission," in *IEEE Symp. New Frontiers in Dynamic Spectr. (DySPAN).* IEEE, 2007, pp. 516–523.

[17] P. Sutton, K. Nolan, and L. E. Doyle, "Cyclostationary signatures for rendezvous in OFDM-based dynamic spectrum access networks," in *IEEE Symp. New Frontiers in Dynamic Spectr. (DySPAN)*, Apr. 2007, pp. 220–231.

[18] A. Tkachenko, D. Cabric, and R. W. Brodersen, "Cyclostationary feature detector experiments using reconfigurable BEE2," in *IEEE Symp. New Frontiers in Dynamic Spectr. (DySPAN)*, Apr. 2007, pp. 216–219.

[19] G. Ganesan and Y. Li, "Cooperative spectrum sensing in cognitive radio networks," in *IEEE Symp. New Frontiers in Dynamic Spectr. (DySPAN)*, Nov. 2005, pp. 137–143.

[20] D. Cabric, A. Tkachenko, and R. W. Brodersen, "Spectrum sensing measurements of pilot, energy, and collaborative detection," in *IEEE Mil. Commun. Conf. (MILCOM)*, Oct. 2006, pp. 1–7.

[21] G. Ganesan and Y. Li, "Cooperative spectrum sensing in cognitive radio networks," in *IEEE Symp. New Frontiers in Dynamic Spectr. (DySPAN)*, Nov. 2005, pp. 137–143.

[22] Z. Li, F. Yu, and M. Huang, "A distributed consensus-based cooperative spectrum-sensing scheme in cognitive radios," *IEEE Trans. Veh. Technol.*, vol. 59, no. 1, pp. 383–393, Jan. 2010.

[23] J. Bazerque and G. Giannakis, "Distributed spectrum sensing for cognitive radio networks by exploiting sparsity," *IEEE Trans. Signal Process.*, vol. 58, no. 3, pp. 1847–1862, Mar. 2010.

[24] S. Zhang, C. Tepedelenliolu, M. K. Banavar, and A. Spanias, "Distributed node counting in wireless sensor networks in the presence of communication noise," *IEEE Sensors J.*, vol. 17, no. 4, pp. 1175–1186, Feb. 2017.

[25] ——, "Max-consensus using the soft maximum," in *Asilomar Conf. Signals, Syst. Comput.*, Nov. 2013, pp. 433–437.

[26] S. Zhang, C. Tepedelenliolu, M. K. Banavar, and A. Spanias, "Max consensus in sensor networks: Non-linear bounded transmission and additive noise," *IEEE Sensors Mag.*, vol. 16, no. 24, pp. 9089–9098, Dec. 2016.

[27] S. Zhang, C. Tepedelenlioglu, J. Lee, H. Braun, and A. Spanias, "Cramer-rao bounds for distributed system size estimation using consensus algorithms," in *Sensor Signal Process. Defence (SSPD)*, Sept. 2016, pp. 1–5.

[28] R. Santucci, M. K. Banavar, S. Zhang, A. Spanias, and C. Tepedelenlioglu, "OFDM-based distributed estimation for rich scattering environments," in *Sensor Signal Process. Defence (SSPD)*, Sept. 2014, pp. 1–5.

[29] S. Zhang, J. Lee, C. Tepedelenlioglu, and A. Spanias, "Distributed estimation of the degree distribution in wireless sensor networks," in *IEEE Global Commun. Conf. (GLOBECOM)*, Dec. 2016, pp. 1–6.

[30] A. Ewaisha and C. Tepedelenlioğlu, "Optimal power control and scheduling for real-time and non-real-time data," *IEEE Trans. Veh. Technol. (to-appear)*, 2017.

[31] ——, "Joint scheduling and power control for delay guarantees in heterogeneous cognitive radios," *IEEE Trans. Wireless Commun.*, vol. 15, no. 9, pp. 6298–6309, Sept. 2016.

[32] ——, "Power control and scheduling under hard deadline constraints for on-off fading channels," in *IEEE Wireless Commun. Netw. Conf. (WCNC)*, Mar. 2017, pp. 1–6.

[33] A. Ewaisha and C. Tepedelenlioglu, "Delay optimal joint scheduling-and-power-control for cognitive radio uplinks," in *IEEE Global Commun. Conf. (GLOBECOM)*, Dec. 2016, pp. 1–6.

[34] A. S. A.E. Ewaisha and T. ElBatt, "Optimization of channel sensing time and order for cognitive radios," in *IEEE Wireless Commun. Netw. Conf. (WCNC),*, Mar. 2011, pp. 1414–1419.

[35] B. Wang and K. Liu, "Advances in cognitive radio networks: A survey," *IEEE J. Sel. Topics Signal Process.*, vol. 5, no. 1, pp. 5–23, Feb. 2011.

[36] Y. Chen, G. Yu, Z. Zhang, H. h. Chen, and P. Qiu, "On cognitive radio networks with opportunistic power control strategies in fading channels," *IEEE Trans. Wireless Commun.*, vol. 7, no. 7, pp. 2752–2761, July 2008.

[37] W. Wang, T. Peng, and W. Wang, "Optimal power control under interference temperature constraints in cognitive radio network," in *IEEE Wireless Commun. Netw. Conf. (WCNC)*, Mar. 2007, pp. 116–120.

[38] S. A. Jafar and M. J. Fakhereddin, "Degrees of freedom for the MIMO interference channel," *IEEE Trans. Inf. Theory*, vol. 53, no. 7, pp. 2637–2642, July 2007.

[39] M. Gastpar, "On capacity under receive and spatial spectrum-sharing constraints," *IEEE Trans. Inf. Theory*, vol. 53, no. 2, pp. 471 –487, Feb. 2007.

[40] K. Hamdi, W. Zhang, and K. Ben Letaief, "Joint beamforming and scheduling in cognitive radio networks," in *IEEE Global Telecommun. Conf. (GLOBECOM)*, Nov. 2007, pp. 2977 –2981.

[41] H. Islam, Y.-C. Liang, and A. T. Hoang, "Distributed power and admission control for cognitive radio networks using antenna arrays," in *IEEE Symp. New Frontiers in Dynamic Spectr.(DySPAN)*, Apr. 2007, pp. 250 –253.

[42] X. Kang, Y.-C. Liang, H. Garg, and L. Zhang, "Sensing-based spectrum sharing in cognitive radio networks," *IEEE Trans. Veh. Technol.*, vol. 58, no. 8, pp. 4649–4654, Oct. 2009.

[43] S. Stotas and A. Nallanathan, "Enhancing the capacity of spectrum sharing cognitive radio networks," *IEEE Trans. Veh. Technol.*, vol. 60, no. 8, pp. 3768–3779, Oct. 2011.

[44] M. Khoshkholgh, K. Navaie, and H. Yanikomeroglu, "Access strategies for spectrum sharing in fading environment: Overlay, underlay, and mixed," *IEEE Trans. Mobile Comput.*, vol. 9, no. 12, pp. 1780–1793, Dec. 2010.

[45] H. Song, J.-P. Hong, and W. Choi, "On the optimal switching probability for a hybrid cognitive radio system," *IEEE Trans. Wireless Commun.*, vol. 12, no. 4, pp. 1594–1605, Apr. 2013.

[46] J. Oh and W. Choi, "A hybrid cognitive radio system: A combination of underlay and overlay approaches," in *IEEE Veh. Technol. Conf. (VTC)*, Sept. 2010, pp. 1–5.

[47] Z. Yan, X. Zhang, and W. Wang, "Outage performance of relay assisted hybrid overlay/underlay cognitive radio systems," in *IEEE Wireless Commun. Netw. Conf. (WCNC)*, Mar. 2011, pp. 1920–1925.

[48] T. W. Ban, W. Choi, B. C. Jung, and D. K. Sung, "Multi-user diversity in a spectrum sharing system," *IEEE Trans. Wireless Commun.*, vol. 8, no. 1, pp. 102 –106, Jan. 2009.

[49] R. Zhang and Y.-C. Liang, "Investigation on multiuser diversity in spectrum sharing based cognitive radio networks," *IEEE Commun. Lett.*, vol. 14, no. 2, pp. 133 –135, Feb. 2010.

[50] C. Masouros, F. Khan, T. Ratnarajah, and M. Sellathurai, "On the diversity gains of user scheduling in the cognitive radio parallel access channel," in *IEEE Global Telecommun. Conf. (GLOBECOM)*, Dec. 2011, pp. 1 –5.

[51] F. Khan, T. Ratnarajah, and M. Sellathurai, "Multiuser diversity analysis in spectrum sharing cognitive radio networks," in *Proc. 5th Int. Conf. Cog. Radio Oriented Wireless Netw. Commun. (CROWNCOM)*, June 2010, pp. 1 –5.

[52] A. Ghasemi and E. S. Sousa, "Fundamental limits of spectrum-sharing in fading environments," *IEEE Trans. Wireless Commun.*, vol. 6, no. 2, pp. 649 –658, Feb. 2007.

[53] A. Tajer and X. Wang, "Multiuser diversity gain in cognitive networks," *IEEE/ACM Trans. Netw.*, vol. 18, no. 6, pp. 1766 –1779, Dec. 2010.

[54] ——, "Multiuser diversity gain in cognitive networks with distributed spectrum access," in *43rd Annu. Conf. Inf. Sci. Syst. (CISS)*, Mar. 2009, pp. 135 –140.

[55] R. Zeng and C. Tepedelenlioglu, "Underlay cognitive multi-user diversity with random number of secondary users," *IEEE Trans. Wireless Commun.*, vol. 13, no. 10, pp. 5571–5581, Oct. 2014.

[56] M. K. Karakayali, G. J. Foschini, and R. A. Valenzuela, "Network coordination for spectrally efficient communications in cellular systems," *IEEE Wireless Commun.*, vol. 13, no. 4, pp. 56–61, 2006.

[57] N. Devroye, P. Mitran, and V. Tarokh, "Achievable rates in cognitive radio channels," *IEEE Trans. Inf. Theory*, vol. 52, no. 5, pp. 1813–1827, May 2006.

[58] A. Jovicic and P. Viswanath, "Cognitive radio: An information-theoretic perspective," *IEEE Trans. Inf. Theory*, vol. 55, no. 9, pp. 3945–3958, Sept. 2009.

[59] P. Yang, L. Luo, and J. Qin, "Outage performance of cognitive relay networks with interference from primary user," *IEEE Commun. Lett.*, vol. 16, no. 10, pp. 1695–1698, 2012.

[60] D. Li, "Cognitive relay networks: opportunistic or uncoded decode-and-forward relaying?" *IEEE Trans. Veh. Technol.*, vol. 63, no. 3, pp. 1486–1491, 2014.

[61] F. Guimaraes, D. da Costa, T. Tsiftsis, C. Cavalcante, and G. Karagiannidis, "Multiuser and multirelay cognitive radio networks under spectrum-sharing constraints," *IEEE Trans. Veh. Technol.*, vol. 63, no. 1, pp. 433–439, 2014.

[62] Y. Han, A. Pandharipande, and S. H. Ting, "Cooperative spectrum sharing via controlled amplify-and-forward relaying," in *IEEE 19th Int. Symp. Personal, Indoor and Mobile Radio Commun. (PIMRC 2008)*. IEEE, 2008, pp. 1–5.

[63] ——, "Cooperative decode-and-forward relaying for secondary spectrum access," *IEEE Trans. Wireless Commun.*, vol. 8, no. 10, pp. 4945–4950, 2009.

[64] Y. Han, S. H. Ting, and A. Pandharipande, "Cooperative spectrum sharing protocol with selective relaying system," *IEEE Trans. Commun.*, vol. 60, no. 1, pp. 62–67, 2012.

[65] D. Michalopoulos and G. Karagiannidis, "Performance analysis of single relay selection in rayleigh fading," *IEEE Trans. Wireless Commun.*, vol. 7, no. 10, pp. 3718–3724, Oct. 2008.

[66] M. Eltayeb, K. Elkhalil, H. Bahrami, and T. Al-Naffouri, "Opportunistic relay selection with limited feedback," *IEEE Trans. Commun.*, vol. 63, no. 8, pp. 2885–2898, Aug. 2015.

[67] W. Su, J. Matyjas, and S. Batalama, "Active cooperation between primary users and cognitive radio users in heterogeneous ad-hoc networks," *IEEE Trans. Signal Process.*, vol. 60, no. 4, pp. 1796–1805, Apr. 2012.

[68] Y. Yan, J. Huang, and J. Wang, "Dynamic bargaining for relay-based cooperative spectrum sharing," *IEEE J. Select. Areas Commun.*, vol. 31, no. 8, pp. 1480–1493, 2013.

[69] O. Simeone, Y. Bar-Ness, and U. Spagnolini, "Stable throughput of cognitive radios with and without relaying capability," *IEEE Trans. Commun.*, vol. 55, no. 12, pp. 2351–2360, Dec. 2007.

[70] R. Zeng and C. Tepedelenlioglu, "Fundamental BER performance trade-off in cooperative cognitive radio systems with random number of secondary users," *Asilomar Conf. Signal, Syst, and Comput. (Asilomar)*, Nov. 2016.

[71] ——, "Optimal achievable rate trade-off in cooperative cognitive radio systems," *IEEE Int. Conf. Acoust. Speech Signal Process. (ICASSP)*, Mar 2017.

[72] ——, "Fundamental performance trade-offs in cooperative cognitive radio systems," *IEEE Trans. Cogn. Commun. Netw.*, vol. 3, no. 2, pp. 169–179, June 2017.

[73] S. I. Hussain, M. M. Abdallah, M.-S. Alouini, K. Qaraqe, and M. Hasna, "Relay selection in underlay cognitive networks with fixed transmission power nodes," *Trans. Emerging Telecommun. Tech.*, vol. 24, no. 7-8, pp. 734–747, 2013. [Online]. Available: http://dx.doi.org/10.1002/ett.2691

[74] H. Ding, J. Ge, D. da Costa, and Z. Jiang, "Asymptotic analysis of cooperative diversity systems with relay selection in a spectrum-sharing scenario," *IEEE Trans. Veh. Technol.*, vol. 60, no. 2, pp. 457–472, Feb. 2011.

[75] V. N. Q. Bao, T. Duong, D. Benevides da Costa, G. Alexandropoulos, and A. Nallanathan, "Cognitive amplify-and-forward relaying with best relay selection in non-identical rayleigh fading," *IEEE. Commun. Lett.*, vol. 17, no. 3, pp. 475–478, Mar. 2013.

[76] L. Fan, X. Lei, T. Q. Duong, R. Hu, and M. Elkashlan, "Multiuser cognitive relay networks: Joint impact of direct and relay communications," *IEEE Trans. Wireless Commun.*, vol. 13, no. 9, pp. 5043–5055, 2014.

[77] K. Doppler, M. Rinne, C. Wijting, C. B. Ribeiro, and K. Hugl, "Device-to-device communication as an underlay to LTE-advanced networks," *IEEE Commun. Mag.*, vol. 47, no. 12, pp. 42–49, Dec. 2009.

[78] A. Asadi, Q. Wang, and V. Mancuso, "A survey on device-to-device communication in cellular networks," *IEEE Commun. Surveys Tuts.*, vol. 16, no. 4, pp. 1801–1819, Fourthquarter 2014.

[79] P. Phunchongharn, E. Hossain, and D. I. Kim, "Resource allocation for device-to-device communications underlaying LTE-advanced networks," *IEEE Wireless Commun.*, vol. 20, no. 4, pp. 91–100, Aug. 2013.

[80] B. Kaufman, J. Lilleberg, and B. Aazhang, "Spectrum sharing scheme between cellular users and ad-hoc device-to-device users," *IEEE Trans. on Wireless Commun.*, vol. 12, no. 3, pp. 1038–1049, Mar. 2013.

[81] C. H. Yu, O. Tirkkonen, K. Doppler, and C. Ribeiro, "Power optimization of device-to-device communication underlaying cellular communication," in *IEEE Int. Conf. Commun. (ICC)*, June 2009, pp. 1–5.

[82] ——, "On the performance of device-to-device underlay communication with simple power control," in *IEEE Veh. Technol. Conf. (VTC)*, Apr. 2009, pp. 1–5.

[83] N. Lee, X. Lin, J. G. Andrews, and R. Heath, "Power control for D2D underlaid cellular networks: Modeling, algorithms, and analysis," *IEEE J. Sel. Areas Commun*, vol. 33, no. 1, pp. 1–13, Jan. 2015.

[84] P. Jnis, V. Koivunen, C. B. Ribeiro, K. Doppler, and K. Hugl, "Interference-avoiding MIMO schemes for device-to-device radio underlaying cellular networks," in *IEEE 20th Int. Symp. Pers., Indoor and Mobile Radio Commun. (PIMRC)*, Sept. 2009, pp. 2385–2389.

[85] H. Tang, C. Zhu, and Z. Ding, "Cooperative MIMO precoding for D2D underlay in cellular networks," in *IEEE In. Conf. Commun. (ICC),*, June 2013, pp. 5517–5521.

[86] X. Lin, R. W. Heath, and J. G. Andrews, "The interplay between massive MIMO and underlaid D2D networking," *IEEE Trans. Wireless Commun.*, vol. 14, no. 6, pp. 3337–3351, June 2015.

[87] J. C. Li, M. Lei, and F. Gao, "Device-to-device (D2D) communication in MU-MIMO cellular networks," in *IEEE Global Commun. Conf. (GLOBECOM)*, 2012, pp. 3583–3587.

[88] B. Zhou, H. Hu, S. Q. Huang, and H. H. Chen, "Intracluster device-to-device relay algorithm with optimal resource utilization," *IEEE Trans. Veh. Technol.*, vol. 62, no. 5, pp. 2315–2326, June 2013.

[89] T. M. Cover and J. A. Thomas, *Elements of Information Theory*, 2nd ed., ser. Wiley Series in Telecommunications and Signal Processing. Wiley-Interscience, 2006.

[90] Y. Pei and Y.-C. Liang, "Resource allocation for device-to-device communications overlaying two-way cellular networks," *IEEE Trans. Wireless Commun.*, vol. 12, no. 7, pp. 3611–3621, July 2013.

[91] Y. Han, A. Pandharipande, and S. Ting, "Cooperative decode-and-forward relaying for secondary spectrum access," *IEEE Trans. Wireless Commun.*, vol. 8, no. 10, pp. 4945–4950, Oct. 2009.

[92] Y. Han, A. Pandharipande, and S. H. Ting, "Cooperative spectrum sharing via controlled amplify-and-forward relaying," in *IEEE 19th Int. Symp. Pers., Indoor and Mobile Radio Commun. (PIMRC)*, Sept. 2008, pp. 1–5.

[93] G. Zhang, K. Yang, P. Liu, and J. Wei, "Power allocation for full-duplex relaying-based D2D communication underlaying cellular networks," *IEEE Trans. Veh. Technol.*, vol. 64, no. 10, pp. 4911–4916, Oct. 2015.

[94] X. Li, C. Tepedelenlioğlu, and H. Şenol, "Channel estimation for residual self-interference in full duplex amplify-and-forward two-way relays," *IEEE Trans. Wireless Commun.*, vol. 16, no. 8, pp. 4970–4983, Aug. 2017.

[95] ——, "Optimal training for residual self-interference in full duplex one-way relays," *IEEE Trans. Commun.*, 2017. [Online]. Available: http://arxiv.org/abs/1709.06140

[96] H. Şenol, X. Li, and C. Tepedelenlioğlu, "Rapidly time-varying channel estimation for full duplex amplify-and-forward one-way relaying networks," *IEEE Trans. Signal Process.*, 2017.

[97] R. Zeng and C. Tepedelenlioglu, "Multiple device-to-device users overlaying cellular networks," in *IEEE Wireless Commun. Netw. Conf. (WCNC)*, Mar. 2017, pp. 1–6.

[98] M. Shaked and J. G. Shanthikumar, *Stochastic orders and their applications*. Academic Press, 1994.

[99] ——, *Stochastic Orders*. Springer, 2006.

[100] A. Muller and D. Stoyan, *Comparison methods for stochastic models and risks*. John Wiley and Sons, 2002.

[101] W. Feller, *An Introduction To Probability Theory And Its Applications, 2Nd Ed.* Wiley India Pvt. Ltd., 2009.

[102] A. W. Marshall, I. Olkin, and B. C. Arnold, *Inequalities: Theory of Majorization and Its Applications*, 2nd ed. Springer New York Dordrecht Heidelberg London, 2011.

[103] D. J. Daley. and P. Narayan, "Series expansions of probability generating functions and bounds for the extinction probability of a branching process," *J. Appl. Probability*, vol. 17, no. 4, pp. 939 –947, Dec. 1980.

[104] N. de Brujin, *Asymptotic Methods In Analysis.* Amsterdam: North-Holland, 1958.

[105] A. B. Narasimhamurthy, C. Tepedelenlioglu, and Y. Zhang, "Multi-user diversity with random number of users," *IEEE Trans. Wireless Commun.*, vol. 11, no. 1, pp. 60 –64, Jan. 2012.

[106] J. Jensen, "Sur les fonctions convexes et les ingalits entre les valeurs moyennes," *Acta Mathematica*, vol. 30, no. 1, pp. 175–193, 1906. [Online]. Available: http://dx.doi.org/10.1007/BF02418571

[107] A. Goldsmith, *Wireless Communications*, 1st ed. NY: Cambridge : Cambridge University Press, 2005.

[108] D. Gesbert and M.-S. Alouini, "How much feedback is multi-user diversity really worth?" in *IEEE Int. Conf. Commun.*, vol. 1, 2004, pp. 234–238.

[109] O. Filio, V. Kontorovich, and F. Ramos-Alarcon, "Time-energy limited feedback algorithms for multiuser diversity scenarios on nakagami fading channels," *IEEE Trans. Commun.*, vol. 60, no. 4, pp. 1045–1057, Apr. 2012.

[110] D. N. C. Tse and P. Viswanath, *Fundamentals of Wireless Communication*, 1st ed. Cam-bridge: Cambridge University Press, June 2005.

[111] L. L. Cam, "An approximation theorem for the poisson binomial distribution," *Pacific J. Mathematics*, vol. 10, no. 4, pp. 1181 –1197, Dec. 1960.

[112] P. J. Downey, "An Abelian theorem for completely monotone functions," June 1993, available online at ftp://ftp.cs.arizona.edu/ reports/1993/TR93-15.ps.Z.

[113] M. Hanif, H.-C. Yang, and M.-S. Alouini, "Receive antenna selection for underlay cognitive radio with instantaneous interference constraint," *IEEE Signal Process. Lett.*, vol. 22, no. 6, pp. 738–742, 2015.

[114] J. Laneman, D. Tse, and G. W. Wornell, "Cooperative diversity in wireless networks: Efficient protocols and outage behavior," *IEEE Trans. Inf. Theory.*, vol. 50, no. 12, pp. 3062–3080, Dec. 2004.

[115] A. Sendonaris, E. Erkip, and B. Aazhang, "User cooperation diversity. Part I. System description," *IEEE Trans. Commun.*, vol. 51, no. 11, pp. 1927–1938, Nov. 2003.

[116] A. Ribeiro, X. Cai, and G. Giannakis, "Symbol error probabilities for general cooperative links," *IEEE Trans. Wireless Commun.*, vol. 4, no. 3, pp. 1264–1273, May 2005.

[117] M. Simon and M.-S. Alouini, *Digital communication over fading channels*. New York: Wiley, 2005.

[118] M. Hasna and M.-S. Alouini, "Harmonic mean and end-to-end performance of transmission systems with relays," *IEEE Tran. Commun.*, vol. 52, no. 1, pp. 130–135, Jan. 2004.

[119] H. David and H. Nagaraja, *Order Statistics*. New York: Wiley, Aug. 2003.

[120] C. Tepedelenlioglu, Y. Zhang, and O. Rahman, "Asymptotic BER analysis of a simo multiuser diversity system," *IEEE Trans. Veh. Tech.*, vol. 58, no. 9, pp. 5330–5335, Nov. 2009.

[121] M. Abramowitz and I. Stegun, *Handbook of Mathematical Functions, With Formulas, Graphs, and Mathematical Tables*, 9th ed. New York: Dover, 1970.

[122] A. Bletsas, A. Khisti, D. Reed, and A. Lippman, "A simple cooperative diversity method based on network path selection," *IEEE J. Sel. Areas Commun.*, vol. 24, no. 3, pp. 659–672, Mar. 2006.

[123] J. Pérez, J. Ibánez, L. Vielva, and I. Santamaria, "Closed-form approximation for the outage capacity of orthogonal STBC," *IEEE Commun. Lett.*, vol. 9, no. 11, pp. 961–963, Nov. 2005.

[124] J. Pérez, J. Ibánez, L. Vielva, D. J. Pérez-blanco, and I. Santamaría, "Tight closed-form approximation for the ergodic capacity of orthogonal STBC," *IEEE Trans. Wireless Commun.*, vol. 6, no. 2, pp. 452–457, Feb. 2007.

[125] H. A. David and H. N. Nagaraja, *Order statistics*. Wiley Online Library, 1981.

[126] H. N. Nagaraja, P. K. Sen, and D. F. Morrison, *Statistical Theory and Applications: Papers in Honor of Herbert A. David*, 1st ed. Springer-Verlag New York, 1996.

[127] A. Rajan, C. Tepedelenlioglu, and R. Zeng, "A unified fading model using generalized gamma convolutions," in *2017 IEEE Wireless Commun. Netw. Conf. (WCNC)*, Mar. 2017.

[128] A. Rajan, C. Tepedelenliolu, and R. Zeng, "A unified approach for modeling fading channels using infinitely divisible distributions," *IEEE Trans. Veh. Technol.*, vol. PP, no. 99, pp. 1–1, 2017.

[129] R. Schilling, R. Song, and Z. Vondraček, *Bernstein Functions: Theory and Applications*. Walter de Gruyter, 2010.

[130] S. Sanayei and A. Nosratinia, "Opportunistic beamforming with limited feedback," *IEEE Trans. Wireless Commun.*, vol. 6, no. 8, pp. 2765–2771, Aug. 2007.

[131] R. Larson, R. P. Hostetler, and B. H. Edwards, *Calculus*, 8th ed. Cengage Learning, 2005.

APPENDIX A

PROOF OF THEOREM 5

Defining $y := e^{-x}$ and integrating by substitution,

$$\begin{aligned}
\mathrm{E}_{\mathcal{N}}\left[\overline{C}(\rho,\mathcal{N})\right] &= \rho\int_0^{\infty}\frac{1-U_{\mathcal{N}}(1-e^{-x})}{1+\rho x}dx \\
&= \int_0^1 \frac{1-U_{\mathcal{N}}(1-y)}{1-\rho\log y}\left(\frac{\rho}{y}\right)dy \\
&= \int_0^{\frac{\sqrt{\log\lambda}}{\lambda}} \frac{1-U_{\mathcal{N}}(1-y)}{1-\rho\log y}\left(\frac{\rho}{y}\right)dy + \int_{\frac{\sqrt{\log\lambda}}{\lambda}}^1 \frac{1-U_{\mathcal{N}}(1-y)}{1-\rho\log y}\left(\frac{\rho}{y}\right)dy
\end{aligned} \tag{A.1}$$

For the first term after the third equality in (A.1), we have the following inequalities according to the lower bound in (2.7):

$$0 < \int_0^{\frac{\sqrt{\log\lambda}}{\lambda}} \frac{U_{\mathcal{N}}(1-y)}{1-\rho\log y}\left(\frac{\rho}{y}\right)dy < \int_0^{\frac{\sqrt{\log\lambda}}{\lambda}} \frac{\lambda y}{1+\rho\log(\lambda)}\left(\frac{\rho}{y}\right)dy \tag{A.2}$$

$$= \frac{\rho\sqrt{\log(\lambda)}}{1+\rho\log(\lambda)-(\rho/2)\log(\log(\lambda))} \tag{A.3}$$

The right hand side in (A.2) holds because the denominator of the integrand is replaced with its lower limit. It can be seen that the upper bound after the equality in (A.3) yields $O\left(1/\sqrt{\log(\lambda)}\right)$ and has limit 0 as $\lambda\to\infty$. This implies that the first term in (A.1) should have limit 0. The second term in (A.1) has the upper and lower bounds given by,

$$\begin{aligned}
&\int_{\frac{\sqrt{\log\lambda}}{\lambda}}^1 \frac{1-U_{\mathcal{N}}\left(1-\frac{\sqrt{\log(\lambda)}}{\lambda}\right)}{(1-\rho\log(y))}\left(\frac{\rho}{y}\right)dy \\
&< \int_{\frac{\sqrt{\log\lambda}}{\lambda}}^1 \frac{1-U_{\mathcal{N}}(1-y)}{1-\rho\log(y)}\left(\frac{\rho}{y}\right)dy \\
&< \int_{\frac{\sqrt{\log\lambda}}{\lambda}}^1 \frac{1-U_{\mathcal{N}}(0)}{1-\rho\log(y)}\left(\frac{\rho}{y}\right)dy
\end{aligned} \tag{A.4}$$

in which the lower and upper bounds are obtained by bounding the numerator since $U_{\mathcal{N}}(1-y)$ is a monotonically decreasing function of y. Defining a normalized random variable $\mathcal{N}' = \mathcal{N}/\lambda$ which has mean value 1 and variance $\sigma^2_{\mathcal{N}'} = o(1)$ as $\lambda\to\infty$, using the upper bound in (2.7) we have:

$$\begin{aligned}
U_{\mathcal{N}'}(s) &\leqslant 1-(1-s)+\frac{\sigma^2_{\mathcal{N}'}}{2}(1-s)^2 \\
&= s+\frac{\sigma^2_{\mathcal{N}'}}{2}(1-s)^2
\end{aligned} \tag{A.5}$$

and

$$U_{\mathcal{N}}(s) = U_{\mathcal{N}'}(s^{\lambda}) \leqslant s^{\lambda} + \frac{\sigma^2_{\mathcal{N}'}}{2}(1-s^{\lambda})^2. \tag{A.6}$$

Moreover, the numerator of the lower bound in (A.4) can be further lower bounded as following:

$$1 - U_{\mathcal{N}}\left(1 - \frac{\sqrt{\log(\lambda)}}{\lambda}\right) \geqslant 1 - \left(1 - \frac{\sqrt{\log(\lambda)}}{\lambda}\right)^{\lambda} - \frac{\sigma^2_{\mathcal{N}'}}{2}\left(1 - \left(1 - \frac{\sqrt{\log(\lambda)}}{\lambda}\right)^{\lambda}\right)^2 \tag{A.7}$$

Therefore, the upper and lower bounds in (A.4) turn out to be

$$\left(1 - g(\lambda) - \frac{\sigma^2_{\mathcal{N}'}}{2}\left(1-g(\lambda)\right)^2\right)\log\left(1 + \rho\log(\lambda) - \frac{\rho}{2}\log(\log(\lambda))\right) \tag{A.8}$$

and

$$(1 - U_{\mathcal{N}}(0))\log\left(1 + \rho\log(\lambda) - \frac{\rho}{2}\log(\log(\lambda))\right) \tag{A.9}$$

respectively, where $g(\lambda) = \left(1 - \frac{\sqrt{\log(\lambda)}}{\lambda}\right)^{\lambda}$. In (A.8), when condition (b) holds,

$$\lim_{\lambda\to\infty}\left(g(\lambda) + \frac{\sigma^2_{\mathcal{N}'}}{2}\left(1-g(\lambda)\right)^2\right)\log(1+\log(\lambda)) = 0 \tag{A.10}$$

and in (A.9), when condition (a) holds

$$\lim_{\lambda\to\infty} U_{\mathcal{N}}(0)\log(1+\rho\log(\lambda)) = 0. \tag{A.11}$$

Hence, both (A.8) and (A.9) converge to $\log\left(1 + \rho\log(\lambda) - (\rho/2)\log(\log(\lambda))\right)$ as $\lambda \to \infty$. Moreover,

$$\begin{aligned}
\log\left(1 + \rho\log(\lambda) - \frac{\rho}{2}\log(\log(\lambda))\right) &= \log\left((1+\rho\log(\lambda))\left(1 - \frac{\frac{\rho\log(\log(\lambda))}{2}}{\log(1+\rho\log(\lambda))}\right)\right) \\
&= \log(1+\rho\log(\lambda)) + \log\left(1 - \frac{\frac{\rho\log(\log(\lambda))}{2}}{\log(1+\rho\log(\lambda))}\right) \\
&= \log(1+\rho\log(\lambda)) + O\left(\log(\log(\lambda))/\log(\lambda)\right)
\end{aligned} \tag{A.12}$$

as $\lambda \to \infty$. Therefore, considering the fact that $\log(\log(\lambda))/\log(\lambda)$ decays faster that $1/\sqrt{\log(\lambda)}$, (A.3) and (A.12) complete the proof.

APPENDIX B

THEOREM 5 HOLDS FOR PB SU DISTRIBUTION

Following the definition in Section 2.3.4, we have $\sum_{i=1}^{L} p_i = \lambda$ and $\sigma_{\mathcal{W}}^2 = \sum_{i=1}^{L} p_i(1-p_i)$. Since $\Pr[\mathcal{W}=0] = \prod_{i=1}^{L}(1-p_i) = U_{\mathcal{W}}(0)$ and $\log(1-p_i) < -p_i$, we have

$$\log\left(\prod_{i=1}^{L}(1-p_i)\right) = \sum_{i=1}^{L}\log(1-p_i) < \sum_{i=1}^{L}(-p_i) = -\lambda, \tag{B.1}$$

equivalently, $0 < \Pr[\mathcal{W}=0] < e^{-\lambda}$, which implies that condition a is satisfied. Furthermore, it is obvious that $\sigma_{\mathcal{W}}^2 < \sum_{i=1}^{L} p_i = \lambda$, hence condition (b) holds.

APPENDIX C

PROOF OF THEOREM 9

$\mathcal{Z} \leq_{\text{Lt}} \mathcal{X}$: to show $U_{\mathcal{Z}}(z) \leq U_{\mathcal{Y}}(z)$ first we take logarithm to $U_{\mathcal{Z}}(z)$ and $U_{\mathcal{Y}}(z)$ and we get

$$\log(U_{\mathcal{Z}}(z)) - \log(U_{\mathcal{Y}}(z)) = \frac{pr}{1-p}(z-1) - r\log\left(\frac{1-p}{1-pz}\right). \tag{C.1}$$

By shuffling the terms we rewrite the problem as comparing $\frac{p}{1-p} - \log(1-p) + \log(1-pz)$ with 0. Taking the first derivative with respect to z we get

$$\frac{\partial\left(\frac{p}{1-p} - \log(1-p) + \log(1-pz)\right)}{\partial z} = \frac{p}{1-p} - \frac{p}{1-pz} \geq 0 \tag{C.2}$$

for all $0 \leq z \leq 1$. This implies that (C.1) is an monotonically increasing function of z with the maximum value 0 at $z = 1$.

$\mathcal{X} \leq_{\text{Lt}} \mathcal{Y}$: to show $U_{\mathcal{X}}(z) \geq U_{\mathcal{Y}}(z)$ first we take logarithm to $U_{\mathcal{X}}(z)$ and $U_{\mathcal{Y}}(z)$ and we get

$$\log(U_{\mathcal{X}}(z)) - \log(U_{\mathcal{Y}}(z)) = Lp(z-1) - L\log\left(1-p+pz\right). \tag{C.3}$$

By rearranging the terms we rewrite the problem as comparing $s - \log(1+s)$ with 0, where $s = p(z-1)$. Taking the first derivative with respect to s we get

$$\begin{aligned}\frac{\partial\left(s - \log(1+s)\right)}{\partial s} &= 1 - \frac{1}{s+1} \\ &= \frac{s}{1+s} \leq 0\end{aligned} \tag{C.4}$$

for all $0 \leq z \leq 1$. This implies that (C.3) is an monotonically decreasing function of z with the minimum value 0 at $z = 1$.

$\mathcal{Y} \leq_{\text{Lt}} \mathcal{W}$: First we express all success probabilities of $\mathcal{W}$, denoted as p_i, in vector form so that $\boldsymbol{p} = [p_1 \quad p_2 \quad \dots \quad p_i]$. To show that $U_{\mathcal{Y}}(z) \geq U_{\mathcal{W}}(z)$ we notice that the equality is achieved when $\boldsymbol{p} = [\lambda/L \quad \lambda/L \quad \dots \quad \lambda/L]$ which is denoted as $\boldsymbol{p}_{\text{bin}}$. By applying Theorem 3 it can be seen that $U_{\mathcal{W}}(z) = \prod_{i=1}^{L}(1-p_i+p_iz)$ is a Shur-concave function of $\boldsymbol{p}$ since $\log(1-p_i+p_iz)$ is concave of p_i. Second, we assume there exists at least one probability vector of $\mathcal{W}$, denoted as $\boldsymbol{w} = [w_1 \quad w_2 \quad \dots \quad w_i]$, and $\boldsymbol{w} \prec \boldsymbol{p}_{\text{bin}}$. Then we have

$$w_1 = \max_i w_i \leq \lambda/L, \tag{C.5}$$

so that

$$\sum_{i=1}^{L} w_i \leq \sum_{i=1}^{L} w_1 \leq \lambda \tag{C.6}$$

which will violate the condition $\sum_{i=1}^{L} w_i = \lambda$ unless $\boldsymbol{w} = \boldsymbol{p}$. This indicates that $\boldsymbol{p}_{\text{bin}}$ is majorized by any other arbitrary probability vector $\boldsymbol{w}$ of $\mathcal{W}$, and $U_{\mathcal{Y}}(z, \boldsymbol{p}) = U_{\mathcal{W}}(\boldsymbol{p}_{z,\text{bin}}) \geq U_{\mathcal{W}}(z, \boldsymbol{w})$ at every value of z.

Hence, we have $U_{\mathcal{Z}}(z) \geq U_{\mathcal{X}}(z) \geq U_{\mathcal{Y}}(z) \geq U_{\mathcal{W}}(z)$, equivalently it can be concluded that $\mathcal{Z} \leq_{\text{Lt}} \mathcal{X} \leq_{\text{Lt}} \mathcal{Y} \leq_{\text{Lt}} \mathcal{W}$, which completes the proof.

APPENDIX D

PROOF OF THEOREM 10

Before proving Theorem 10, we first show the asymptotic behavior of the beta function $B(x,y)$ and lower incomplete gamma function $\gamma(x,y)$ in the high y regime.

For the beta function we have

$$\begin{aligned} B(x,y) &= \frac{\Gamma(x)\Gamma(y)}{\Gamma(x+y)} \\ &= \Gamma(y)\frac{\sqrt{2\pi(x-1)}\left(\frac{x-1}{e}\right)^{x-1}}{\sqrt{2\pi(x+y-1)}\left(\frac{x+y-1}{e}\right)^{x+y-1}} \\ &= \Gamma(y)\sqrt{\frac{x-1}{x+y-1}}\left(\frac{x-1}{x+y-1}\right)^{x-1}\left(\frac{1}{x+y-1}\right)^{y}e^{y}. \end{aligned} \tag{D.1}$$

By Stirling's formula [101, pp. 50-53] on the gamma function, $\Gamma(x) = x! \approx \sqrt{2\pi x}\left(\frac{x}{e}\right)^{x}$ when x is large, we obtain that

$$\begin{aligned} B(x,y) &= \Gamma(y)\sqrt{\frac{x-1}{x+y-1}}\left(\frac{x-1}{x+y-1}\right)^{x-1}\left(\frac{1}{x+y-1}\right)^{y}e^{y} \\ &= \Gamma(y)\sqrt{\frac{x-1}{x+y-1}}\left(1-\frac{y}{x+y-1}\right)^{x-1}(x+y-1)^{-y}e^{y} \\ &= \Gamma(y)e^{-y}x^{-y}e^{y} + o(x^{-y}) \\ &= \Gamma(y)x^{-y} + o(x^{-y}). \end{aligned} \tag{D.2}$$

where $\Gamma(\cdot)$ is Gamma function defined as $\Gamma(t) = \int_0^\infty x^{t-1}e^{-x}dx$.

For the lower incomplete gamma function, we have the following approximation

$$\gamma(x,y) = \Gamma(x) - \Gamma(x,y) = \Gamma(x) + o(1) \tag{D.3}$$

as $y \to \infty$, where $\Gamma(x,y) = \int_y^\infty t^{x-1}e^{-t}dt$ is the upper incomplete gamma function.

Substituting (D.2) and (D.3) into (3.25) and we obtain

$$\begin{aligned} \overline{\mathrm{P}}_{\mathrm{e_{all}}}^{\mathrm{HM}}(N,M) &= \frac{\alpha^3}{1+\eta\beta_1}\exp(-\eta\alpha_N c)\gamma(\eta c+1, \exp(\alpha_N))MB(M, 1+\eta\beta_4) \\ &\approx K\Gamma(1+\eta c)N^{-\eta c}M\Gamma(1+\eta\beta_4)M^{-1-\eta\rho} \\ &= K\Gamma(1+\eta c)\Gamma(1+\eta\beta_4)N^{-\eta c}M^{-\eta\beta_4} \end{aligned} \tag{D.4}$$

and

$$\begin{aligned} \overline{\mathrm{P}}_{\mathrm{e_{all}}}^{\mathrm{MM}}(N,M) &= \frac{\alpha^3}{1+\eta\beta_1}NB(N, 1+\eta\rho)MB(M, 1+\eta\beta_4) \\ &\approx KN\Gamma(1+\eta\rho)N^{-1-\eta\rho}M\Gamma(1+\eta\beta_4)M^{-1-\eta\rho} \\ &= K\Gamma(1+\eta\rho)\Gamma(1+\eta\beta_4)N^{-\eta\rho}M^{-\eta\beta_4} \end{aligned} \tag{D.5}$$

where $K = \frac{\alpha^3}{1+\eta\beta_1}$. Let $t = \frac{N}{N+M}$, for the harmonic mean upper bound case, the optimization problem in Theorem 10 can be reduced to

$$\begin{aligned} \text{maximize} \quad & f(t) = t^{-\eta c}(1-t)^{-\eta\beta_4} \\ \text{s.t.} \quad & 0 \le t \le 1. \end{aligned} \tag{D.6}$$

We define $g(t) = \log(f(t)) = \log(t^{-\eta c}(1-t)^{-\eta\beta_4})$, and take the second derivative of $g(t)$ with respect to t and obtain

$$\frac{d^2 g(t)}{t^2} = \frac{\eta\beta_4}{1-t} + \frac{\eta c}{t^2} \geq 0. \tag{D.7}$$

Consequently, $g(t)$ is convex over $0 \leq t \leq 1$ and has a unique minimum. Solving $dg(t)/dt = 0$, we conclude that $\overline{\mathrm{P}}_{\mathrm{e_{all}}}^{\mathrm{HM}}(N, M)$ can be minimized at $t^*_{\mathrm{HM}} = c/(c+\beta_4)$. Similarly, $\overline{\mathrm{P}}_{\mathrm{e_{all}}}^{\mathrm{MM}}(N, M)$ can be proved to be minimized at $t^*_{\mathrm{MM}} = \rho/(\rho+\beta_4)$, which completes the proof.

APPENDIX E

PROOF OF THEOREM 11

The sum rate of the proposed CR system can be expressed as

$$\overline{\mathrm{C}}_{\mathrm{all}}(N,M) = \overline{\mathrm{C}}_{\mathrm{P}}(N) + \overline{\mathrm{C}}_{\mathrm{S}}(M) \tag{E.1}$$

It has been shown in [55] that

$$\overline{\mathrm{C}}_{\mathrm{S}}(M) = \log(\log(M)) + O\left(\frac{1}{\sqrt{\log(M)}}\right). \tag{E.2}$$

It has been proved in [130] that if a family of positive i.i.d. random variables $\{\mathcal{X}_n\}$ with finite mean ν_n and variance σ_n^2 satisfy $\nu_n \to \infty$ and $\frac{\sigma_N^2}{\nu_n} \to 0$ as $n \to \infty$, then we have

$$\mathrm{E}[\log(1+\mathcal{X}_n)] = \log(1+\nu_n) + o(\log(1+\nu_n)). \tag{E.3}$$

When N is large, either the harmonic mean or the min-max upper bound is applied, from equation (3.4) it can be seen that the family of i.i.d. random variables γ_{P} have finite mean $\mathrm{E}[\gamma_{\mathrm{P}}] = \mathrm{E}[\gamma_{\mathrm{D}}] + \mathrm{E}[\gamma_{\mathrm{R}}^*] = \beta_1 + \rho\log(N)$ or $\mathrm{E}[\gamma_{\mathrm{P}}] = \beta_1 + c\log(N)$, and variance $\mathrm{var}[\gamma_{\mathrm{P}}] = {\beta_1}^2 + \pi^2/6$ [120]. Then, $\mathrm{E}[\gamma_{\mathrm{P}}] \to \infty$ and $\frac{\mathrm{var}[\gamma_{\mathrm{P}}]}{\mathrm{E}[\gamma_{\mathrm{P}}]} \to 0$ as $N \to \infty$. Hence we apply (E.3) and obtain that

$$\overline{\mathrm{C}}_{\mathrm{P}}(N) = \frac{1}{2}\log(\log(N)) + o(\log(\log(N))). \tag{E.4}$$

Hence,

$$\overline{\mathrm{C}}_{\mathrm{all}}(N,M) = \frac{1}{2}\log(\log(N)) + \log(\log(M)) + O\left(\frac{1}{\sqrt{\log(M)}}\right) + o(\log(\log(N))). \tag{E.5}$$

Let $t = \frac{N}{N+M}$, the optimization problem is equivalent to

$$\begin{aligned} \text{maximize} \quad & h(t) = \frac{1}{2}\log(\log(Lt)) + \log(\log(L(1-t))) \\ \text{s.t.} \quad & 0 \le t \le 1. \end{aligned} \tag{E.6}$$

Since $\log(N)$ is a non-decreasing concave function of t, $h(t)$ is also concave in t. Taking the first order derivative of $h(t)$ with respect to t and set it to zero, we have the following equation of the optimal ratio t^* as

$$\frac{3t^* - 1}{2t\log(t) - (1-t^*)\log(1-t^*)} = \frac{1}{\log(L)}. \tag{E.7}$$

It is easily seen that as $L \to \infty$, $t^* \to 1/3$, which completes the proof.

APPENDIX F

PROOF OF THEOREM 13

For the PU, due to the Jensen's inequality, any randomization of the number of SUs always deteriorates the achievable rate performance of the selected user [55]. Hence the achievable rate of the PU $\mathrm{E}_{\mathcal{N}}[\overline{\mathrm{C}}_{\mathrm{P}}(\mathcal{N})]$ can be upper bounded as:

$$\mathrm{E}_{\mathcal{N}}[\overline{\mathrm{C}}_{\mathrm{P}}(\mathcal{N})] \leq \overline{\mathrm{C}}_{\mathrm{P}}(\mathrm{E}[\mathcal{N}]), \tag{F.1}$$

which scales like $\frac{1}{2}\log(\log(\lambda t))$ as $\lambda \to \infty$ from (3.30). $\mathrm{E}_{\mathcal{N}}[\overline{\mathrm{C}}_{\mathrm{P}}(\mathcal{N})]$ is also lower bounded by removing the direct link from PU to the PR, and we have

$$\mathrm{E}_{\mathcal{N}}[\overline{\mathrm{C}}_{\mathrm{P}}(\mathcal{N})] \geq \mathrm{E}[\log(1+\gamma_{\mathrm{R}}^{*})]. \tag{F.2}$$

Using Theorem 5 in [55], the $\mathrm{E}[\log(1+\gamma_{\mathrm{R}}^{*})]$ can be shown to scale like $\frac{1}{2}\log(\log(\lambda t)) + O(1/\sqrt{\log(\lambda)})$ as $\lambda \to \infty$. Consequently, both the upper bound and lower bound on $\mathrm{E}_{\mathcal{N}}[\overline{\mathrm{C}}_{\mathrm{P}}(\mathcal{N})]$ converge to each other, and applying the squeeze theorem we have

$$\mathrm{E}_{\mathcal{N}}[\overline{\mathrm{C}}_{\mathrm{P}}(\mathcal{N})] = \frac{1}{2}\log(\log(\lambda t)) + O\left(\frac{1}{\sqrt{\log(\lambda)}}\right) + o(\log(\log(\lambda))) \tag{F.3}$$

as $\lambda \to \infty$. For the selected SU, from Theorem 5 in [55] we have

$$\mathrm{E}_{\mathcal{M}}[\overline{\mathrm{C}}_{\mathrm{S}}(\mathcal{M})] \to \log(\log(\lambda(1-t))) + O\left(\frac{1}{\sqrt{\log(\lambda(1-t))}}\right). \tag{F.4}$$

Hence, combining (F.3) and (F.4), we have for large λ,

$$\mathrm{E}_{\mathcal{N},\mathcal{M}}[\overline{\mathrm{C}}_{\mathrm{all}}(\mathcal{N},\mathcal{M})] = \frac{1}{2}\log(\log(\lambda t)) + \log(\log(\lambda(1-t))) + O\left(\frac{1}{\sqrt{\log(\lambda(1-t))}}\right) + o(\log(\log(\lambda))). \tag{F.5}$$

The rest of the proof is very similar to the proof of Theorem 11 that minimizing $\mathrm{E}_{\mathcal{N},\mathcal{M}}[\overline{\mathrm{C}}_{\mathrm{all}}(\mathcal{N},\mathcal{M})]$ is equivalent to minimizing $\overline{\mathrm{C}}_{\mathrm{all}}(N,M)$ by replacing L with λ.

APPENDIX G

PROOF OF THEOREM 14

$R_N(\gamma_{\mathrm{TC}_i})$ in (4.15) is the remainder of the N^{th} order Taylor series, whose absolute value can be upper-bounded by [131, p. 654]

$$|R_N(\gamma_{\mathrm{TC}_i})| \leq \frac{U}{N!} \left|(\gamma_{\mathrm{TC}_i} - \mu)^N\right|, \tag{G.1}$$

where U satisfies

$$\left| \frac{\partial^{N+1} \log\left(1 + \frac{P_{\mathrm{D}}\alpha}{P_{\mathrm{D}}(1-\alpha)+\frac{1}{x}}\right)}{\partial x^{N+1}} \right| \leq U, \quad \forall\ x. \tag{G.2}$$

The upper-bound U in (G.2) can be derived as

$$\begin{aligned} \left| \frac{\partial^{n} \log\left(1 + \frac{P_{\mathrm{D}}\alpha}{P_{\mathrm{D}}(1-\alpha)+\frac{1}{\gamma_{\mathrm{TC}_i}}}\right)}{\partial \gamma_{\mathrm{TC}_i}^{n}} \right| &= (n-1)! \left(\frac{P_{\mathrm{D}}^n}{(1+P_{\mathrm{D}}\gamma_{\mathrm{TC}_i})^n} - \frac{P_{\mathrm{D}}^n(1-\alpha)^n}{(1+P_{\mathrm{D}}(1-\alpha)\gamma_{\mathrm{TC}_i})^n} \right) \\ &\leq (n-1)! P_{\mathrm{D}}^n = U. \end{aligned} \tag{G.3}$$

Therefore, substituting (G.3) into (G.1), the remainder $\mathbb{E}\left[R_N(\gamma_{\mathrm{TC}_i})\right]$ averaged over γ_{TC_i} in (4.15) can be upper-bounded by

$$\left|\mathbb{E}\left[R_N(\gamma_{\mathrm{TC}_i})\right]\right| \leq \mathbb{E}\left[\left|R_N(\gamma_{\mathrm{TC}_i})\right|\right] = \frac{P_{\mathrm{D}}^{N+1}\mathbb{E}\left[\left|(\gamma_{\mathrm{TC}_i} - \mu)^{N+1}\right|\right]}{N+1}, \tag{G.4}$$

where the inequality in (G.4) is due to the convexity of the absolute value function.

From the binomial theorem, the n^{th} order central moment of exponentially distributed γ_{TC_i} can be expressed as

$$\mathbb{E}[|(\gamma_{\mathrm{TC}_i} - \mu)^n|] \leq \mathbb{E}[(\gamma_{\mathrm{TC}_i} + \mu)^n] = \mathbb{E}\left[\sum_{i=0}^{n} \binom{n}{i} \gamma_{\mathrm{TC}_i}^{n-i} \mu^i\right] \tag{G.5}$$

$$= \sum_{i=0}^{n} \binom{n}{i} \mathbb{E}\left[\gamma_{\mathrm{TC}_i}^{n-i}\right] \mu^i = \sum_{i=0}^{n} \frac{n!}{i!} \mu^{n-i}\mu^i = n!\mu^n \sum_{i=0}^{n} \frac{1}{i!} \tag{G.6}$$

$$\leq n!\mu^n \sum_{i=0}^{\infty} \frac{1}{i!} = n!\mu^n e, \tag{G.7}$$

where the inequality in (G.5) holds since γ_{TC_i} is a positive random variable. $\mathbb{E}\left[\gamma_{\mathrm{TC}_i}^{i}\right] = i!\mu^i$ in (G.6) is the i^{th} order moment of the exponentially distributed γ_{TC_i} with parameter μ. The equality in (G.7) holds since $\sum_{i=0}^{\infty} \frac{1}{i!} = e$.

Substituting (G.7) into (G.4), the upper-bound on the average remainder is derived as

$$\mathbb{E}\left[\left|R_N(\gamma_{\mathrm{TC}_i})\right|\right] \leq eN!P_{\mathrm{D}}^{N+1}\mu^{N+1}. \tag{G.8}$$

It can be seen that for any finite number N, the right hand side of the inequality in (G.8) scales like μ^{N+1} as $\mu \to 0$. Let $\mathbb{E}[T_N(\gamma_{\mathrm{TC}_i})]$ denote the N^{th} term in the sum in (4.15), then its absolute value $|\mathbb{E}[T_N(\gamma_{\mathrm{TC}_i})]|$ is upper-bounded as

$$\begin{aligned}
|\mathbb{E}[T_N(\gamma_{\mathrm{TC}_i})]| &\leq \mathbb{E}[|T_N(\gamma_{\mathrm{TC}_i})|] \\
&= \mu^N (N-1)! \left(\frac{P_{\mathrm{D}}^N}{(1+P_{\mathrm{D}}^N \mu^N} - \frac{P_{\mathrm{D}}^N (1-\alpha)^N}{(1+P_{\mathrm{D}}(1-\alpha)\mu)^N} \right) \sum_{i=0}^{n} \frac{1}{i!} \\
&\leq \mu^N (N-1)! P_{\mathrm{D}}^N e, \qquad \text{(G.9)}
\end{aligned}$$

which scales as μ^N as $\mu \to 0$. Hence, the remainder term approaches 0 faster than the N^{th} order term as $\mu \to 0$. This indicates that the Taylor series in (4.15) can be truncated at any finite order N, and remain tight when μ is small, which completes the proof.

APPENDIX H

PROOF OF THEOREM 15

The expectation in Theorem 15 is with respect to γ_{TC_i} and $\mathcal{Z}$. Therefore the approximation will require a multivariate Taylor series expansion around the mean values of these random variables:

$$\mathbb{E}\left[\log\left(1+\frac{P_{\mathrm{D}}(1-\alpha)\gamma_{\mathrm{TR}_i}}{P_{\mathrm{D}}(1-\alpha)\mathcal{Z}+1}\right)\right] = \log\left(1+\frac{P_{\mathrm{D}}(1-\alpha)\mu}{P_{\mathrm{D}}(1-\alpha)(M-1)\beta+1}\right)$$
$$+\sum_{n=1}^{N}\sum_{k=0}^{n}\binom{n}{k}D_k^n\log\left(1+\frac{P_{\mathrm{D}}(1-\alpha)\mu}{P_{\mathrm{D}}(1-\alpha)(M-1)\beta+1}\right)\mathbb{E}\left[(\gamma_{\mathrm{TR}_i}-\mu)^{n-k}\right]\mathbb{E}\left[(\mathcal{Z}-(M-1)\beta)^k\right]$$
$$+\mathbb{E}\left[R_N(\gamma_{\mathrm{TR}_i},\mathcal{Z})\right], \tag{H.1}$$

where $D_k^n f(x,y)$ denotes the n^{th} order mixed derivative of function $f(x,y)$ with respect to x and y, and is defined as

$$D_k^n f(x,y) = \frac{\partial^n f(x,y)}{\partial x^k \partial y^{n-k}} \quad \text{for } k=0,1,...n. \tag{H.2}$$

It can be shown from the Taylor's Theorem [131, Theorem 9.19] that the the absolute value of the N^{th} order Taylor series remainder in (H.1) is upper-bounded by

$$|R_N(\gamma_{\mathrm{TR}_i},\mathcal{Z})| \leq U\frac{\left|\sum_{k=0}^{N+1}\binom{N+1}{k}(\gamma_{\mathrm{TR}_i}-\mu)^{N+1-k}(\mathcal{Z}-(M-1)\beta)^k\right|}{(N+1)!}, \tag{H.3}$$

where U satisfies

$$\left|\sum_{k=0}^{N+1}\binom{N+1}{k}D_k^{N+1}\log\left(1+\frac{P_{\mathrm{D}}(1-\alpha)x}{P_{\mathrm{D}}(1-\alpha)y+1}\right)\right| \leq U, \qquad \forall\ x \text{ and } y. \tag{H.4}$$

Substituting (H.2) into (H.4), the upper-bound U can be derived as

$$\begin{aligned}\left|\sum_{k=0}^{N+1}\binom{N+1}{k}D_k^{N+1}\log\left(1+\frac{P_{\mathrm{D}}(1-\alpha)\gamma_{\mathrm{TR}_i}}{P_{\mathrm{D}}(1-\alpha)\mathcal{Z}+1}\right)\right| &= \left|\sum_{k=0}^{N+1}\binom{N+1}{k}E-F\right| \\ &\leq \sum_{k=0}^{N+1}\binom{N+1}{k}|E|+|F| \\ &= \left(2^{N+1}+1\right)N!P_{\mathrm{D}}^{N+1}(1-\alpha)^{N+1} \\ &= U, \end{aligned} \tag{H.5}$$

where

$$E = (-1)^N\frac{N!P_{\mathrm{D}}^{N+1}(1-\alpha)^{N+1}}{\left(1+P_{\mathrm{D}}(1-\alpha)(\gamma_{\mathrm{TR}_i}+\mathcal{Z})\right)^{N+1}}, \tag{H.6}$$

$$F = (-1)^N\frac{N!P_{\mathrm{D}}^{N+1}(1-\alpha)^{N+1}}{\left(1+P_{\mathrm{D}}(1-\alpha)\mathcal{Z}\right)^{N+1}}. \tag{H.7}$$

Equation (H.5) holds since $\sum_{k=0}^{N+1}\binom{N+1}{k} = 2^{N+1}$, and $|E|$ and $|F|$ are both upper-bounded by $N!P_{\mathrm{D}}^{N+1}(1-\alpha)^{N+1}$.

Therefore, the absolute value of the remainder in (H.3) averaged over γ_{TR_i} and $\mathcal{Z}$ can be upper-bounded by

$$\begin{aligned}
&|\mathbb{E}\left[R_N(\gamma_{\mathrm{TR}_i}, \mathcal{Z})\right]| \leq \mathbb{E}\left[|R_N(\gamma_{\mathrm{TR}_i}, \mathcal{Z})|\right] \\
&\leq \frac{U}{(N+1)!}\sum_{k=0}^{N+1}\binom{N+1}{k}\mathbb{E}\left[\left|(\gamma_{\mathrm{TR}_i}-\mu)^{N+1-k}\right|\right]\mathbb{E}\left[\left|(\mathcal{Z}-(M-1)\beta)^{k}\right|\right] \qquad \text{(H.8)} \\
&\leq Ue\sum_{k=0}^{N+1}(N+1-k)!\mu^{N+1-k}\beta^{k}\sum_{l=0}^{k}\binom{k}{l}M^{k-l}\prod_{n=0}^{l-1}(M+n), \qquad \text{(H.9)}
\end{aligned}$$

which goes to 0 for any finite $N+1$ as $\mu, \beta \to 0$. Especially when β is related to μ through a proportionality constant, $|\mathbb{E}\left[R_N(\gamma_{\mathrm{TR}_i}, \mathcal{Z})\right]|$ scales like μ^{N+1}. Let $\mathbb{E}[T_N(\gamma_{\mathrm{TR}_i}, \mathcal{Z})]$ denote the N^{th} term in the sum in (H.1), then its absolute value $|\mathbb{E}[T_N(\gamma_{\mathrm{TR}_i}, \mathcal{Z})]|$ is upper-bounded as

$$\begin{aligned}
&|\mathbb{E}[T_N(\gamma_{\mathrm{TR}_i}, \mathcal{Z})]| \leq \mathbb{E}[|T_N(\gamma_{\mathrm{TR}_i}, \mathcal{Z})|] \qquad \text{(H.10)} \\
&\leq \mu^N(2^N+1)(N-1)!P_{\mathrm{D}}^N(1-\alpha)^N e\sum_{k=0}^{N}(N-k)!\sum_{l=0}^{k}\binom{k}{l}M^{k-l}\prod_{n=0}^{l-1}(M+n), \qquad \text{(H.11)}
\end{aligned}$$

which scales as μ^N. Hence, the remainder term approaches 0 faster than the N^{th} order term as $\mu \to 0$. This indicates that the Taylor series in (H.1) can be truncated at any finite order N and remain tight when μ and β are small. Let $N = 2$, and we have the second order approximation of $\overline{R}_{\mathrm{D}}^{\mathrm{II}}(\mu, M)$ in (4.33) at small μ and β, which completes the proof.